Simulation of Large Scale Pedestrian Flow

Von der Fakultät für Mathematik und Physik der
Universität Stuttgart zur Erlangung der Würde eines
Doktors der Naturwissenschaften (Dr. rer. nat.)
genehmigte Abhandlung

Vorgelegt von
Mohamed Hedi Dridi
aus Tunis (Tunesien)

Hauptberichter: Prof. Dr. Günter Wunner
Mitberichter: Prof. Dr. Günter Haag

Tag der mündlichen Prüfung: 7. Oktober 2015

1. Institut für Theoretische Physik
Universität Stuttgart
Stuttgart 2015

CONTENTS

Contents **3**

List of abbreviations **7**

Abstract **9**

Zusammenfassung **11**

1 Introduction **17**
1.1 Aims of study, motivation and requirements 18
1.1.1 Aims of study: Why / where pedestrian traffic control? . . . 19
1.1.2 Motivation and requirements / specifications 20
1.2 Dissertation outline 20

2 Simulation of the motion of pedestrians **23**
2.1 Introduction 23
2.2 Existing approaches in microscopic and macroscopic models 24
2.3 Microscopic models 24
2.3.1 Social force model 24
2.3.2 2D cellular automata 26
2.3.3 Microscopic swarm model 27
2.4 Macroscopic model 29
2.5 Hybrid model: Discrete and continuous crowds 29
2.6 Some empirical data 30
2.6.1 Physical parameters 33
2.6.2 Corridor experiment 35
2.6.3 Fundamental diagram 38
2.6.4 Different conditions 38
2.6.5 Bottleneck and arc formation 40
2.6.6 Different fundamental diagrams 45
2.7 Pedestrian forces and motion (in PedFlow) 46
2.7.1 PedFlow force models 47

2.7.2 General description of will force . . . 47
2.8 Internal forces . . . 49
2.8.1 Desired direction $\vec{z}$ . . . 49
2.8.2 Internal forces –far range . . . 52
2.8.3 Internal forces –intermediate range . . . 54
2.8.4 External forces . . . 56
2.9 Data structures . . . 58
2.9.1 Data carried by the individual . . . 59
2.9.2 Geographic data . . . 60
2.9.3 Fixed triangular background grid . . . 60
2.9.4 Pedestrian data . . . 60
2.9.5 Example: Walking through a narrow passage . . . 62
2.9.6 Example: Evacuation of aircraft . . . 65
2.10 Pressure forces . . . 67
2.10.1 Introduction . . . 67
2.10.2 Classification of crowds and crowd accidents . . . 68
2.10.3 Crowd forces . . . 68
2.10.4 Value of crush force and lasting time . . . 69
2.10.5 Comfortable space in crowds . . . 70
2.10.6 Pushing mechanisms . . . 70
2.10.7 Contact pressure measurement of in-line pushing . . . 72
2.10.8 Leaning victim/pushers and no-leaning victim/pushers . . . 72
2.10.9 Conclusion . . . 75

3 List of parameters influencing the pedestrian movement 77
3.1 Introduction . . . 77
3.2 Conditions . . . 78
3.2.1 Panic condition (emergency) . . . 78
3.2.2 Causes of panic . . . 80
3.3 Types of crowds . . . 80
3.4 Ethnic groups and culture parameters . . . 81
3.5 Age parameter and subject selection . . . 82
3.6 Physical fitness (or level of exhaustion) . . . 83
3.7 Pedestrian radius parameters . . . 84
3.8 Climatic parameters (weather conditions) . . . 85
3.9 Psychology parameters . . . 85
3.10 Illustration . . . 86
3.11 Pedestrian database . . . 87
3.11.1 Data management . . . 87

4 Analysis of the Video Recording in Hajj 2009 (Mataf Area) 89
4.1 Introduction . . . 89
4.1.1 Data collection and type of observation . . . 89
4.1.2 Goals . . . 90
4.2 Estimation of crowd density . . . 91
4.2.1 Data . . . 93
4.2.2 Methods . . . 94
4.2.3 Automatic estimation of crowd density . . . 98
4.2.4 Data analysis . . . 99
4.3 Method of determining the pedestrian speed . . . 100
4.3.1 Methods . . . 103
4.3.2 Automatic estimation of pedestrian walking speeds . . . 110
4.4 Comparison of walking speeds . . . 111
4.5 Analysis of the pilgrims movement on the Mataf . . . 115
4.5.1 Echo effect with 'Adobe After Effects' ® . . . 116
4.5.2 Conclusion . . . 117

5 Microscopic simulation of the Mataf 119
5.1 Introduction . . . 119
5.1.1 Motivation . . . 120
5.1.2 Observations in the simplified model . . . 120
5.1.3 The Haram mosque building description . . . 121
5.1.4 Simulation of the simplified model . . . 122
5.1.5 Simulation of the enhanced model . . . 123
5.2 Mataf capacity estimation . . . 125
5.2.1 Fundamental Diagram . . . 125
5.2.2 Calculations . . . 126
5.3 Mobile Mataf geometry . . . 127
5.3.1 Concepts and evaluations . . . 127
5.3.2 Simulation . . . 128
5.4 Mataf capacities estimation . . . 129
5.5 Conclusion . . . 131

6 Validation 133
6.1 Validation and verification techniques . . . 133
6.1.1 A short overview . . . 133
6.1.2 Introduction to crowd simulation tool validation . . . 133
6.2 Calibration and validation of the PedFlow model . . . 137
6.2.1 Validation through comparison with other models . . . 138

6.2.2 Validation through visualization and comparison with the real world . . . 145
6.3 Validation of PedFlow using the optical flow method . . . 147
6.3.1 The optical flow method . . . 148
6.3.2 Motion analysis and object tracking . . . 150
6.4 Pedestrian tracking using OpenCV software . . . 151
6.4.1 Results . . . 152
6.4.2 Discussion . . . 153
6.4.3 Conclusions . . . 154

7 The new design of Mataf and further investigations 157
7.1 Recommendations for the future Hajj planning and development . 157

8 Conclusions and Recommendations 161
8.1 Conclusions . . . 161
8.2 Further research recommendations . . . 162

A Publications related to this thesis 165

Acknowledgments 167

Bibliography 169

LIST OF ABBREVIATIONS

Symbol	Used for
$\vec{v_i}$	actual velocity of individual i
$\vec{v_d}$	desired velocity of individual i
$\bar{v_i}$	average walking velocity of individual i
m_p	mass of each individual
R_i	radius of individual i
$\vec{f}_{will}$	the will force:= self-driven force of individual
$\vec{f}_i^s$	self-driven force of individual i
$\vec{f}_{ij}$	force on individual i by individual j
$\vec{f}_{iw}$	force on individual i by wall w
τ_i	relaxation time of individual i
d_{ij}	distance between the centre of mass of i and j
d_{iw}	distance of person i to wall w
A	constant (2 $\times 10^3$)
B	constant (0.08 m)
K	1.2 $\times 10^5$kgs^{-2}
κ	2.4 $\times 10^5$kgm^{-1}s^{-1}
n_{ij}	normalized vector pointing from person j to i
t_{ij}	tangential direction
n_{iw}	direction of i perpendicular to wall w
t_{iw}	direction tangential to w
δv_{ij}^t	tangential velocity difference i.e. $((v_j - v_i).t_{ij})$
v_{min}	minimum desired velocity of an individual
v_{max}	maximum desired velocity of an individual
ρ_p	pedestrian density
D	person projected area per square meter (pm^2/m^2)
$I(x,t)$	image intensity function
(PM)	Predtechenskii and Milinskii fundamental diagram

ABSTRACT

Pedestrian simulation is a challenging and fruitful application area for particle simulation, especially in places where many people are gathered (e.g. the Hajj, sports and concert events). Traffic and transportation domains take advantage of this simulation as well. Here the design and implementation involves interesting issues and particle-based modelling allows for the reproduction of pedestrian behaviour to a level of detail beyond pure collision-free locomotion. In this dissertation we will present a prototypical study: a simulation of pedestrian movement throughout the entire Haram area in the city of Mecca, Saudi Arabia, during the busiest Hajj hours. The objectives of this study are twofold: firstly to gather data for accurate predictions for designers and decision makers, and secondly to show, verify and validate that through the use of simulation tools it is possible to reproduce realistic scenarios.

Typical questions in pedestrian motion planning and design are: How many minutes would be needed to evacuate a football stadium or a pop concert arena? Where is the best place for pedestrian information or a poster wall to be placed? How many exit signs should be distributed over the area and where should they be placed? How many minutes does a pedestrian need to go from point A to point B in the overcrowded places? Are transfer times still realistic when the pedestrians are not familiar with the layout? For better planning in this area a better understanding of human behaviour is required and one way to achieve this is to improve the tools available for pedestrian planning (such as pedestrian micro simulation). In particular, particle-based simulation has become an attractive paradigm for modelling and simulating pedestrian decision-making and behaviour because it supports a one-to-one correspondence between the subject of observation and the simulated particle.

Since pedestrian movement is very complex, a computing method has to be developed to simulate the crowded movement of pedestrians on a virtual area. The method is based on the data and relations published by Predtechenski and Milinski [1], resulting from several thousand observations.

In this investigation we have developed two-dimensional space crowd dynamic models to allow for a simulation of high density crowds. This was done

by modifying and enhancing various features on existing microscopic models, respecting the properties of the individuals like social force and Cellular Automata models. We have also studied all existing models and their positive and negative properties to describe a real crowd behaviour. Our target was to describe a comprehensive approach to model a large scale of pedestrian scenarios (like pilgrim mobility in Hajj) through integrating a number of models from different research domains. In this dissertation a model based on discrete theory is developed and classical mechanics such as Newton's laws of motion are used. The sum of all the forces exerted by the particle or acting on this particle is called $\vec{f}$. This force requires intensive modelling efforts that will be considered and implemented as force-vectors. In this work we will discuss the main forces that can be identified as acting on a pedestrian.

This model was developed from image data (so called empirical data) taken from a video camera or data obtained using human observers. We consider the individuals as self-driven particles interacting through social and physical forces, which is one approach that has been used to describe crowd dynamics. The behaviour of the pedestrians can be observed from video tapes and from the given task cycle. Since not all behaviour of pedestrians has a major global effect on the overall capacity, the main affecting behaviour has to be extracted and used as input for the computer model.

ZUSAMMENFASSUNG

Der Extremfall der Fußgängerforschung ist ein dichtes Gedränge zehntausender Menschen, das in Fußballstadien, aber auch bei Pilgern in Mekka auftreten kann. Wenn jeder zwischen anderen eingequetscht ist, kann das Phänomen der Crowd Turbulence auftreten, ein praktisch unkontrollierbares, erdbebenartiges Hin- und Hergeworfenwerden. Dabei kann es zu einer Tragödie mit vielen Toten kommen. Meine Dissertation befasst sich mit der Simulation und dem Management von höhereren Fußgängerdichten in Fußballstadien oder in Pilgerstätten. Diese Software hilft, die Anfänge gefährlicher Turbulenzen früher zu erkennen, sie schlägt Alarm und die Sicherheitskräfte können eingreifen.

Je genauer die Simulation ist, umso besser lassen sich Gebäude, Kreuzfahrtschiffe oder Bahnhöfe planen. Unnötiges Gedränge oder gar Panik werden so vermieden. Modellrechnungen haben beispielsweise gezeigt, dass einfache Mittel den „Durchfluss“ an Notausgängen verbessern können. Ein Pfeiler genügt, denn er spaltet die schiebende Menschenmasse. So sinkt der Druck auf die Tür, durch die sich alle so schnell wie möglich zwängen wollen.

Das Fußgängerverhalten wird durch ein mikroskopisches Modell beschrieben, welches die Motivation eines Fußgängers und die Beeinflussung durch seine wahrgenommene Umwelt anhand von sogenannten sozialen Kräften beschreibt. Beispielsweise wird die Orientierung in Richtung eines Ziels und der Wunsch, mit einer bestimmten Geschwindigkeit voranzukommen, durch eine Antriebskraft beschrieben. Die Validierung dieses Modells benötigt empirische Daten. Das in dieser Arbeit angewandte Auswertungsverfahren der Untersuchung bei hoher Dichte der Fußgängerströme basiert auf Beobachtungen, Photographien und Videoaufnahmen.

Mit dem dramatischen demographische Anstieg der Bevölkerung der Welt werden immer mehr Sicherheitskräfte bei jedem Ereignis (z.B. Fußballspiele und Musikkonzerte) benötigt. Die Sportarenen können gegenwärtig 100 000 und mehr Zuschauer aufnehmen. Geschlossene Sporthallen und Konzertsäulen nehmen 10 000 bis 12 000 Menschen auf. So werden in unserer heutigen Zeit die öffentlichen Gebäude immer gigantischer, damit sie mehr Zuschauer aufnehmen können. Die Aufgabe von Architekten und Ingenieuren ist, die Kapazitäten dieser

Gebäude zu vergrößern und die erforderliche Sicherheit für die Besucher herzustellen. Eine der wichtigen erforderlichen Maßnahmen für die Sicherheit der Menschen ist die laminare Strömung oder Bewegung der Fußgänger. Engpässe und Engstellen in einem geschlossenen oder offenen Bereich zu erkennen, kann sehr hilfreich sein, um bestimmte zukünftige Gefahren zu erkennen und zu vermeiden. Die fatalen Unfälle passieren am meisten in diesen Engpassbereichen, da die Menschendichte dort schnell steigt. Die meisten Verwundeten sterben an Kreislaufschwäche und Mangel an Sauerstoff. Die Gefahr, dass ein Chaos in einem Fußballspiel ausbricht, ist heute allgegenwertig, da die Zahl gewalttätiger Fußball-Hooligans überall auf dem Globus weiter steigt, wie vielen Polizeiprotokollen zu entnehmen ist.

Typische Fragen in der Fußgängerbewegungsplanung und im Design sind: Wie viele Minuten werden benötigt, um ein Fußballstadion oder eine Pop-Konzert-Arena zu evakuieren? Wo ist der beste Platz für Fußgänger-Informationen oder wo werden Plakate platziert? Wie viele Ausgangs-Schilder sollten über die Fläche verteilt werden, und wo sollen sie aufgestellt werden? Wie viele Minuten benötigt ein Fußgänger, um an überfüllten Plätzen vom Punkt A zum Punkt B zu gelangen? Sind die Wegezeiten noch realistisch, wenn der Fußgänger nicht mit dem Grundriss vertraut ist? Für eine bessere Planung in diesem Bereich ist ein besseres Verständnis des menschlichen Verhaltens erforderlich, und ein Weg, dies zu erreichen, ist es, die für die Fußgänger-Planung (wie z.B. die Fußgängermikrosimulation) verfügbaren Werkzeuge zu verbessern. Insbesondere hat sich die partikelbasierte Simulation zu einem attraktiven Paradigma für die Modellierung und Simulation der Entscheidungsfindung und des Verhaltens von Fußgängern entwickelt, weil sie eine Eins-zu-Eins-Entsprechung zwischen dem Subjekt der Beobachtung und den simulierten Teilchen ermöglicht.

Da die Fußgängerbewegung ein sehr komplexer Vorgang ist, wurde in der vorliegenden Arbeit ein Berechnungsverfahren entwickelt, um die Bewegung der Fußgänger auf überfüllten Flächen in einer virtuellen Umgebung zu simulieren. Die Methode basiert auf den Daten und Beziehungen von Predtechenski und Milinski [1], die aus mehreren tausend Beobachtungen resultieren. In dieser Untersuchung wurden zweidimensionale Modelle der Dynamik von Menschenmassen entwickelt, die eine Simulation bei hoher Dichte erlauben. Dies wurde durch die Modifizierung und Weiterentwicklung verschiedener Funktionen in bestehenden mikroskopischen Ansätzen erreicht, wobei die Eigenschaften der Individuen wie die soziale Kraft aber auch Zelluläre-Automaten-Modelle einbezogen wurden. Weiterhin wurden alle vorhandenen Modelle und deren positive und negative Eigenschaften untersucht, um das Verhalten von Menschenmassen realistisch zu beschrieben. Ziel war es, einen umfassenden Ansatz zu gewinnen, um eine große

Bandbreite an Fußgänger-Szenarien (wie die Mobilität der Pilger im Hajj) durch die Integration einer Reihe von Verfahren aus verschiedenen Forschungsbereichen zu modellieren. In dieser Arbeit wird ein Modell entwickelt, das auf diskreter Theorie basiert und auf die klassische Mechanik, wie Newtons Gesetze der Bewegung, zurückgreift. Die Summe der Kräfte, die durch die Partikel ausgeübt werden oder auf diese einwirken, wird mit $\vec{f}$ bezeichnet. Diese Kräfte erfordern eine intensive Studie, die in Kraft-Vektoren resultiert. In dieser Arbeit werden die wichtigsten Kräfte diskutiert, für die eine Auswirkung auf den Fußgänger identifiziert werden kann.

Das Modell dieser Arbeit wurde basierend auf Bilddaten (sogenannten empirischen Daten), die von einer Videokamera aufgenommen wurden oder unter Verwendung menschlicher Beobachter gewonnen wurden, entwickelt. Die Menschen werden als autonome Teilchen betrachtet, die durch soziale und physische Kräfte wechselwirken. Das Verhalten der Fußgänger kann in Videoaufnahmen und anhand eines gegebenen Tätigkeitsablaufs beobachtet werden. Da nicht jedes Verhalten der Fußgänger einen großen globalen Effekt auf den Gesamtablauf hat, wurden die wesentlichen Verhaltenseigenschaften extrahiert und als Eingabe für das Computermodell verwendet.

Diese Arbeit konzentriert sich auf die Verbesserung der Bewegung der Massenmenschenströme, um potentielle Gefahren zu erkennen und Aktionen und Maßnahmen zur Gefahrenabwehr und Prävention zu erarbeiten. Die eingeführten Prozesse sind detailliert in dieser Doktorarbeit dargestellt. Innerhalb des Forschungsbereichs werden „Fußgängerbewegungen“ aufgebaut, um unterschiedliche Entwicklungsszenarien zu simulieren. Ziel dieser Simulationen ist die Verbesserung der Qualität und der Fluidität der Fußgängerströme an Stellen mit höherer Dichte. Diese Arbeit befasst sich mit Orten, an denen die Personendichte mehr als 5 Personen/m^2 beträgt. An diesen Orten stellt die Menschendichte (in Stadien und Pilgerstätten) eine große Gefahr dar. Die Bewegung und die Sicherheit der Menschen innerhalb und außerhalb öffentlicher Gebäude (Sportarenen, Bahnhöfe, Konzertgebäude oder Eingangspavillons) stellt eine große Herausforderung für die Manager und Sicherheitskräfte dar. Flughäfen oder öffentliche Gebäude, Konzerthallen mit kritischer Infrastruktur und hohe Menschenströme (wie an Verkehrskreuzungen und unterirdische Metrostationen), als auch Privathäuser, Unternehmen und Produktionsabteilungen haben eine funktionelle Bestimmung, mit der die Regeln, nach denen man die Bewegung der Menschen steuert, eng verbundenen sind. Alle diese Anlagen, insbesondere der Bereich der Sicherheit unterirdischer ÖPNV-Anlagen könnte von der Computersimulation dieser Arbeit profitieren. Die Ergebnisse der Simulation können helfen, Menschenleben zu retten und Gefahren zu minimieren. Die Ergebnisse der Simula-

tion lieferten eine Vielzahl von Kennwerten wie z.B. Engstellenbereiche, Dichten auf dem Mataf-Bereich oder Belastungen und Kapazität von Moschee-Anlagen. Mit der Simulation wurden Engpässe und Hindernisse identifiziert und Empfehlungen für Maßnahmen sowie Nachweise der Wirkungen dieser Maßnahmen erarbeitet.

Ziele der Studie , Motivation und Anforderungen

Im Gegensatz zu makroskopischen Modellen betrachten mikroskopische Fußgänger-Studien das detaillierte Zusammenspiel der Fußgänger, um ihre Bewegung im Fußgängerverkehrsfluss zu kontrollieren. Dies bedeutet, dass das Verhalten der einzelnen Partikel in der Strömung in Betracht gezogen und ihre Interaktion registriert wird. Sowohl die physischen als auch die psychischen Einflussparameter jedes Objekts in der Bewegung muss im Fußgängerstrom berücksichtigt werden, um eine so realistische Simulation wie möglich zu erreichen. Frühere Arbeiten zur Quantifizierung mikroskopischer Fußgängerströme untersuchten in erster Linie die Simulation der Bewegung von Personen. Blue [2] verwendet zum Beispiel ein Zelluläre-Automaten-Modell, um die Ausbildung von Bewegungslinien zu generieren. Wenn auch nicht auf Gruppen von Menschen angewandt, verwendete Reynolds [3] ein Agenten-basiertes Modell, um das Zusammenströmen an einem Ort zu simulieren, indem er eine kleine Anzahl einfacher Regeln für die Wechselwirkung der einzelnen Agenten annahm. Auf ähnliche Weise verwendeten Helbing, Molnar und Vicsek [4] ein Modell sozialer Kräfte, um die Linienausbildung und eine physische Blockade an Engpässen in Paniksituationen aufzuzeigen.

Ziele der Studie : Warum / wo den Fußgängerverkehr kontrollieren?

Die genaue Vorhersage der Fußgängerbewegung kann verwendet werden, um potenzielle Sicherheitsrisiken und die operative Entwicklung bei Veranstaltungen, bei denen viele Menschen versammelt sind, zu beurteilen. Wie bereits erwähnt, sind Beispiele für solche Situationen Sport- und Musikveranstaltungen, Kinos, Theater, Museen, Konferenzzentren, Wallfahrtsorte und Orte der Anbetung oder Straßendemonstrationen, aber auch die Evakuierung von Flugzeugen, Schiffen und Zügen sind Fälle, in denen die Vorhersage der Fußgängerbewegung vorteilhaft verwendet werden kann.

Menschenmassen sind ein Teil unseres täglichen Lebens. Während die meisten Zuschauer sicher sind, könnte es für einige gefährlich sein: zum Beispiel im Jahr 2006 wurden viele Pilger während der Steinigung des Teufels auf der

Jamarat-Brücke getötet (zerdrückt) [5]. Im vergangenen Jahr wurden – nach aktuellen Nachrichteninformationen – am Eingang zum Festivalgelände der Loveparade in Duisburg 18 Menschen getötet und rund 80 Menschen verletzt. Solche Effekte in Menschenmassen sind nicht auf Außenanlagen begrenzt; zum Beispiel müssen Architekten, die Großgebäude entwerfen (z.B. Arenen und Hörsäle), die Verhaltensweisen an Ausgängen verstehen. So können gute Modelle den Massen sehr hilfreich sein.

In der heutigen Zeit ist es wesentlich wichtiger als jemals zuvor, die Dynamik von Menschenmassen zu verstehen. Die Bevölkerung ist dramatisch gewachsen und in räumlich begrenzten Bereichen steigt die Gefahr, zerdrückt oder verletzt zu werden, ständig. Um Ereignisse, an denen viele Individuen beteiligt sind, bewältigen zu können, ist die Entwicklung von Modellen wichtig, die für die Evakuierung verwendet werden können und in der Lage sind, eine große Anzahl von Fußgängern zu simulieren.

Motivation und Anforderungen / Spezifikationen

Für Fälle, in denen die Vorhersage von vielen (> 100 000) Personen über einen längeren Zeitraum betrachtet wird (z.B. Pilgerstätten), müssen die Daten optimal verarbeitet werden, um eine Simulation in einer angemessenen Zeit durchführen zu können. Die Simulation muss > 100 000 Fußgänger beinhalten und einen hohen Grad an Realismus (Genauigkeit) der Geographie, in der sich die Fußgänger bewegen, erreichen. Die Genauigkeit muss für die Arten oder Gruppen und die Verhaltensweisen der Masse erreicht werden. Auf der anderen Seite muss die Simulation in Echtzeit mit einer hohen Geschwindigkeit ausgeführt werden. Das System muss flexibel sein, um Leitsysteme für Menschenmassen einbeziehen zu können.

Für die Hram-Moschee in Makkah wurde auf der Basis einer detaillierten Fußgängerzählung eine partikelbasierte Mikrosimulation der Fußgängerbewegungen aufgebaut, um unterschiedliche Entwicklungsszenarien zu simulieren. Die Daten umfassen das Einströmen und den Abfluss von Personen sowie die Fußgängerdichten und Geschwindigkeiten während unerschiedlicher Zeiten. Daraus wurde eine umfangreiche Datenbank erstellt. Die gleichzeitige Simulation von 50 000 Pilgern wurde durchgeführt.

Aufbau der Dissertation

- Ziele der Studie, Motivation und Anforderungen
- Simulation der Bewegung von Fußgängern

- Liste der Einflussparameter auf die Fußgängerbewegung
- Die Analyse der Video-Aufnahme des Hajj 2009
- Simulationsergebnisse des Mataf- und Sa'y-Bereichs
- Simulationsergebnisse der mobilen Mataf
- Validierung
- Das neue Design der Mataf und weitere Untersuchungen
- Schlussfolgerungen und Empfehlungen

Diese Arbeit entstand in Kooperation mit der Firma SL-Rasch, Oberaichen, dem Center of Research Excellence in Hajj and Omrah – HajjCORE, Sau¸-di-A¸-rabien (http://www.hajjcore.org), und dem 1. Institut für Theoretische Physik der Universität Stuttgart.

CHAPTER 1

INTRODUCTION

Crowd simulation has found its way into computer science, computer visualizations and the computer simulation of oriented building construction and crowd management [1]. Without the claim of being exhaustive, we mention microscopic and macroscopic simulation models like the social force model (Helbing and Molnar, 1997) [6] and cellular automata [7]. The models were devised for different purposes and aspects, with different proportions of hardware, software and simulation. The above mentioned models will be discussed in our investigation, encompassing: modules and sensors, data inputs, outputs, visualizations and their processing. These pedestrian models are based on macroscopic (Fruin, 1971a,b, Bord, 1985) [8, 9, 10] or microscopic behavior (Blue and Adler, 1998; Gips and Marksjo, 1985; Helbing, 1991; Helbing and Molnar, 1995; Helbing and Vicsek, 1999; Lovas, 1994; Okazaki, 1979; Okazaki and Matsushita, 1993; Thompson and Marchant, 1995a,b; Watts, 1987) [7, 11, 6, 12, 13, 14, 15, 16, 17, 18]. Every model has its own philosophy to treat the movement of a crowd from different points of view. The famous example of a microscopic model describing crowd dynamics is the Social Force Model, where individuals are represented as self-driven particles interacting through social and physical forces. Macroscopic models do not pay attention to the individuals, they look at the behaviour of the entire flow.

In recent years, there has been increasing interest in modelling crowd and evacuation dynamics. Pedestrian models are based on macroscopic or microscopic behaviour. In this work, we are interested in developing models that can be used for evacuation control strategies. The accurate prediction of pedestrian motion can be used to assess operational performance and potential safety hazards at events where many individuals are gathered. Examples of such situations are sports and music events, cinemas and theatres, museums, conference centres, places of pilgrimage and worship, and street demonstrations. Evacuation from air-planes, ships and trains also represent cases where the prediction of pedestrian motion can be used advantageously.

Our model will be based on microscopic [2, 19] pedestrian simulation models.

The flow of pilgrims will be simulated, based on mathematical models derived from empirical data of pedestrian flows. If we consider a microscopic modelling approach, the pedestrians are treated as particles interacting through social forces called social rules. The evolution and design of this pedestrian simulation model required a lot of information and data. To be able to develop and calibrate a (microscopic) pedestrian simulation model, a number of variables need to be considered. For the first step of the model development, data was collected using video recordings of the Hajj 2009 in Mecca, and the coordinates of the head paths of pedestrians were taken through image processing. For the observation of pedestrian flows a Sony camera was used. This observation was made in different places where the pilgrims perform their rituals. Many variables can be gathered to describe the behaviour of pedestrians from different points of view. This dissertation describes how to obtain variables from video recordings and simple image processing that can represent the movement of pedestrians (pilgrims) and its variables.

This work focuses on describing and modelling the human behaviour from a point of view different to what has been known until now in crowd dynamics. Additionally we emphasize the importance of incorporating human psychological and physiological factors into the models.

1.1 Aims of study, motivation and requirements

In contrast to macroscopic models, microscopic pedestrian studies consider the detailed interaction of pedestrians to control their movement in pedestrian traffic flow. This means that the behaviour of every single particle in the flow is considered and its interaction is registered. Both the physical and psychological parameters influencing the movement of every entity in the pedestrian flow must be considered to achieve as realistic a simulation as possible. Previous work in quantifying microscopic pedestrian flows and crowd dynamics have been studied primarily through simulating the motion of individuals. For example, Blue [2] used a cellular automata model to generate emergent lane formation. Though not for groups of people, Reynolds [3] used an agent-based model to generate flocking behaviour using a small set of simple interacting rules for each agent. Along a similar line, Helbing, Molnar, and Vicsek [4] used a social force model to demonstrate lane formation and the physical jamming at bottlenecks during panics and stampedes.

All these models need empirical data for calibration and verification of the simulation model. For this reason we used different tools and developed different methods to collect the microscopic data and to analyse microscopic pedestrian

flow. One can recognize that the pedestrian data collection is still very much in its infancy. The microscopic pedestrian flow characteristics need to be understood. Manual, semi-manual and automatic image processing data collection systems were developed. It was found that the microscopic speed resembles a normal distribution with a mean of 1.38 m/second and standard deviation of 0.37 m/second. The acceleration distribution also bore a resemblance to normal distribution with an average of 0.68 m/ square second.

A two-dimensional space crowd dynamic based on microscopic pedestrian simulation models was also developed. Both the Microscopic Video Data Collection and Microscopic Pedestrian Simulation Model generate a database called the PedGUI database. The formulations of the flow performance or microscopic pedestrian characteristics are explained. The sensitivity of the simulation and relationship between the flow performances are described. Validation of the simulation using real world data is then explained through the comparison between average instantaneous speed distributions of the real world data with the result of the simulations. For verification and validation, data was provided by the Institute of Hajj research and the Ministry of Hajj, consisting of layout information, pilgrim numbers and Hajj schedules. We augmented this data with camera-based observations at several stairways, gates and the piazza inside and outside the Haram in Mecca. The simulation model was then applied for some experiments to a hallway, some corridors, bottlenecks and panic situations. This was done in order to gain more understanding of pedestrian behaviour in one-way and counter-flow situations, to know the behaviour of the system if the number of pedestrians increases with time, to evaluate a policy of lane-formation in bidirectional flow, to observe segregation towards pedestrian crossings and to inspect performance at the crossing. All of these experiments and observations were needed later to understand high density crowd behaviour. One can deduce that the microscopic pedestrian studies have been successfully applied to give a better understanding of the behaviour of microscopic pedestrians flow, predict the theoretical and practical situation and evaluate some design methods before their implementation.

1.1.1 Aims of study: Why / where pedestrian traffic control?

The accurate prediction of pedestrian motion can be used to assess the potential safety hazards and operational performance at events where many individuals are gathered. As already mentioned examples of such situations are sports and music events, cinemas and theatres, museums, conference centres, places of pilgrimage and worship, street demonstrations. Evacuation from air-planes, ships

and trains also represent cases where the prediction of pedestrian motion can be used advantageously.

Crowds are a part of our everyday lives. Whilst most crowds are safe, some can be dangerous: for example in 2006 many pilgrims were killed (crushed) during the stoning of the devil on the Jamarat Bridge [5]. Last year according to current news information, 18 people have died and around 80 people have been injured at the entrance to the festival grounds, in the love parade in Duisburg city. Crowd effects are not limited to these exterior settings; for example, architects designing large venues (e.g. arenas and lecture theatres) need to understand crowd exit behaviours. Thus, good models of crowds can be very helpful to many professionals.

Today we need to understand how to alter crowd dynamics more than any time before, the population has grown dramatically and in presence of restraint places the danger of crush or injuries increases all the time. To manage situations with many individuals we are interested in developing models that can be used for evacuation control strategies and to simulate a large scale of pedestrians.

1.1.2 Motivation and requirements / specifications

For cases where the prediction of many (>100 000) individuals over a long time is considered (e.g. pilgrimage centres), optimal data structures must be used in order to carry out a simulation in a reasonable time. The simulation must accommodate >100 000 pedestrians and must achieve high degrees of realism (accuracy) in the geography where the pedestrians move. The accuracy must be achieved for the types/groups and the behaviours of the crowd. On the other hand the simulation must run in real-time with a high speed of execution. The system must be flexible in order to incorporate in-line crowd management systems.

1.2 Dissertation outline

- Aims of study, motivation and requirements.
- Simulation of the motion of pedestrians.
- List of parameters influencing the pedestrian movement.
- Analysis of the video taking in Hajj 2009.
- Simulation results of Mataf and Sa'y area.
- Simulation results of mobile Mataf.

- Validation.
- The new design of Mataf and further investigations.
- Conclusions and recommendations.

CHAPTER 2

SIMULATION OF THE MOTION OF PEDESTRIANS

2.1 INTRODUCTION

Many approaches and models have been developed to study crowd behaviour [4, 3]. Microscopic models or particle based models attempt to describe the behaviour of every individual in the crowd. They consist of single particles that interact through social and physical forces, which is known as the Helbing Model [20]. The force that drives the particles from the rest to its desired velocity is referred to as self-driven force. The collision avoidance force is represented through a repulsive force which depends on the distance between the particles. This model is inspired by the gas-kinematic models [20], therefore there is an analogy between the behaviour of particles in a gas and the behaviour of pedestrians in a crowd. But this model has a lot of deficiencies to display the reality. In the swarm microscopic model the collision force is given through lateral incompressibility of the particles. The movement of pedestrians is influenced by many parameters and attributes (e.g. fitness, psychology,...) and the investigation of this topic is still in its beginning stages. Because all these models need empirical data, we will describe and illustrate a summary about the collected individual pedestrian data and fundamental diagrams. Following this approach, we will discuss the PedFlow model [21] and explain how the characteristic pedestrian forces are defined and implemented in this model. In the last section we will describe the forces that come into play in case of crowd crush or dangerous situations. We will give a large description about the pressure and friction forces in case of body contact. Following this we will present results and analysis.

2.2 Existing approaches in microscopic and macroscopic models

In recent years, several models for the movement of crowds have been proposed. One can distinguish between two general approaches: microscopic and macroscopic models. In the microscopic scope (range), pedestrians are treated as individual entities (particles). The particle interactions in this model are determined by physical and social rules as well as the interactions between the particles with their physical surrounding. In this context we cite, the social-force models (see [22] and the references therein), the cellular automata, e.g [23, 24], queuing models e.g. [25], or continuum dynamic approaches like [26]. For an extensive survey of different microscopic approaches we refer to [27].

The origin of the microscopic models for pedestrian behaviour can be traced back to the work of Reynolds in the years 1987 and 1999 [3, 28]. This model was extended by the sociological factors introduced in [29], psychological effects in [30], social forces [19, 31, 32, 33], and other models of pedestrian behaviour [34, 35, 36]. Many methods have been developed to describe the short range forces responsible for the collision avoidance between nearby pedestrians. These include geometrically-based algorithms [37, 38, 39, 40, 41, 42], grid-based methods [43, 44, 45] and force-based methods [46, 47, 48, 33].

In contrast to microscopic models, macroscopic models treat the pedestrians flow as continuum homogeneous mass that behaves like a fluid without considering the behaviour of single individuals. Many methods use concepts familiar from fluid and gas dynamics, see [49]. Modelling pedestrian dynamics as a fluid can be traced back to [8, 9]. More recent models are based on optimal transportation methods [50], mean field games (see [51] for a general introduction) or non-linear conservation laws [52].

Finally some of the models based on such techniques are listed in the following paragraph.

2.3 Microscopic models

2.3.1 Social force model

The social force model was developed by Helbing and Molnár [19], improved by Lakoba in 2005 [47] and has been expanded to contain physical contact forces in case of high density crowd or panic situation [4, 27]. The social force model has its origin in gas-kinetic models [20]. Social forces are a quantity to describe the motivation to follow a set of social rules that guide the pedestrian movement. In

this model the personal space is considered as well as following others at a safe distance and avoiding to get too close to walls and obstacles.

For a crowd consisting of N individuals, the force acting on the ith person is denoted by $\vec{f_i}$ and is given by

$$\vec{f_i} = \vec{f_i^s} + \sum_{i \neq j; j=1}^{N} \vec{f_{ij}^I} + \sum_{k=1}^{M} \vec{f_{ik}^w} \tag{2.1}$$

where $\vec{f_i^s}$ denotes the self-driven force that drives an individual towards their desired velocity, $\vec{f_{ij}^I}$ denotes the interaction force between pedestrians, and $\vec{f_{ik}^w}$ denotes the obstacles avoidance force (out of a total of M wall surfaces). The self-driven force is proportional to the difference between an individual's desired velocity v_d and a desired direction $\hat{e}_i$, and their actual velocity $\vec{v}_i$. τ_i is referred to as the relaxation time and corresponds to the finite amount of time that is required for people to react and physically change their velocity. Thus the self-driven force is given by

$$\vec{f_i^s} = \frac{m_i(v_d \hat{e}_i - \vec{v}_i)}{\tau_i} \tag{2.2}$$

where m_i denotes the mass of the ith individual.

The person-person interaction force consists of two main components, a social interaction term and a physical interaction term. The social interaction term is modelled as a repulsive force from other individuals that decreases with distance and illustrate the autonomous sphere of the individual. The distance between individuals i and j is given by

$$d_{ij} = \|\vec{r}_i - \vec{r}_j\| - R_i - R_j \tag{2.3}$$

where $\vec{r}$ is the position of an individual and R is their radius, (i.e. people are modelled as circles). The social interaction force is presented as an exponential function that decreases with distance, with the magnitude of the interaction given by the parameter α and the distance over which it is active given by the parameter β, so that the entire expression for this term is given by $\alpha e^{(-d_{ij}/\beta)}$.

In cases of dense crowds, physical contact between individuals occurs and can become a significant factor. The physical interactions consist of a body compression term and a tangential friction term. The compressional term acts along the unit vector, $\hat{n}_{ij}$, given by

$$\hat{n}_{ij} = \frac{\vec{r}_i - \vec{r}_j}{\|\vec{r}_i - \vec{r}_j\|} \tag{2.4}$$

with a magnitude given by the parameter κ. The frictional component acts along the tangential unit vector $\hat{t}_{ij}$ which is orthogonal to $\hat{n}_{ij}$, and is proportional to the

difference in tangential velocity given by

$$\Delta v_{ij}^t = (\vec{v}_i - \vec{v}_j) \cdot \hat{t}_{ij} \tag{2.5}$$

The magnitude of this sliding frictional term can be set using the parameter κ. Combining the social and physical forces together yields:

$$\vec{f}_{ij}^I = [\alpha^I e^{(-d_{ij}/\beta^I)} + \kappa^I g(d_{ij})]\hat{n}_{ij} - [\kappa^I g(d_{ij})\Delta v_{ij}^t]\hat{t}_{ij} \tag{2.6}$$

where the function $g(x)$ is zero if x is positive and returns $-x$ if x is negative, so that there is no contribution from the physical forces when people are not in contact.

The equation describing the interactions between a person and a wall has the same form as the social interactions between people, and is given by:

$$\vec{f}_{ik}^W = [\alpha^W e^{(-d_{ik}/\beta^W)} + \kappa^W g(d_{ik})]\hat{n}_{ik} - [\kappa^W g(d_{ik})\vec{v}_i.\hat{t}_{ik}]\hat{t}_{ik} \tag{2.7}$$

where d_{ik} is now the minimum distance separating individual i from the kth wall, $\hat{n}_{ik}$ is the unit vector along this minimum distance, and $\hat{t}_{ik}$ is perpendicular to $\hat{n}_{ik}$. Two pedestrian phenomena were described by these equations: Lane formation and door oscillation [22].

Here we can mention some of the current shortcomings of this model. First, the model has never been validated with the real world data or phenomena. According to many publications, the researchers of the social force model are more focused on the physical interactions to explain biological and physical behaviours rather than the real pedestrian traffic flow. The psychological factors in case of panic situation are never introduced. Second, this model cannot describe the behaviour of individuals like in reality and as a consequence, the result of many simulations are not realistic.

2.3.2 2D cellular automata

At the beginning the Cellular automaton (plural: cellular automata) model has been developed to simulate transportation and car traffics. In the last decade, there were many attempts using Cellular automata to simulate pedestrian dynamics [53, 54].

The model considers the pedestrians as entities (automata) in cells. The geometries where the pedestrians are moving are given as a regular grid of cells, each one in a finite number of states. The occupancy of a cell depends on the state in the neighbourhood cells. Time is also discrete, and the state of a cell at time t is a function of the states of a finite number of cells (called its neighbourhood) at time t - 1. These neighbours are a selection of cells relative to the specified cell,

and do not change (though the cell itself may be in its neighbourhood, it is not usually considered as a neighbour). Each cell has the same rule for its update, based on the values in its neighborhood [55, 56, 57].

However, this approach is limited to geometries, where the walking direction does not change. Therefore, it is not possible to simulate situations where movement is not from left to right but, e.g., towards an exit. To do this, the walking direction has to be determined taking into account external information like signage. Just recently Burstedde [55] has proposed a 2D Cellular Automaton model with different kinds of floor fields: a static (S) and a dynamic (D) one. The static floor field is a scalar field representing the distance to either the exit or the destination cells measured by a Manhattan metric, i.e., the number of steps across edges between this cell and the exit.

A more extensive description of this model can be found in [55]. One of the interesting results of this approach is its ability to reproduce lane formation without explicitly taking into account the interaction between persons. Therefore, lane formation can be found also in (spatially) discrete models. The static field S enables route choice, whereas D is modified by the pedestrians and introduces long-range interactions.

Burstedde et al's work is a $v_{max} = 1$ solution where particles may only move one cell per iteration/generation. Particles may move in 1 of 9 directions with probabilities denoted by M_{ij} (one direction is to stay put). Each particle may have its own local probability grid. If the target cell is occupied, the particle stays put.

One of the shortcoming of the Cellular Automaton model is that it does not reflect the real behaviour of the pedestrians. Through the cellular based model the behaviour of pedestrians seems rough visually and cannot be identified. The pedestrian gives the impression of jumping from one cell to another. Blue and Adler (2000) [54] till this moment don't give an excellent idea on validation of the microscopic model using the existing model fundamental diagram.

2.3.3 Microscopic swarm model

The microscopic swarm model called also Flocking Model was introduced by Craig W. Reynolds [3]. The technique to simulate animal flocking, sets the stage for further studies of crowd simulation. Each agent in the simulation is called a "boid". A complex crowd behaviour can be achieved through individual agents following simple rules.

Compared with human movement in specific situations, swarms can have the same properties of crowds. The microscopic swarm model represents the detailed

Figure 2.1: Swarm.

interaction of agents to control their movement in any agent arena. The microscopic swarm model is a mathematical model where every agent has three variables of force. The development of this model was inspired by the escape panic model [19, 58, 59, 60], the bird flocking behavioural model [3] and the pedestrian traffic model [61]. The model and simulation is designed to capture the individual swarm member and is able to record its movement characteristics.

- The microscopic swarm model and simulation is a physical force based model similar to the social force model with forward and repulsion forces as the main force driver [60].
- This model allows any collision by giving an additional radius to the agents and a repulsive force assignment when two of the radii collide.
- The developed model uses mass parameters beside force variables that can be measured.
- The collision avoidance algorithm is influenced by the Reynolds steering behaviour model [62, 63].

2.4 Macroscopic model

In macroscopic models the pedestrian behaviour is considered by a continuum approach, where the movement of large crowds exhibits many of the properties of fluid motion. Therefore the crowd behaviour is treated as a fluid. In this concept detailed interactions are overlooked and the model's characteristics are shifted toward parameters such as flow rate $f(\rho)$, concentration ρ (also known as traffic density), and average speed $\bar{v}$, all being functions of 2-D space (x, y) and time (t). This class of model uses hyperbolic partial differential equations. The idea to model the pedestrian behaviour like a fluid was first introduced by (Fruin, 1971a,b [8, 9]) and adopted by (Bord, 1985 [10]), where macroscopic models where developed using (a) fluid dynamics theory, (b) continuum mechanics (Navier-Stokes equations). The shortcomings of this way to understand complex crowd phenomena is due to the assumption that pedestrians behave similar to fluids, which cannot explain all kinds of crowd behaviours. The pedestrians-pedestrians and pedestrians-obstacles interactions will not be recognized by macroscopic models. Macroscopic models don't pay attention to individuals, rather they treat the entire pedestrian flow. This approach is well suited for understanding the rules governing the global behaviour of pedestrian flow for which individual characteristics are not that important.

2.5 Hybrid model: Discrete and continuous crowds

The Hybrid Model was developed by Narain et al. [64] and inspired by microscopic and macroscopic models. In local behaviour the model can be referred to the concept of [28, 19] and other microscopic approaches. Considering the global behaviour of pedestrian flow the model was close to the fluid dynamics models using a continuum theory to model pedestrians behaviour [65, 26]. This approach is considered to be a new way to model high density pedestrian behaviour, using agents which are discrete and a single system which is continuous. According to the developer of this model, it can deal with the simulation of dense crowds containing up to thousands of pedestrians (also called agents) which are unidirectionally incompressible and result in dense scenarios which an acceleration of inter-agent collision avoidance.

Inspired by the previous works on continuum models for medium-density crowds [65, 26], it has been noted that crowds at high density show behaviour similar to granular flows [66] where the individual movements are restricted by the nearby surroundings.

The main idea of this approach is to consider the microscopic or discrete

aspect of each individual and the macroscopic properties of the entire pedestrian flow within low, and more interesting in high density, crowds through Lagrangian representation of individuals with a coarser Eulerian crowd model. In case of high density crowds the particles or agents which become incompressible, that means the avoidance forces between the agents rise when the agents are close together, whereas in free movement the particles are compressible. This model proposes a new mathematical formulation to better understand and illustrate the crowd behaviour recognition.

2.6 Some empirical data

Meso, Macro and Micro Models, all need empirical data. Some of most important previous measurements in crowd dynamics are the experiments performed by Predtetschenski and Milinski in Russia (russ: 1969, germ: 1971) [1]. Up to this moment, there is a serious deficiency in empirical data regarding crowd dynamics, especially crowd panic. Therefore we have analysed video recordings of the Tawaf in Mecca during the Hajj 2009. Numerous methods for extracting pedestrian data to analyse the microscopic pedestrian flow have been developed, but all these tools are still in their preliminary stage. Many methods were developed to help in pedestrian data collection for example manual, semi-automated and automated image processing. All obtained data must be integrated into crowd management systems. The microscopic data collection obtained through analysing a set of video recording and the microscopic pedestrian simulation model create a database called "Pedestrian GUI database" see (chapter:3). This data is used to describe the behaviour of individual pedestrians in the microscopic regime. The validation of the simulation tools is achieved through the comparison between average instantaneous speed distributions of the real world with the result of the simulations.

Image processing is a well known method used to extract data from digitized images. This method is applied in different ways in many science areas, for example in modern sciences and technologies, environments surveillance, building security, events and traffic in order to maintain safety and order. This method requires a combination of movement detection and tracking to determine the behaviour of pedestrians in scenes, followed by analysis in locating suspicious behaviour. This issue will be detailed in chapter: 4.

Monitoring natural pedestrian flow movement by implementation of the photographic method, one can determine a characteristic part of the flow. As we can see in figure 2.4 the camera must be placed in the center of the observed area or sector and perpendicular to the axis of vision. The observations are done during

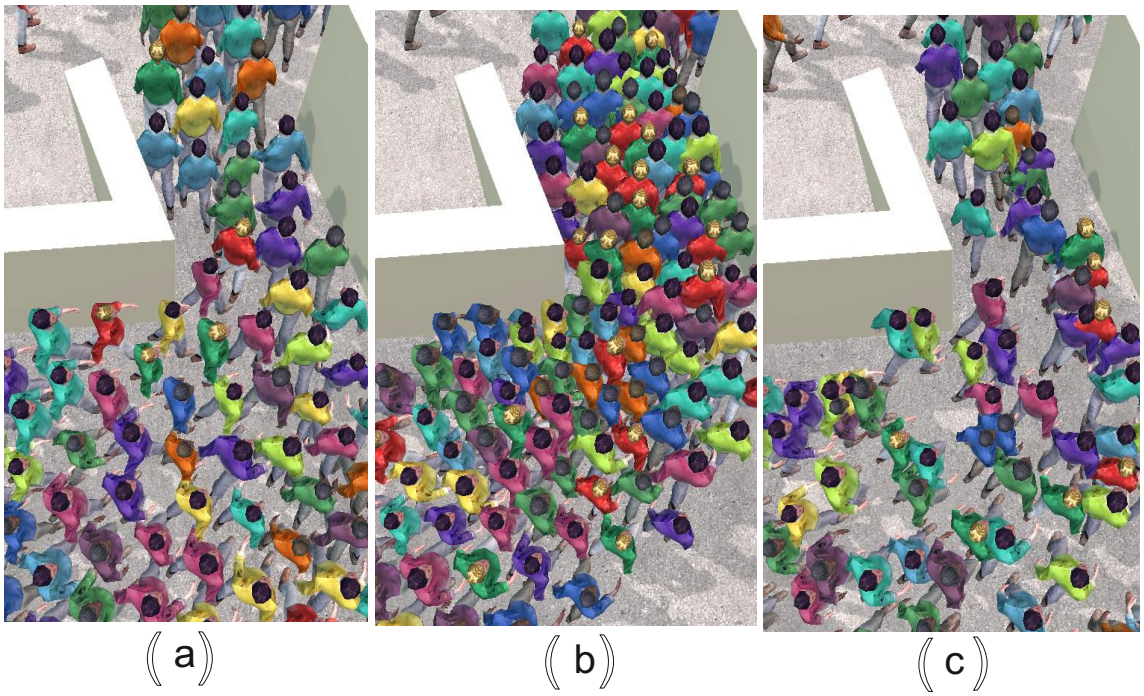

Figure 2.2: Bottleneck simulation results using the hybrid model. Time snapshots of agents attempting to exit through a narrow doorway, (a) with both the unilateral incompressibility constraint (UIC) projection and pairwise collision resolution, (b) without UIC, (c) without collision resolution [64]. If all pedestrians converge to the same exit at the same time, the passage will be blocked after a short time. Note that the pedestrians blocking each other are causing so called arc formation, (see fig. 2.12).

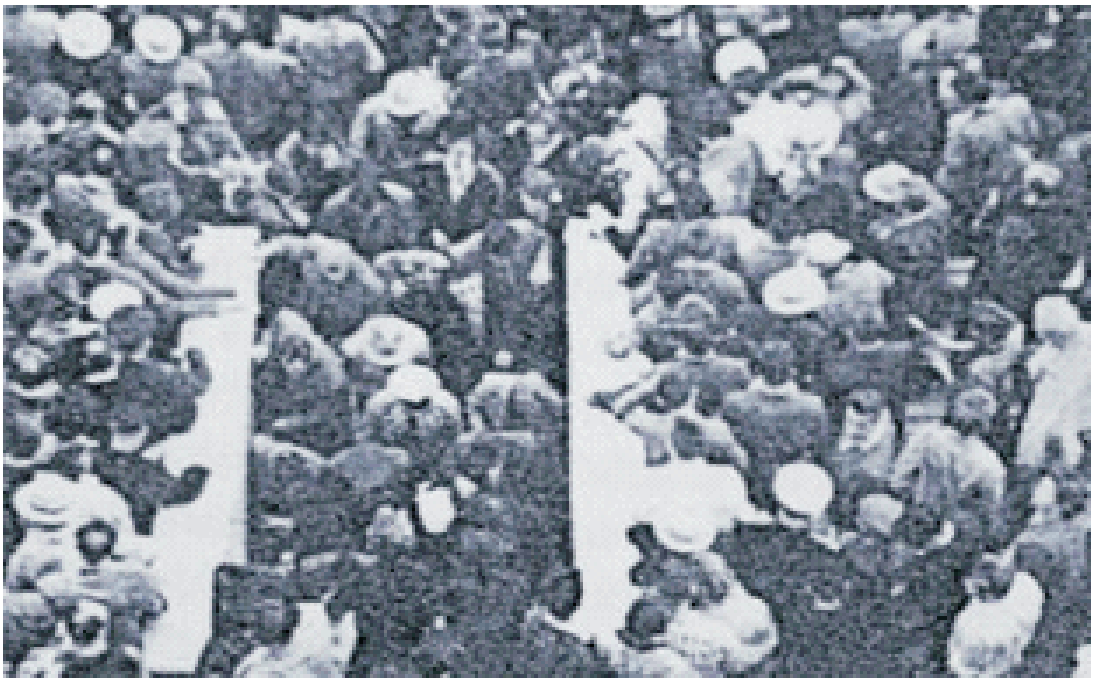

Figure 2.3: Observation of crowd movements; Top view.

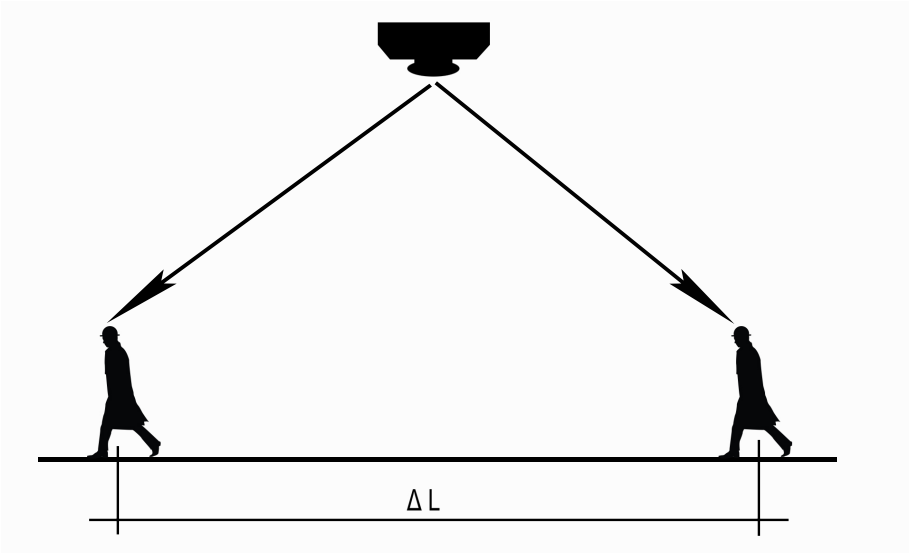

Figure 2.4: Scheme for pedestrian observation with help of photos and filming.

defined time intervals. If the parameters of the hallway are known (the width and length of the observed sector), it is possible to calculate the intensity and the density of the pedestrian flow at a specific time. With help of this type of observation, the density of flow can be determined at any time, especially at the rush hours.

Typical measures used in the literature for the pedestrian flow are:

- Given a number of pedestrians N_p walking at time t through a corridor with width b and length l, a density of the form

$$\rho(t) = \frac{N_p}{bl}; [1/m^2] \tag{2.8}$$

  expressed in persons per unit area can be defined.

- Its inverse, i.e. the value

$$g(t) = \frac{bl}{N_p}; [m^2] \tag{2.9}$$

  expressed in square meters per person describes the space of the corridor available for one person.

- The fraction of the ground area occupied by all persons can be calculated with

$$\gamma(t) = \frac{\sum A_p}{bl}; [m^2\, m^{-2}] \tag{2.10}$$

  if the sum of the perpendicular projections of the individual body areas A_p on the ground, (see figures 2.4 and 2.5) is known, where $\sum A_p = N_p A_p\ [m^2]$.

Since the area A_p occupied by one person depends on its state of motion, the values of the quantities defined here will differ for moving or stationary pedestrians.

2.6.1 Physical parameters

The crowd behaviour is a very complex system driven by the individual decisions of agents with respect to their aims and destinations, environmental obstacles, and other surrounding circumstances. These physical parameters have a significant impact on the behaviour of the crowd in the case of an emergency. For accuracy and more realistic simulation, the physical factor must be considered in the input of the simulation. The size of the particle can be a determining factor in the reliability of the simulation results.

The parameters of a pedestrian flow and crowd density depend on the number of the persons composing the crowd. The measurements of the persons depend on their physical values, their age, and their clothes. Critical or dangerous

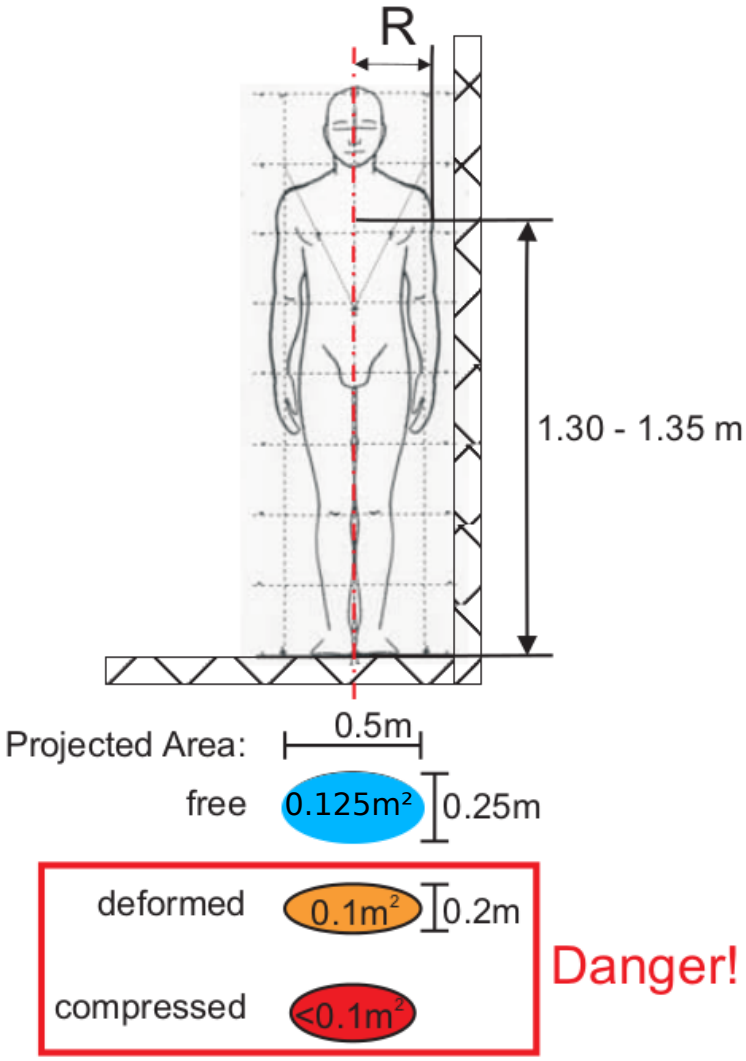

Figure 2.5: Projected area: Pedestrian Area Module (PAM), i.e. the surface A occupied by a pedestrian, is used as a more manageable unit [m^2]. The PAM occupied by a motionless pedestrian can be calculated considering an elliptical or a rectangular form. According to Predtetschenski and Milinski [1], the average surface occupied by a motionless pedestrian is $A_0 = w_0 \cdot d_0$, where w_0 and d_0 are the average lateral width and depth of a human body taken in the height of the human shoulder (approximately 1.30 m above the ground) and measured not less than 0.6 m. When a pedestrian is walking, a greater surface is required, that is, $A = w \cdot d$. Both the terms w and d can be expressed as a function of the walking velocity v. In addition, the lateral width could be made sensitive to the deck acceleration, since pedestrians tend to walk with their legs more widespread when the surface is laterally moving, as stressed by various authors (e.g. [67]).

situations are demonstrated by the red frame, (see fig. 2.5), in this area the individual's body will be pressed or deformed; detailed studies are shown in the section (2.10), Pressure Forces.

Type of Person	Projected area (m^2)
Children	0.04 – 0.06
Adolescent	0.06 – 0.09
Grown-up in summer clothes	0.100
Grown-up in inter season	0.113
Grown-up in winter clothes	0.125
Grown-up in inter season clothes with briefcase	0.180
Grown-up in inter season clothes with light luggage	0.240
Grown-up in inter season clothes with heavy luggage	0.390

Table 2.1: Set of different individual projected areas [1].

The table 2.1 shows the projected area for different types of pedestrians. Many measurements on persons with different ages and different clothes were made and the average values demonstrated in this table. The area of the individuals corresponded to the area of the individual's breast (thorax) height. For more realistic crowd simulation, the differences in human body area between all individuals or pedestrians in crowd must be considered and implemented with the correct percentage. For example, sports arenas or pop music concerts concern mostly young fans and people. In the pilgrimage places, people are usually adults or older people.

2.6.2 Corridor experiment

The movement in pedestrian streams includes faster and slower persons. This behaviour forms the typical tail and front parts of a stream.

The observation shows us that in pedestrian flow over long distances, the front and the end parts of the stream are composed of fewer pedestrians, and they move with a higher or lower speed than the main part of the crowd. We can deduce from this experiment that the pedestrian density in the center of stream is bigger than at the edges, (see fig. 2.6). The distribution of pedestrians in the flow is often irregular and has a random character. The distance between the pedestrian changes all the time. Consequently, the local densities are changed permanently in the walkway. This observation has a significant impact on the validation of our simulation tools.

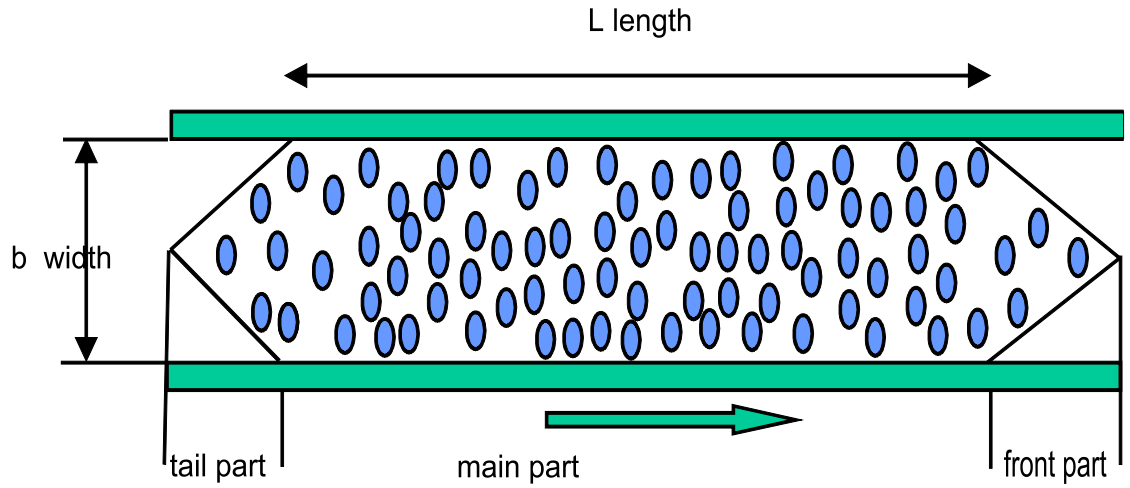

Figure 2.6: Statistical studies. The picture shows a pedestrian stream walking through a hallway. The front part consists of the fastest pedestrians, where the tail part summarizes the slowest walking pedestrians. The main part, which is the largest amount of pedestrians, has a velocity distribution which is between the maximum (front part) and minimum (tail part) velocity.

Type of movement	Walking speed (m/s)
Leisurely stroll	0.6 - 0.8
Walk	0.8 - 1.0
Jog	1.0 - 3.0
Run	3.0 -10.0

Table 2.2: Some collected walking speeds for different types of human movement, [68, 69, 70].

The desired speed of individuals can take different values within expanded borders. The maximum registered speed of humans is around 600 m/min (running 100 m in distance cf. fig. 2.7); The walking speed can be 220 m/min (reached when sport walking over 20 km). Under normal conditions the average speed of humans (excluding athletes) is approximately 60 m/min, in special cases the walking speed can reach 120 to 140 m/min.

The individual's speed fluctuations depend on many factors, which can be very difficult to determine through very complex calculations. Here the age and physical data of humans has a significant impact on their movements, as well as other diverse circumstances. Also, the psychological states of the individuals has a great impact on their movement at a given moment. Therefore, in order to estimate walking speeds, it is inevitable to use sampled data. The statistical method used for sampling the data has to reproduce the correct distribution of walking speeds for a given pedestrian crowd. Important parameters of the crowd

Figure 2.7: Usain Bolt is a Jamaican sprinter widely regarded as the fastest person ever. His 2009 record breaking margin for 100 m, from 9.69 seconds (his own previous world record) to 9.58, is the highest since the start of fully automatic time measurements. His average speed was 10.43 m/s corresponding to 37.54 km/h, [71].

dynamics are the speed of the individuals and the local crowd density, which are related to each other. For high crowd density, the pedestrian movements are much slower, see fundamental diagram figure 2.8.

2.6.3 Fundamental diagram

The density results from the number of pedestrians within a given area. The speed of the pedestrians depends on the density of the pedestrian crowd. However, the intensity resulting from pedestrian movement is not linear with the area occupied by the pedestrians, and it is very hard to predict the capacity for a not yet built environment.

The crowd's speed is a dynamic three-dimensional function [72]. It defines the average speed of individuals located within unit area of floor space at given time t and location $\vec{r} = (x, y)$. The expected number of these individuals is the pedestrian density, written as $\rho(\vec{r}, t)$. The chosen speed and moving direction of these individuals, i.e. the expected velocity is written as $\vec{v}(x, y, t)$. The crowd's speed is subject to the density. The speed monotonically decreases from a "preferred speed" down to zero with the density varying from zero to a present maximum value. The pedestrian flow depends on the physical quantities that are directly connected with the parameters governing the pedestrian movement. It describes the number of pedestrian crossing through a walkway with the width b in a time unit, $\vec{Q}(\vec{r}, t) = \rho(\vec{r}, t)\vec{v}(\vec{r}, t)b$ in [m^2 s^{-1}]. The intensity $\vec{q}$, also called average local flow, $\vec{q}(\vec{r}, t) = \rho(\vec{r}, t)\vec{v}(\vec{r}, t)$ is expressed as a function of the local density $\rho(\vec{r}, t)$ and corresponds to the passage flow of a walkway with width of 1 m. With a certain density reached, $\vec{q}$ reaches a maximum and afterwards falls again, (see fig. 2.8). From this follows that traffic routes, openings and closed areas have a maximal (effective) flow-rates, which is determined by the density $\rho(\vec{r}, t)$ at q_{max}.

2.6.4 Different conditions

The actual walking speeds of the individuals are a results of a list of circumstances and surrounding conditions and depend on the traffic flow characteristics, moreover the free walking speed is influenced by the environmental weather conditions and the fitness condition of a single individual. The effects of the geography and terrain condition on walking speeds are unknown, although from observing pedestrians in real-life or pedestrian motion experiments it can be expected that the elderly would be affected more when walking up or down a grade than the younger. Similarly, it can be expected that old persons would react more strongly to dangerous situations. The figure 2.10 show that the closer the approaching the

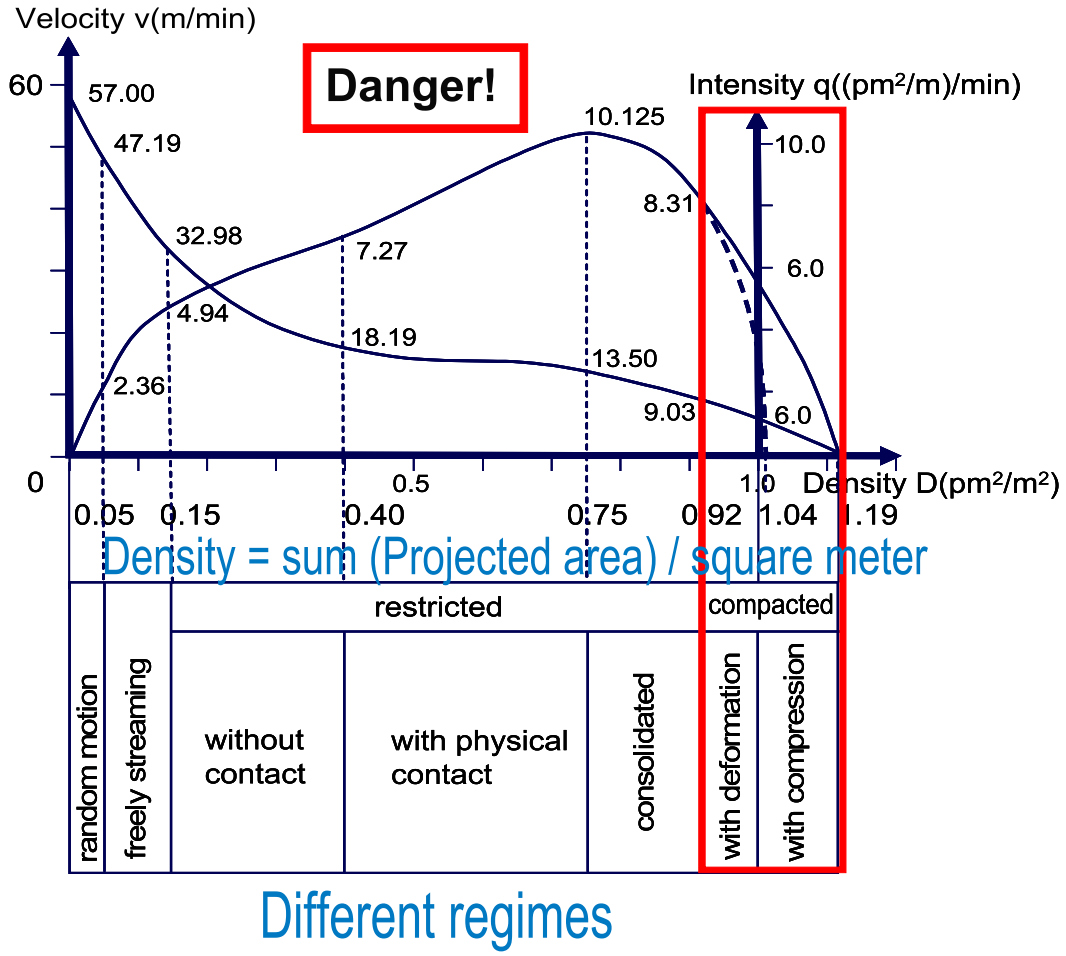

Figure 2.8: Velocity-density diagram: Empirical relation between density (person projected area per square meter pm^2/m^2) and velocity according to Predtetschenski and Milinski [1]. The partition refers to domains with qualitatively different decrease of the velocity. The red rectangle indicates a dangerous area in this curve, where the pedestrian density reaches high values with more than 6 persons/m^2. In this range bodies will be pressed or deformed, resulting in high injury scales with possible fatal consequences.

danger, the faster the mean walking speed of the pedestrians. Finally, the pedestrian speed on pavements, crossways and closed areas is strongly related to the number of pedestrians in the flow. The relationship between speed, flow, and space occupied (i.e. density) for a representative population group has been examined by Predtetschenski and Milinski (russ: 1969, germ: 1971) and others, cf. figures 2.8, 2.10, 2.11 and 2.9.

The walking speed and density of pedestrian flows under different conditions was measured nearly 3600 times [1]. The results of the previous measurement data show that the pedestrians walking speeds are a function of the local densities and the kind of walkway (horizontal, bent, stairs....). Figure2.9 illustrates the results of 360 measurements of pedestrian walking speeds upstairs. The solid curve show the average walking speed.

In figure 2.10, the variation of the walking speed in a horizontal corridor for different types of movements in different (relaxed, normal and dangerous) conditions is illustrated. From the graph we can deduce that in the case of a high density crowd, the average walking speed in all conditions is not to much different.

The maximum q_{max} of the flow rate depends on kind of walkway, as can be seen from figure2.11. From this, the important conclusion follows that horizontal and bent traffic routes just like narrow openings, have both limit or edge flows, which are determined by the density of the values of q_{max}. The values of the intensity of motion correspond to the values of flow rate in a passage with wideness of 1 m.

2.6.5 Bottleneck and arc formation

According to many investigations [73] analyzing a number of crowd disasters shows that: The arc formation and exit congestion occur when all persons run to the nearest exits. In short time the exit will be blocked, the critical capacity of the egress is temporarily exceeded but intensive pressure to use this doorway continues. Usually, to escape a dangerous situation the crowd continues to press ahead because it has no idea of what the conditions are at the bottleneck. The leaning force built by the crowd pressures and acting on the persons from behind at the bottleneck become so huge that it is impossible to resist.

Analysis of more than a dozen serious crowd incidents has shown that in many cases the geometry plan of the buildings, especially the exit area, have played a critical role in the crowd disaster. Pedestrian movement through openings and bottlenecks has turned out until now as a complicated process that must be seriously studied, because dangerous situations have occurred in these crit-

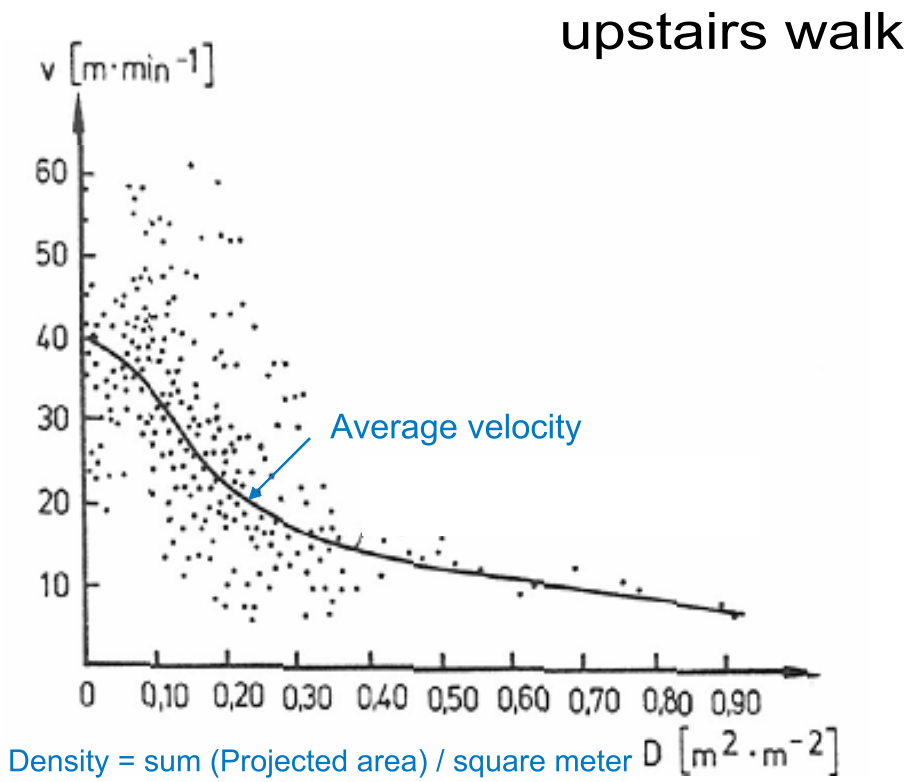

Figure 2.9: Results of practical measurements on walking speed when going up stairs. The solid line indicates the average walking velocity [1].

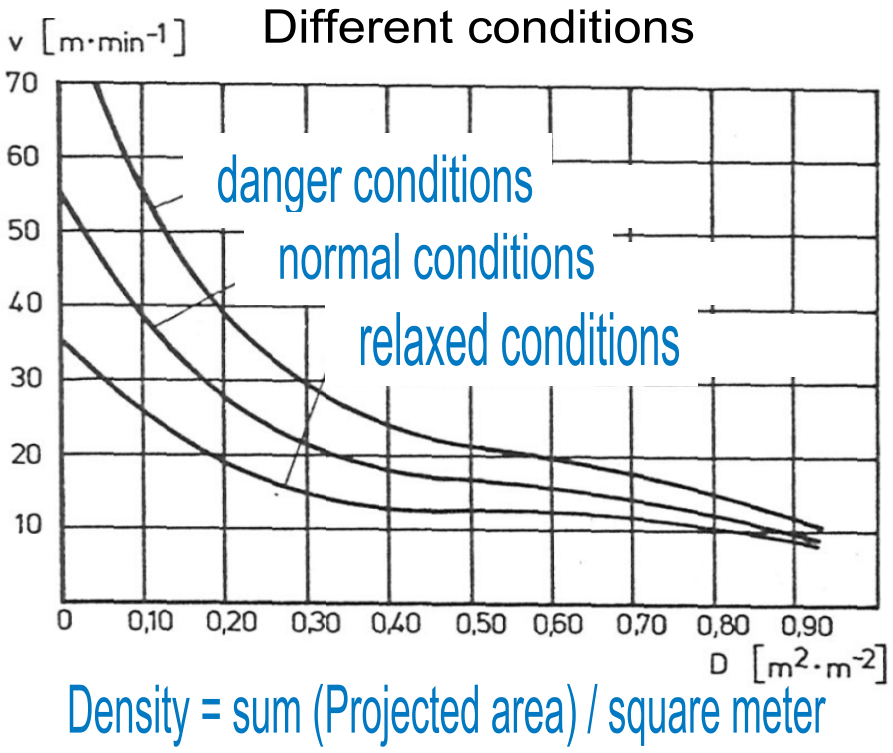

Figure 2.10: Walking speed in a horizontal corridor as a function of density under different conditions. The velocity-density relation differs for various facilities like stairs, ramps, bottlenecks or hallways. Moreover, one has to distinguish between uni- and bidirectional streams. The general situation of pedestrians (normal or dangerous conditions) has a significant impact on this diagram, there are a several effects which can be considered to influence the dependency (see chapter 3.1). [1].

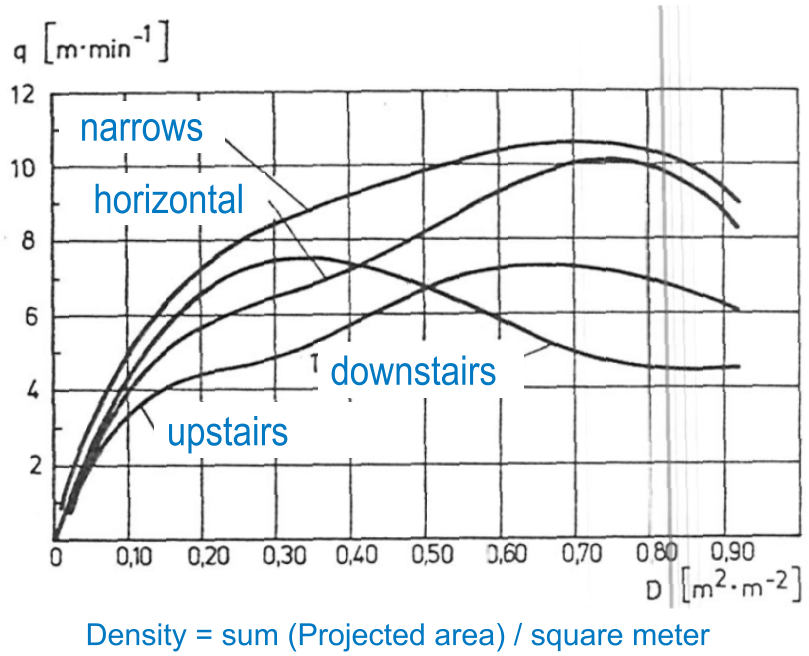

Figure 2.11: Relationship between the flow intensity and the pedestrian density under different conditions. This picture illustrates the average of the local flows $\vec{q}(\vec{r},t) = \rho(\vec{r},t)\vec{v}(\vec{r},t)$ as a function of the local density $\rho(\vec{r},t)$ [1].

ical places. In a crowded environment, it has been observed that most victims were injured or killed by the so called non-controlled behaviours of the crowd, rather than the actual cause (such as fire) of the disaster. Non-controlled crowd behaviours refer to the destructive actions that a crowd may experience during a disaster, such as: stampedes, pushing others out of the way, knocking others down, trampling on others, etc. These actions are responsible for large numbers of injuries and even deaths in crowd disasters. From many observations and a large experience in crowd catastrophes, we can deduce that the most dangerous situation occurs at the exits and bottlenecks of buildings. If an arc is built around any opening, this will be closed and no-one can escape. After a short time, the density around this place increases dramatically. As we can see in figure 2.12 the pedestrians block one another in the direction of the movement which lead to injury situations and body deformation. From this situation an enormous pushing force arises. If the force appears to be towards our desired movement, we cannot decrease its intensity by not moving forward, and therefore no reaction is possible. This method succeeds in reducing shaking behaviour, while still allowing body contact and thus pushing behaviour. Since stopping rules do not apply when the individual is being pushed forward, this achieves the desired emergent result of people appearing to be pushed through doorways when there is a high-density crowd behind them.

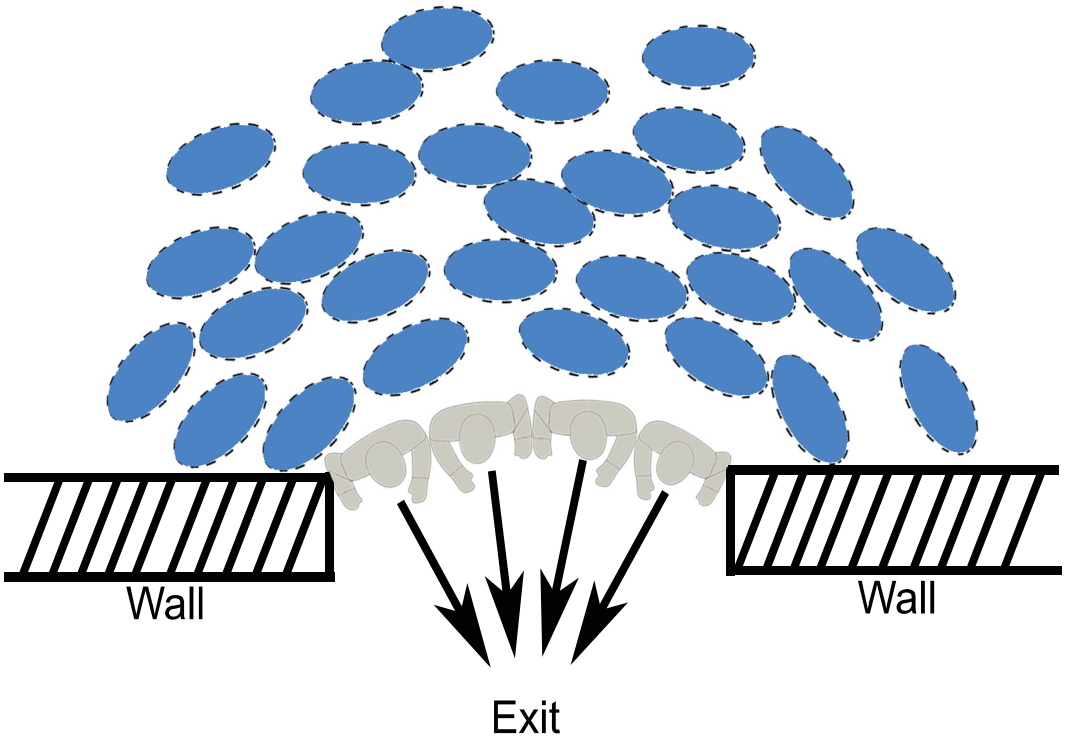

Figure 2.12: Scheme of an arc formation at openings and bottleneck areas. The full ellipses represent pedestrians moving in the same directions. The pedestrians block one another in the direction of the movement and congest the passage area.

2.6.6 Different fundamental diagrams

In the last decades many researches investigated the pedestrian motion from different point of views. Many experiments have been realized of pedestrian velocity in dependency of the environmental characteristics. And many methods have been developed to extract empirical data concerning the pedestrian motion in different conditions. From the comparison of many fundamental diagrams, (see fig. 2.14), we can deduce that there is no big deviation between PM [1], Weidmann [74] and Fruin [9]. The differences are clearly illustrated by the high density values. One can see that the Weidmann fundamental diagram go to zero at the density of 5.4 pedestrians/m^2, however in the Predtechenski and Milinski fundamental diagram the density can achieve 10 pedestrians/m^2. The different initial velocities depend on the fitness level of the walker. Helbing who analysed the crush accident in the Jamarat Bridge in Saudi Arabia 2006 found a density of 9 to 11 pedestrians/m^2 [5]. My own observation of the pilgrims movement in the Mataf area in Hajj 2009, showed that in specific places near the Kaaba of the Mataf area next to the Blackstone, the density is higher than 8 pedestrians/m^2, (see fig. 4.9). Near the Kaaba wall the movement is embedded, and the movement of the pilgrims is greatly restricted due to the extremely high density. The empirical and experimental data concerning the walking behaviour of individuals, is still not complete. This section has illustrate a few investigations of the fundamental walking process by individuals and some properties of the pedestrian flow.

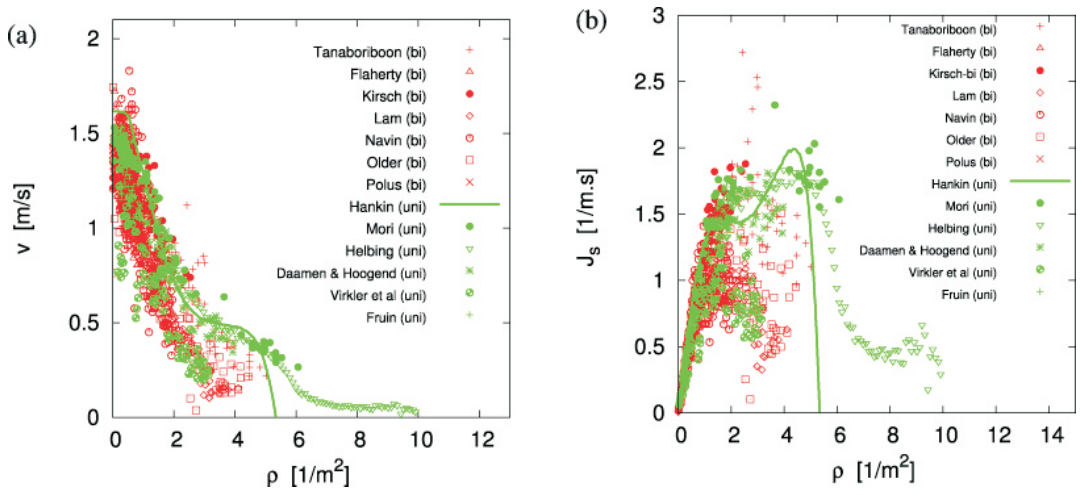

Figure 2.14: (a) Velocity-density fundamental diagrams results from many experiments concerning uni- and bidirectional pedestrian flow and (b) density–intensity diagrams [75].

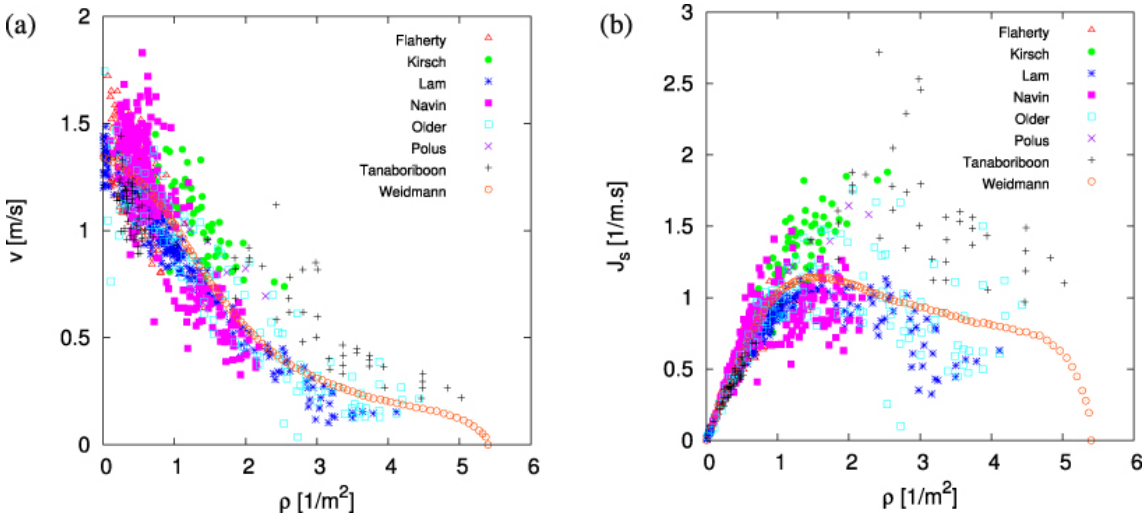

Figure 2.13: (a) Weidmann fundamental diagram in comparison with other diagrams (b) density–intensity diagrams [75].

2.7 Pedestrian forces and motion (in PedFlow)

PedFlow is a microscopic simulation model developed by Löhner Simulation Technologies International, Inc. (LSTI) [21]. In this model individuals are treated as self-driven particles that interact through social and physical rules. Each person in the pedestrian flow has a desired position and desired velocity and adapts his or her current velocity according to the surrounding neighbour; furthermore, each crowd member simultaneously tries to avoid collision with other crowd members and any environmental boundaries. The current velocity and direction of a single individual in the crowd is a result of the circumstances and social interactions. These social forces can be influenced by the environment, other people and internal states.

Force plays an essential role in every crowd model. It can be classified in two major categories, internal and external forces. Forces are characteristics of crowds and crowd disasters. Force has a direct effect on movement: for example force drives people out of rest to their desired velocities, or force can make deviate people from their desired direction. In dangerous crowd situations, force can be the key to decode the fatal consequences (e.g. injuries and death). Many force effects are summarized and documented by Fruin [76].

In this approach the pedestrians are treated as "particles" moving according to Newton's law:

$$m_p \frac{d\vec{v}}{dt} = \vec{f}, \quad \frac{d\vec{r}}{dt} = \vec{v} \tag{2.11}$$

Here m_p, $\vec{v}$ and $\vec{r}$ denote the mass, velocity and position of the pedestrian, and $\vec{f}$

the sum of all forces exerted by it or acting on it. The basic unknown that requires intensive modelling efforts in these equation is the force-vector. In the sequel, we will discuss the main forces that can be identified acting on a pedestrian.

m_p: Pedestrian mass.
$\vec{v}$: Velocity.
θ: Direction.
$\vec{r}$: Position.
$\vec{f}$: Sum of all forces.
R: Characteristic radius.
$Area$: Meaning the pedestrian projected area on the ground.

2.7.1 PedFlow force models

In the PedFlow model, the forces that accelerate a pedestrian are the result of internal (will) and external (collision, signals, etc.) forces. An "individual alert" tries to avoid collisions before they happen, resulting in vanishing external forces. However, if the pedestrian density increases, collision forces will appear, and the ability to move freely will be impaired. The difference between external and internal forces is too rigorous and only serves descriptive purposes in the present context. So, what are the forces that act on the pedestrian?

- Internal forces (active, intentional)
  - Will force (get there in time)
  - Pedestrian collision avoidance forces
  - Wall/Obstacle collision avoidance forces
- External forces (passive, suffered)
  - Physical pedestrians collision forces (physical contact)
  - Physical wall/obstacle collision forces (physical contact)

2.7.2 General description of will force

Each particle is programmed to have a final goal that it wants to reach. The motivation to move towards this goal is given by the driving force, or so called will force $\vec{f}_{will}$ and denotes the self-driven force that drives an individual towards their desired velocity, (see fig. 2.16). The self-driven force is based on a simple error correction term consisting of the difference between an individuals desired velocity, and a desired direction $\vec{z}$, and their actual velocity. This difference in velocity is corrected over a specified time interval τ, referred to as the relaxation

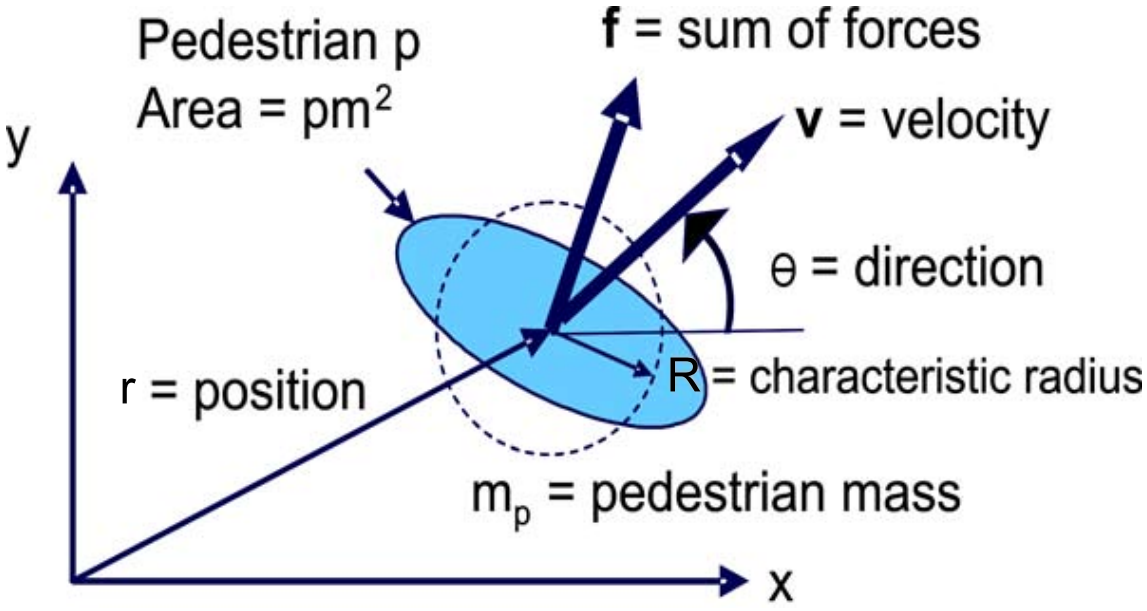

Figure 2.15: Newtonian dynamic representation of a pedestrian "particle".

time, that corresponds to the finite amount of time that is required for people to react and physically change their velocity.

In the following, we denote by will force the force that will accelerate (or decelerate) a pedestrian to achieve the velocity it desires. Given a desired velocity $\vec{v}_d$ and the current velocity $\vec{v}$, this force will be of the form

$$\vec{f}_{will} = g_w(\vec{v}_d - \vec{v}), \tag{2.12}$$

where $g_w = f(\tau)$ is a function of "list of circumstances"

The modeling aspect is included in the function g_w, which in the non-linear case may itself be a function of $\vec{v}_d - \vec{v}$. Suppose g_w is constant, and that only the will force is acting. Furthermore, consider a pedestrian at rest. The pedestrian could start from rest $\vec{v}_0 = 0$ and wants to reach the desired velocity $\vec{v}_d$. In this case, we have: $\vec{f}_{will} = g_w(\vec{v}_d - \vec{v})$, with $\vec{v}(0) = 0$ we have $m_p \frac{d\vec{v}}{dt} = \vec{f}_{will} = g_w(\vec{v}_d - \vec{v})$. The solution of this equation is given by $\vec{v}(t) = \vec{v}_d(1 - e^{-\alpha t})$ with $\frac{d\vec{v}}{dt}(0) = \vec{v}_d\alpha = \vec{v}_d/\tau$ and $\alpha = g_w/m_p = 1/\tau$ We can thus obtain g_w by measuring the time required to reach a percentage (e.g. 90 percent) of the desired velocity, starting from rest, (see fig. 2.17). This time is typically in the range of 0.5 - 1.0 s, but obviously depends on the current state of fitness, stress, climate and terrain condition, and desire to reach a goal. We can define the function $g_w = m_p/\tau$ via "relaxation time" $0.5 < \tau < 1.0$ s. Typical values for the desired velocity $\vec{v}_d$ and relaxation time τ are v_d = 1.35 m/s and τ = O(0.5 to 1.0 s). Medicinal facts and human experience show that older pedestrians walk more slowly than younger pedestrians. This effect

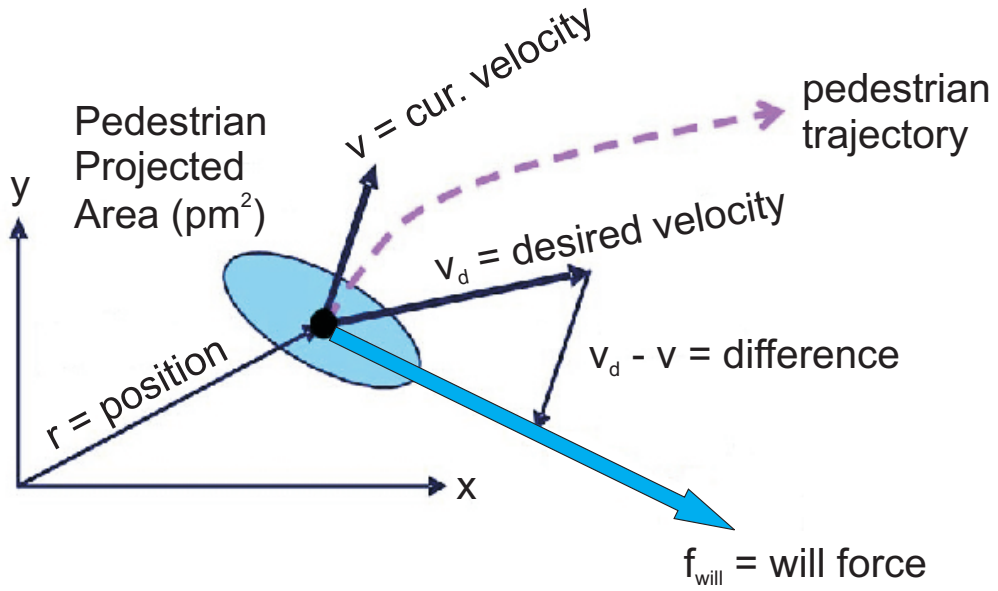

Figure 2.16: The will force $\vec{f}_{will}$ denotes the self-driven force that drives an individual towards their desired velocity.

has a significant impact on the "relaxation time" of a single pedestrian, hence it is easier to assess that younger pedestrians reach their desired velocity faster than older pedestrians.

2.8 Internal forces

2.8.1 Desired direction $\vec{z}$

The desired direction $\vec{z}$ will be considered as the direction of the desired velocity $\vec{v}_d$ of the pedestrian, (See fig. 2.18),

$$\vec{z} = \frac{\vec{v}_d}{|\vec{v}_d|} \tag{2.13}$$

The magnitude of the desired velocity $|\vec{v}_d|$ depends on the fitness of the pedestrian and the motivation/urgency to reach a certain place.

The desired direction of the individuals will be affected by the neighbourhood surrounding at any time and will depend on the type of crowd and the cases considered. All particles in the system have a desired position called the point of interest, if it is possible to reach this desired position in a short time depends on the list of circumstances.

- Without any obstacle and by free movement the desired direction $\vec{z}$ take the direction of the desired position. A single individual has a desired position

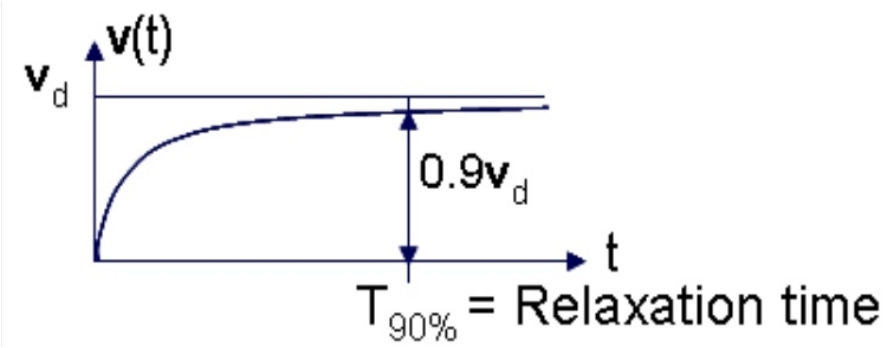

Figure 2.17: Speed-up of an isolated particle to the desired velocity. This difference in velocity is corrected over a specified time interval τ , which is referred to as the relaxation time, that corresponds to the finite amount of time that is required for people to react and physically change their velocity.

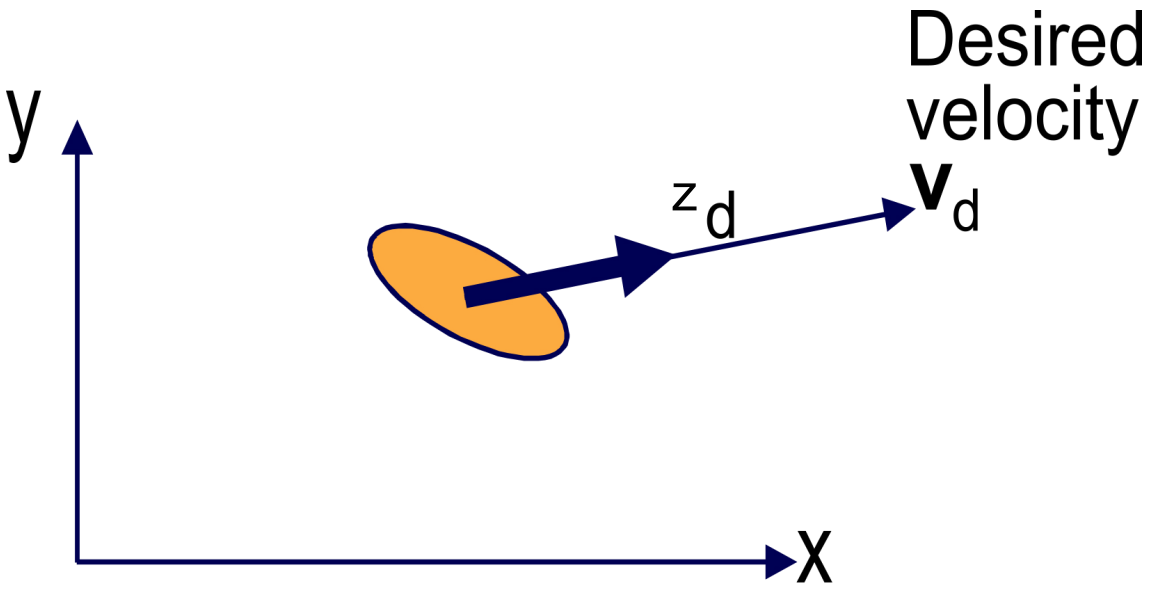

Figure 2.18: Desired direction $\vec{z}$ in dependency of desired velocity.

$\vec{r}_d(t_d)$ as goal, that one would like to reach at a certain time t_d. If there are no time constraints, t_d is simply set to a large number. Given the current position $\vec{r} = (x, y)$, the direction of the velocity is given by

$$\vec{z}_d(t) = \frac{(\vec{r}_d(t_d) - \vec{r})}{|\vec{r}_d(t_d) - \vec{r}|}. \tag{2.14}$$

We denote that $\vec{r}_d(t_d)$ is the individual's desired position reached at desired time t_d (or more) and $\vec{r}(t)$ is the current position, (see fig. 2.19).

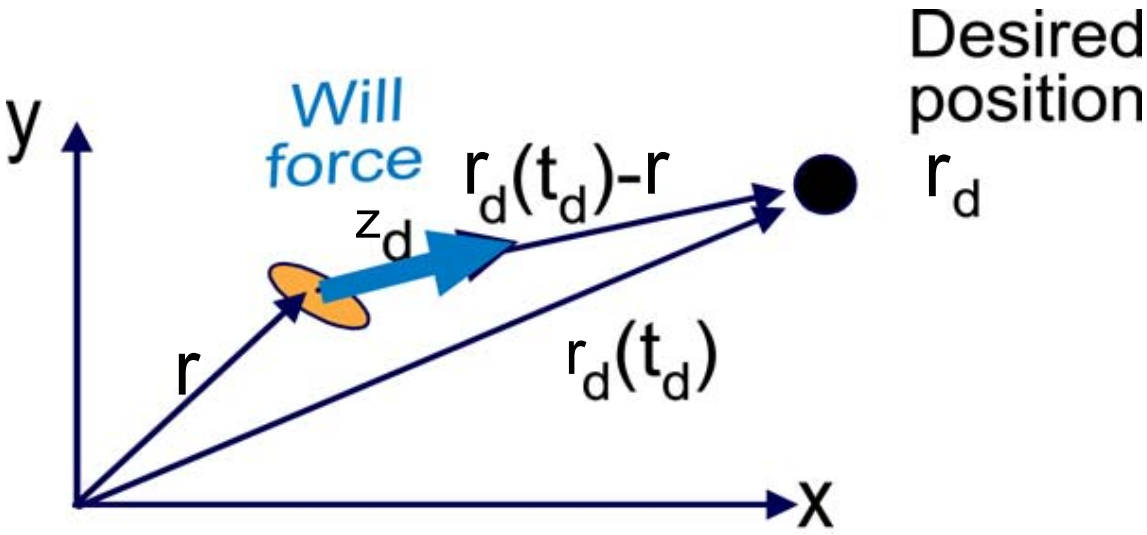

Figure 2.19: Desired position r_d in dependency of the neighbouring situation. This picture illustrates the particle's desired position according to the instantaneous environmental circumstances.

- For members of groups, the goal is always to stay close to the leader. Thus

$$\vec{r}_d(t_d) = \vec{r}_g(t_g) \tag{2.15}$$

becomes the position of the leader, with $\vec{r}_g(t)$ being the group leader position. In this case the desired direction $\vec{z}$ in dependency of group leader position. The blue thick arrow indicates the desired direction of a group member, (see fig. 2.22).

- In the case of an evacuation simulation, the direction is given by gradient of the distance function, d_e, to the closest perceived exit: (see fig. 2.20).

$$\vec{z}(t) = -\frac{\nabla d_e}{|\nabla d_e|} \tag{2.16}$$

$d_e(x, y)$ denotes the distance function to the closest exit and $\nabla d_e(x, y)$ refers to the gradient.

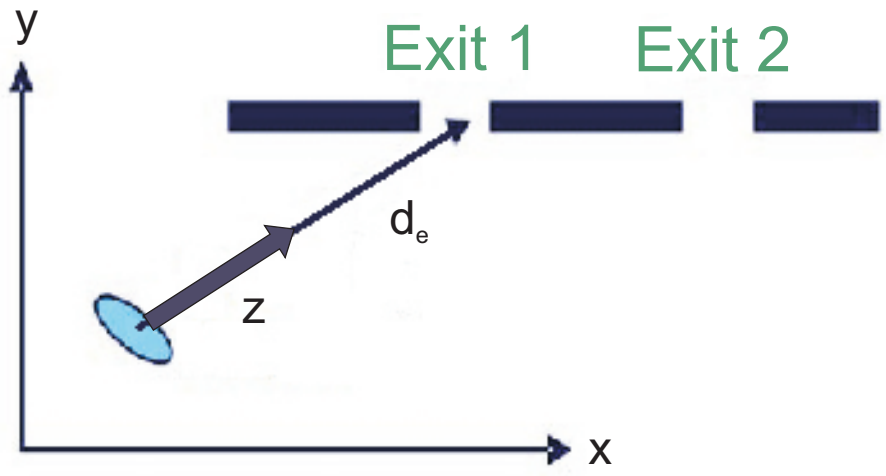

Figure 2.20: Desired direction $\vec{z}$ in dependency of distance to the closest exit. This picture illustrates the particle's desired direction in case of emergency or evacuation.

2.8.2 Internal forces –far range

In normal cases, the will force $\vec{f}_{will}$ takes the direction of the desired velocity $\vec{v}_d$ as shown in figure 2.21.

Traditionally the will forces are specified by a desired velocity of the pedestrian and the trajectory. The will force will be implemented as a vector on the simulation model. However, in the motivation to reach certain places, there are tasks in which the desired motions of individuals are specified by the state of system (list of circumstances) rather than time. For such tasks, desired velocity field control has been proposed. In this chapter, a method to extend our information about the forces that drive the individuals from rest to their desired velocities is evaluated.

- In the case of group movement, the will force takes the direction of the group leader.

  Figure 2.22 illustrates a group of pedestrians following their leader. A group is defined as a physical collection of people following the same route, but who may or may not be part of the same social group, and a "subgroup" is defined as people within the same physical "group" who want to stay together, like friends or family members. Several studies have revealed that smaller subgroups constitute the majority of the people in a crowd. But very few studies are able to model the "subgroup" behaviour. A particular subgroup concerns pedestrians who hold hands. It is recognized that holding

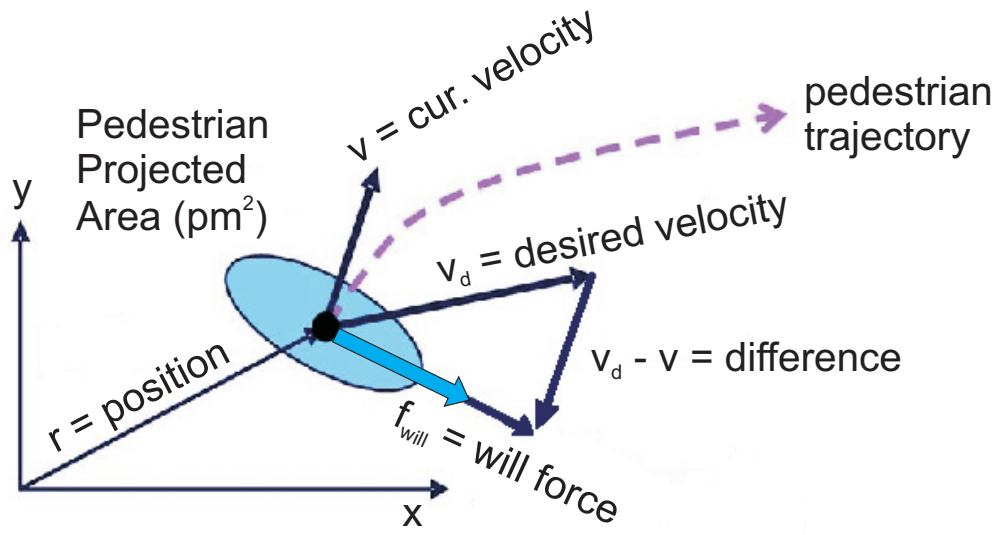

Figure 2.21: Desired velocity. In the real world, each pedestrian has a desired velocity $\vec{v}_d$ towards a desired destination and adapts the current velocity according to the environmental situation.

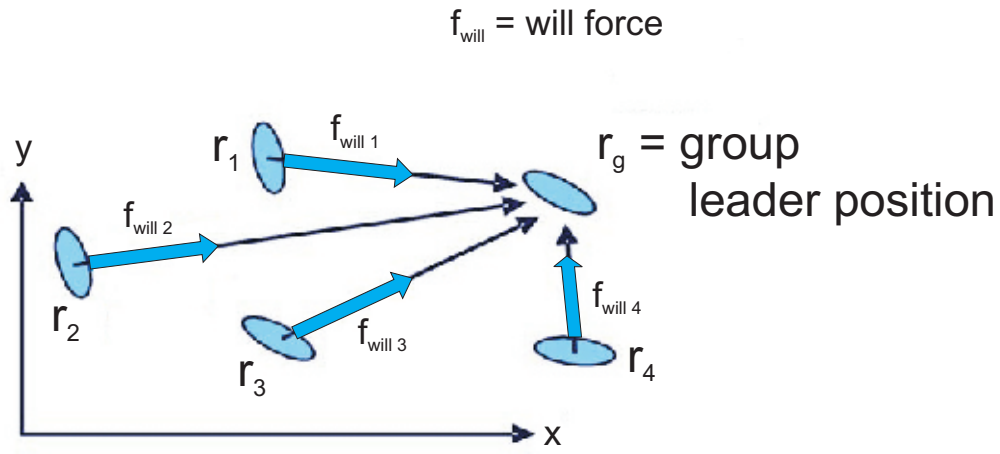

Figure 2.22: "Follow me".

hands is the most effective way of keeping children safe from traffic injury [77]. All the group members take the desired position and the desired velocity of the group leader.

- In the case of an emergency or dangerous situation, the will force takes the direction of the nearest exit and this has dramatic consequences on the behaviour of pedestrians at the exit. They block each other and this builds up a rigid arc from which no one can escape (see fig. 2.23 and 2.12).

Figure 2.23 demonstrate the situation of pedestrians in case of emergency or dangerous situation. The will force points to the direction of the nearest exit. This picture illustrates the situation when people take the proper precaution to prevent potential hazards when they are alerted. For example, in case of an emergency, evacuating the building immediately by using the closest exit and going to the designated meeting location. Panic breaks out, if many individuals attempt to escape an emergency area at the same time, often the emergency exits are blocked in a short time, and the situations have a fatal consequence for survival and leads to injuries or death through crushing people in a crowd. Real world example (fire safety: General Evacuation Procedures): Learn the location of the two nearest exits from your work area (often these are down staircases)[78].

The priority in the emergency or dangerous situations like fire in a building or earthquake are designed to reach each particle the nearest exit in a short time. In first step the particle choose their priority destination after that they can find the beeline towards the nearest exit.

2.8.3 Internal forces –intermediate range

(a) Collision avoidance forces
In the collision avoidance process, autonomous particles need to discover the environment to avoid static and dynamic obstacles. At any time the distance between each obstacle, wall, and the particle i are computed, go both of them closer to each other, then calculate the angle between particle i's desired direction and the line joining the center of particle i and the obstacle. This effect can be seen within the rectangle of influence (figure 2.24). The distance and the angle play a significant role to assess how relevant the obstacle is to the trajectory. When travelling the environment, particles also update their perceived crowd density, which is necessary for their decision making process.

We denote by intermediate range forces that change the motion of an individual in order to avoid an encounter with another. The observation employed here is that all of us will try to avoid a collision by moving away from an encounter

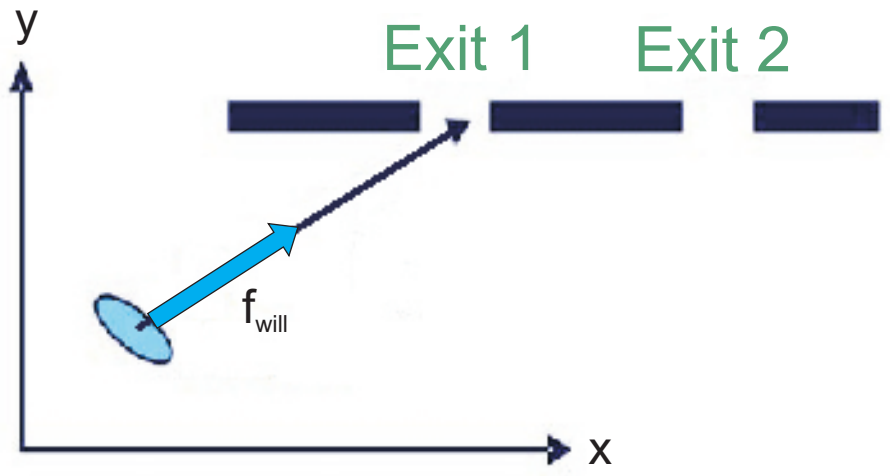

Figure 2.23: Go to nearest exit.

long before it happens. The nature of these forces is such that they act mainly in a direction normal to the current motion of the individual, and therefore do not lead to a significant decrease in velocity. Moreover, this force is only active if a collision is sensed.

Using as a starting point the situation depicted in figure 2.24, given two pedestrians with current coordinates and velocities $\vec{r}_1$, $\vec{v}_1$ and $\vec{r}_2$, $\vec{v}_2$, an encounter may be computed by evaluating the time increment Δt at which the distance between the two is minimized, i.e., $[\vec{r}_1 + \Delta t\vec{v}_1 - (\vec{r}_2 + \Delta t\vec{v}_2)]^2 \rightarrow min$. This results in $[(\vec{r}_1 - \vec{r}_2) + \Delta t_m(\vec{v}_1 - \vec{v}_2)](\vec{v}_1 - \vec{v}_2) = 0$, or $\Delta t_m = -\frac{(\vec{r}_1-\vec{r}_2)(\vec{v}_1-\vec{v}_2)}{(\vec{v}_1-\vec{v}_2)(\vec{v}_1-\vec{v}_2)}$. The minimum distance is given by $\delta_{min} = |(\vec{r}_1 - \vec{r}_2) + \Delta t_m(\vec{v}_1 - \vec{v}_2)|$. Obviously, the force will only become active if $\Delta t > 0$. The general nature of this force is such that it will decrease with distance. How exactly this decrease function looks like is unknown at the present time (it may even be random). We have used a function based on the normalized distance between the pedestrians $d = \frac{|(\vec{r}_1-\vec{r}_2)|}{R_1}$, where R_1 is the characteristic radius of pedestrian 1, which is of the form: $f = f_{max}\frac{1}{(1+d^2)}$. This simple repulsion force may be refined further by considering the directions along and normal to the current velocity vector $\vec{v}_1$, denoted by $\hat{e}_t$ and $\hat{e}_n$, respectively. We can then split the normalized distance d into a tangential and normal component: $d_t = \frac{|\hat{e}_t.(\vec{r}_1-\vec{r}_2)|}{R_1}$, $d_n = \frac{|\hat{e}_n.(\vec{r}_1-\vec{r}_2)|}{R_1}$. This leads to tangential and normal forces of the form: $\vec{f} = -f_{max}\frac{1}{(1+d_t^2)}\hat{e}_t - f_{max}\frac{1}{(1+d_n^2)}\hat{e}_n$. The value of f_{max} can be related to the relaxation time, i.e. it is not too difficult to obtain. We have used f_{max}/m_p = O(4) $\approx$ 4 [m/sec^2].

(b) Avoiding a wall

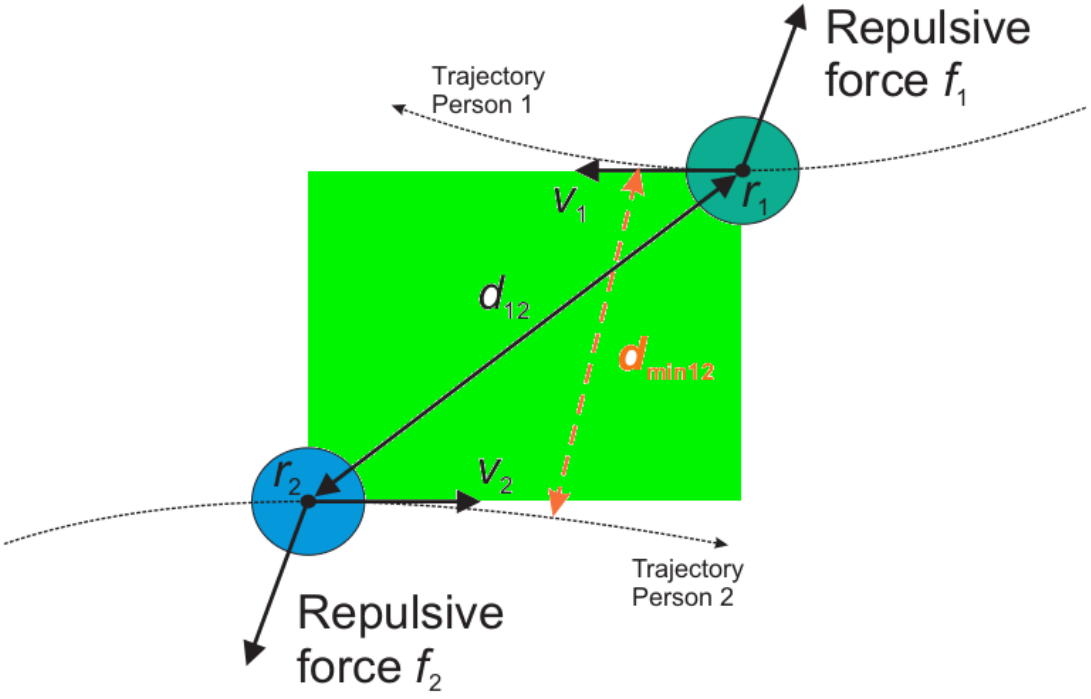

Figure 2.24: Collision avoidance rectangle of influence. Illustration of pedestrian-pedestrian collisions avoidance forces. This force is referred as repulsive force and reaches its max. value at the shortest distance between the particles.

Avoidance forces $f_{repulsive}$ are calculated only for relevant obstacles, walls and agents: i.e. those falling within the rectangle of influence. The avoidance force for obstacle W is illustrated in figure 2.25. The calculation is done in the same way as for the force of the pedestrian-pedestrian repulsion and the same formulas are used. Only the pedestrian-pedestrian distance has to be replaced by the distance of the pedestrian from the wall.

2.8.4 External forces

External forces –near range

- Pedestrian collision: For more realistic crowd simulation and for a description of realistic counter-flows and overtaking behaviours, many attributes influencing the behaviour of people in the real world will be considered. This approach has the ability to simulate human behaviour by setting parameters obtained from many observations related to real human movement. In avoiding an obstacle the factors affecting the tangential forces are:

  – The distance between the particle and any obstacles.

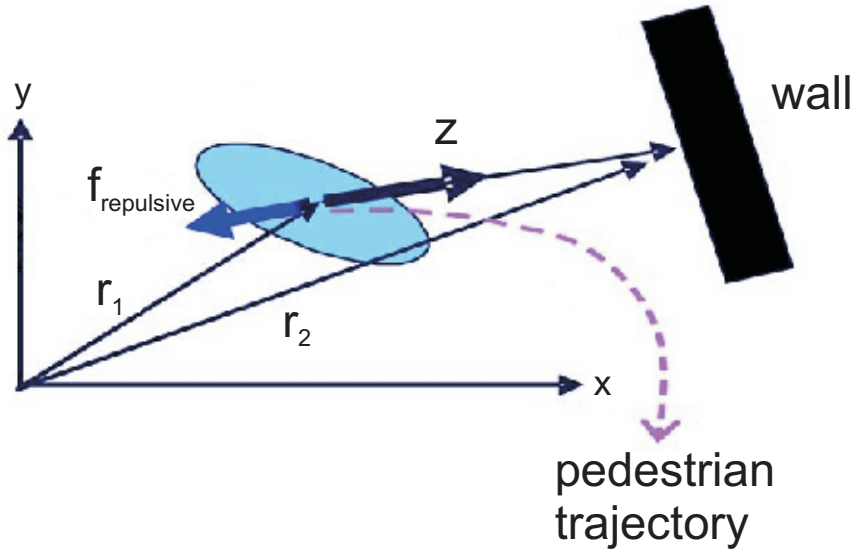

Figure 2.25: Avoiding a wall. This picture illustrate the pedestrian-obstacle collision avoidance. The blue solid arrow shows the direction of the repulsive acting force $f_{repulsive}$ and the dashed arrow indicates the trajectory path of the particle.

- The relative direction and movement of the agents i.e. the direction between the desired velocities vectors ($\vec{v}_1$ and $\vec{v}_2$ for example).
- Crowd density: If an agent enter the interaction rectangle, a tangential force (see fig. 2.24) will be active to change the direction of movement and make a curve in the path to avoid collision. The angle between two agents is used to simulate the individual decision making how to react to a previous collision. For example, in a walking floor, if there is enough space between us and another person, none of us would change the direction. In case of many persons walking in the corridor, the majority of people tend to move to the right. Therefore, when the velocity vectors are almost collinear, the tangential forces pointing to the right. In case an agent 1 detects agent 2 and agent as possible obstacles, then the system computes the distance vector towards agent 1 as follow (d_{21}). Agent 2 is farther away from 1, but since it is moving against agent 1, the system gives this obstacle higher priority.

Once a pedestrian has moved close enough to obstacles or other pedestrians, his velocity will be decreased markedly, (see fig. 2.26). Unlike the long-range forces, these forces act in the direction of the normalised dif-

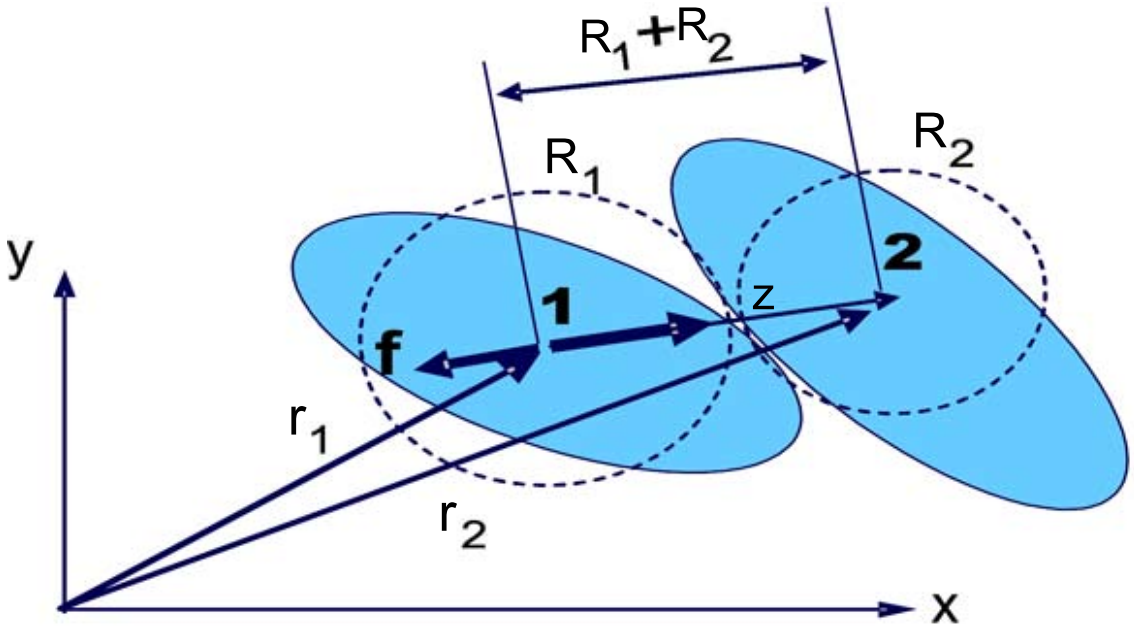

Figure 2.26: Pedestrian collision. Schema illustrate pedestrian-pedestrian body contact or collisions forces. This situation indicate a body friction or body deformation.

ference vector $\vec{z} = \frac{(\vec{r}_2 - \vec{r}_1)}{|\vec{r}_2 - \vec{r}_1|}$. We have used, as before, a force of the form $\vec{f} = -f_{max} \frac{1}{(1+d^2)} \vec{z}$, although the exact nature of this force is unknown at the present time. As before, the value of f_{max} can be related to the relaxation time. We have used f_{max}/m_p = O(4) $\approx$ 4 [m/sec^2].

- Collision with a wall or obstacle: A stream of pedestrians will be enclosed by the walls in or around the structures in which it occurs, (see fig. 2.27). We have assumed that this force acts in the direction of the gradient of the distance-to-wall function $d_w(x)$. This function, which measures the closest distance to a wall from any given location r, is assumed to be known. In practice, it is evaluated in a pre-processing step. As before, we have used, for lack of any deeper knowledge, a function of the form:

$$\vec{f_w} = -f_{max} \frac{1}{(1 + (d_w/R)^2)} . \nabla d_w,$$

with f_{max}/m_p = O(4) $\approx$ 4 [m/sec^2].

$\vec{f}$ denotes the individual-individual interaction force or individual-obstacle force, f_w denotes the collision force due to the wall (out of a total of M wall surfaces).

2.9 Data structures

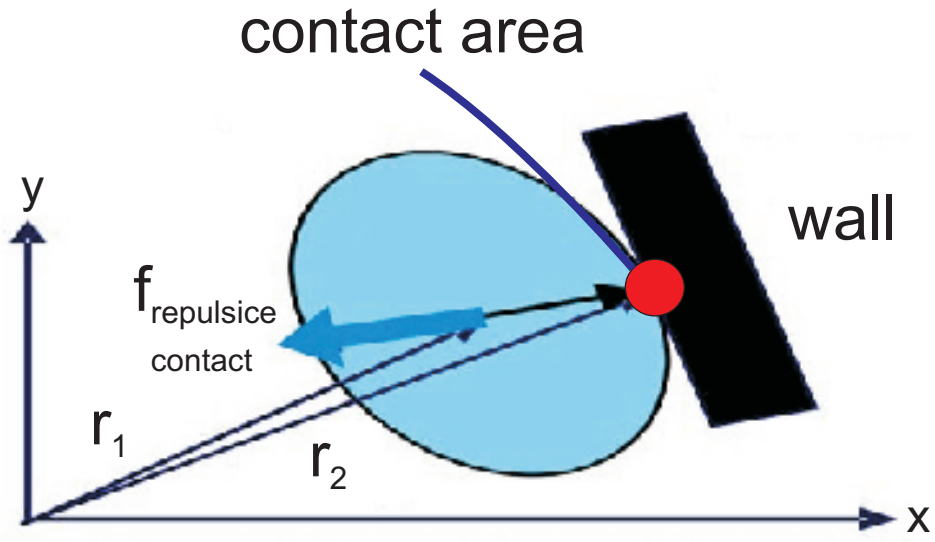

Figure 2.27: Repulsive contact force. The solid blue arrow indicates the direction of the contact repulsive force.

2.9.1 Data carried by the individual

The data concerning a single individual are classified in three categories: physical, emotional and ethnic data. This data, which includes items such as the pedestrian's height, width, fitness, nationality, current physical and mental state, as well as the current motion data (location, velocity, etc.) is stored in arrays attached directly to the pedestrians. In this way, the data becomes easily accessible at any time. In order to save storage, the individual's height, width and fitness are taken from a data-base, i.e. through a table look-up. In this table, the data belonging to a limited number of representative groups is stored, and the individual is tagged as belonging to one of these groups. In order to enhance realism, a random variation number for personal data is also attached to each individual. The savings in storage accrued by this indirect storage assignment are considerable: if we have Nd personal data items, conventional storage would require O(NdNp) items, whereas indirect data assignment only requires O(2Np+NdNg) items. This implies that even for moderate realism, with O(10) data items per person, indirect storage provides savings of O(5). All this data is necessary for more realism in the pedestrian motion simulation.

2.9.2 Geographic data

The environment where the agents navigate is represented in the system as geographic data. The geographic data contain information about the platform within which the particles move, items such as terrain condition (inclination, corridors, escalators, obstacles, etc.), climate data (temperature, humidity, rain, visibility), signs, as well as doors, entrances and emergency exits. All this data is stored in a so-called background grid consisting of triangular elements. This background grid is used to define the geometry of the problem, and is generated automatically using the advancing front method [79]. All geometrical and climatological data is attached to this grid.

2.9.3 Fixed triangular background grid

The geography is stored at (fixed) background nodes and used to define the geometry. The mesh is generated automatically and the data is interpolated (linearly) to the pedestrian position, (see fig. 2.28).

2.9.4 Pedestrian data

- Pedestrian "personal" data types
  - Personal Data (height, width, fitness, nationality, familiarity with surroundings, objectives, etc.)
  - Current Physical and Mental State
  - Current Motion Data (location, velocity, etc.)
- Pedestrian Data Storage
  - Data table for Geno-Types and Objectives/Paths
  - Pedestrian Arrays for Actual Data
  - Pedestrian "personal" Data types

Neighbour data

By far the most time-consuming portion of pedestrian simulations is the evaluation of the interaction between nearest neighbours. The nearest neighbours of every pedestrian must be identified and accounted for at every time step. Assuming an arbitrary cloud of points, a Voronoi tessellation, or its dual, the Delauney triangulation, uniquely defines the nearest neighbours of a point. The Delauney criterion states that the circumcircle of any triangle does not contain any other

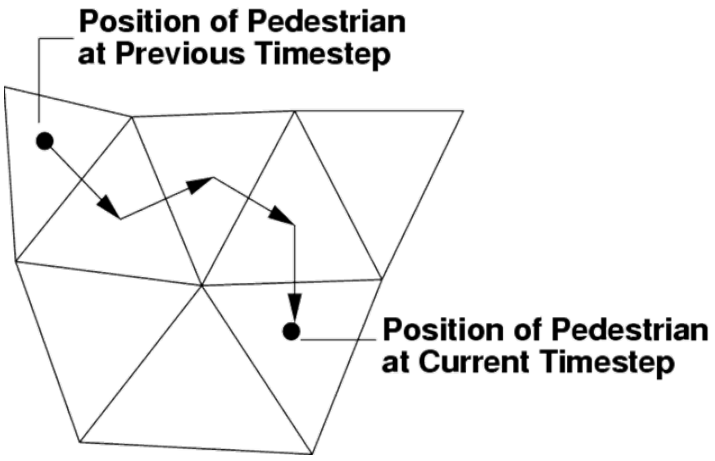

Figure 2.28: Background Grid. All information about the terrain surrounding where the particle moves will be generated with a fixed triangular background grid [21].

point. Another unique way to define a mesh is by minimising the maximum angle for any combination of triangles adjacent to an edge, (see fig. 2.29).

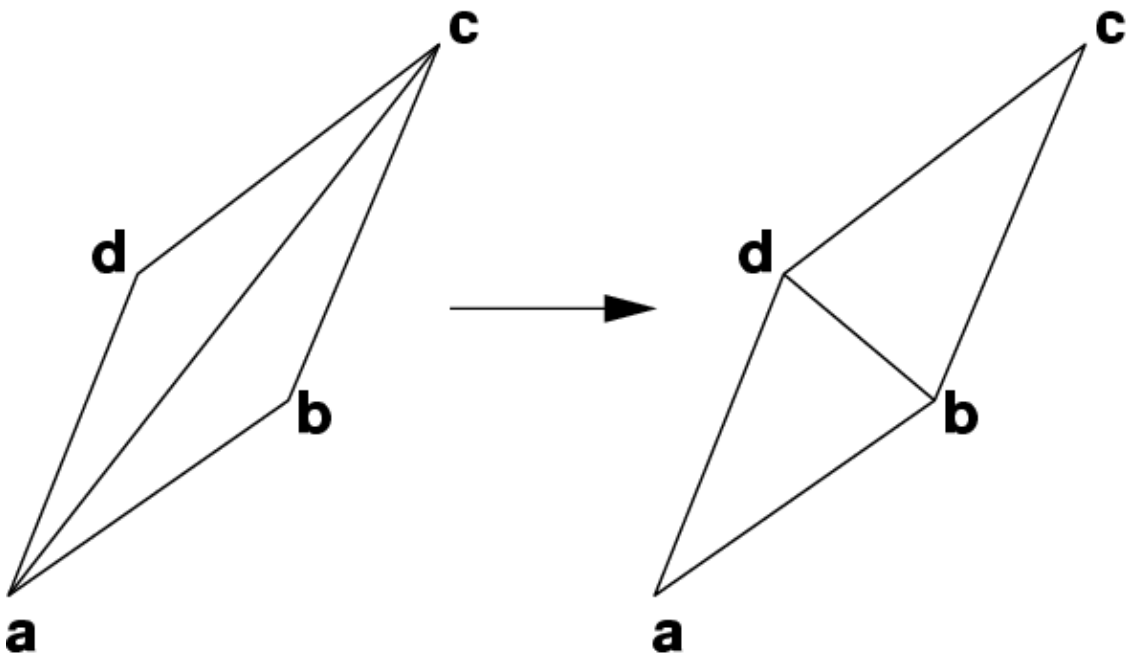

Figure 2.29: Diagonal Swap Using Min-Max Criterion.

For dynamically moving points, the Delauney or min-max criterion will be

violated in parts of the mesh. Every so often (e.g. after every time step), the mesh must be modified in order to restore it. For 2-D grids like the ones contemplated here, this is best achieved by flipping diagonals until the Delauney or min-max criterion have been restored. An edge-based data structure that is well suited for this purpose stores the two points of the edge, the neighbours on either side of the edge, as well as the four edges that enclose the edge, (see fig. 2.30). For boundary edges some of these items will be missing, making it easy to identify them.

On the basis of this method the particle can identify the nearest neighbours (at each Δt).

2.9.5 Example: Walking through a narrow passage

This background grid is used to define the geometry of the problem, and is generated automatically using the advancing front method [79, 81, 82]. All geometrical and climatological data are attached to this grid. This implies that the amount of data stored and used for pedestrian movement depends only on the level of details stored in this mesh, and is proportional to the number of elements in it. For obvious reasons, the size of this mesh (number of elements and points) should be limited to the necessary and available amount of information required for the simulation. One can see that the mesh will be very fine in areas where the density of pedestrians gets higher, (see fig. 2.31). At every instance, a pedestrian will be located in one of the elements of the background grid. This 'host element' is updated continuously with the nearest neighbour tracking procedure.

Pedestrian motion in passages is one of the few cases where reliable empirical data exists. In order to assess the validity of the proposed pedestrian motion model, a typical 'passage flow was selected. The geometry of the problem is shown in figure2.31. Pedestrians enter the domain from the left and exit to the right. For this case, each pedestrian has the goal of reaching first the entrance of the passage, then to traverse it to the other end, and finally to exit on the right. A typical snapshot during one of the simulations is shown in figure2.31.

The pedestrian parameters chosen were as follows:

- Desired velocity $v_d = 1 \pm 0.02$ m/s;
- Relaxation time $\tau = 0.50 \pm 0.1$ s;
- Pedestrian radius $R = 0.2 \pm 0.02$ m.

The problem was run repeatedly with an increasing number of pedestrians entering the domain per time unit. The resulting pedestrian density was measured in the passage, as well as the average velocity. The results obtained are compared

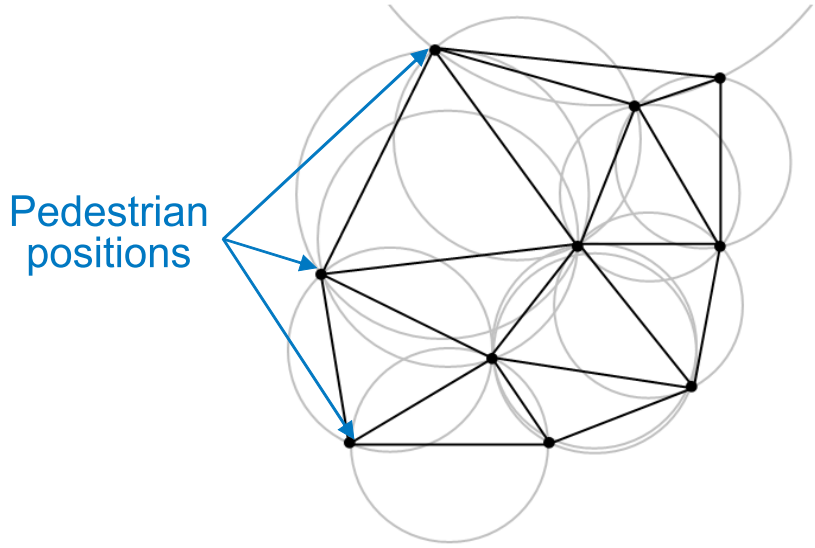

Figure 2.30: Neighbour data. The points represent the particle positions and the circles indicate the particle-particle interaction ranges. Every particle can see and identify the nearest neighbours (at each Δt). In this system pedestrians are moving like a cloud of points, Delauney triangulation (updated) [80].

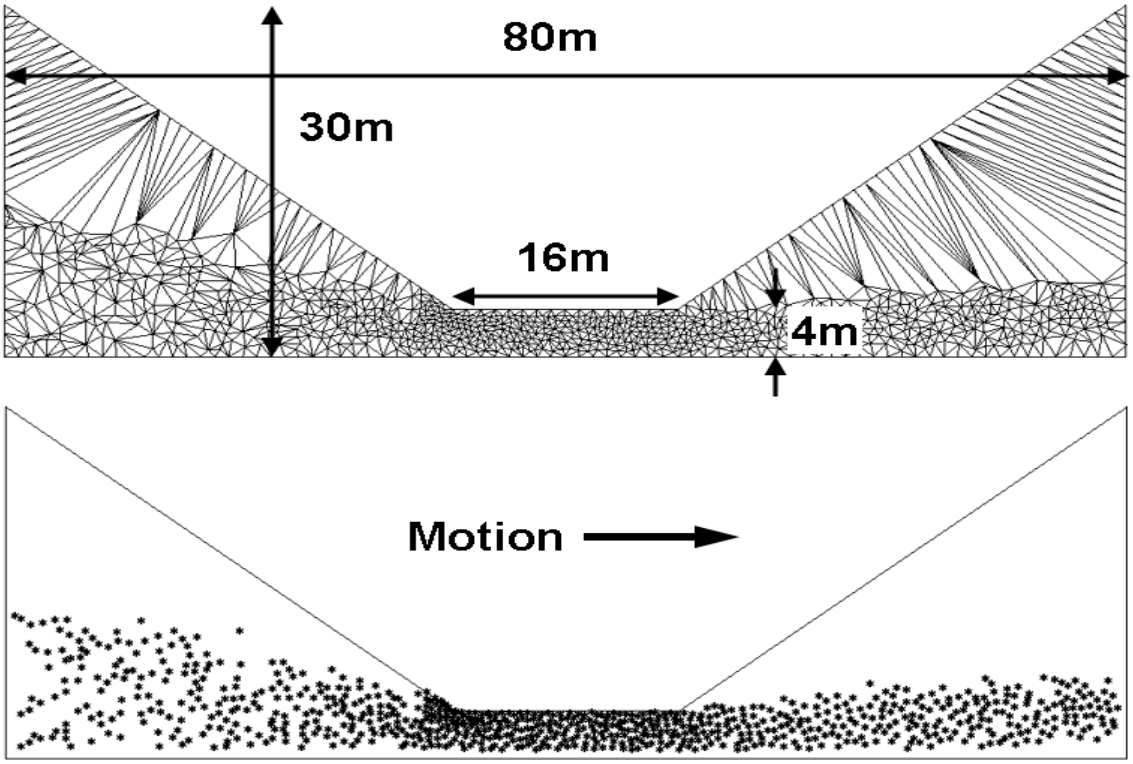

Figure 2.31: Moving grid and position snapshot. This picture shows pedestrians moving through a narrow passage like a cloud of points, Delauney triangulation (updated) [80]. The fine triangulation indicates high density of pedestrians.

with published data in figure 2.32. As one can see, the proposed model provides surprisingly accurate results.

2.9.6 Example: Evacuation of aircraft

The evacuation process of a building or closed area e.g. commercial air-planes or ships is very important to the safety procedure of personnel and passengers. The evacuation training programs proposed by many aviation administration or flight companies have several shortcomings.

Many of them proposed procedures which are not able to achieve a successful evacuations technique; moreover, they were not able to explain either what equipment are functional or which process must be followed during an evacuation. Only evacuations occurred after accidents were studied but not the evacuations emerging from incidents. As a result, a microscopic pedestrian simulation model was used, which can provide the following result:

- How successful evacuations can be performed,
- Assessing potential safety hazards and
- Identifying safety shortcomings before fatal accidents happens.

The simulation of an evacuation scenario is a big challenge for the knowledgeable modeller. In the panic situations there are many factors and parameters governing the movement of pedestrians and influencing the behaviour of crowd. However the time needed to bring all people from the dangerous area to the safe places becomes very important. In this example every pedestrian (agents) start from rest and go to the nearest exit. The inconvenience of this evacuation plan is, that at extremely dangerous situations and due to uncontrolled behaviour of individuals physical jamming and people blocking each other appears at the exits. These studies can help construction engineers and designers providing insight into specific factors, such as crew-member training and passenger behaviour, which affect the outcome of evacuations.

In the simulation technique the goal of every pedestrian is to reach the nearest exit in a short time. The evacuation behaviour has finished as soon as the agents reach their goal. The results show that the majority of agents find their way to the nearest exit. The small number that does not find their way towards the nearest exit can be explained by the fact that the gradient can not built the shortest path due to the positioning of walls in the environment.

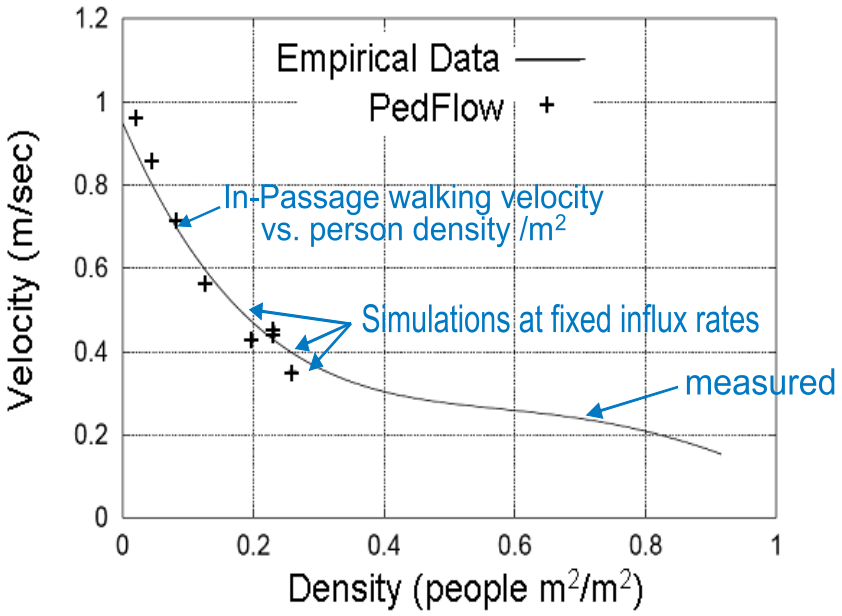

Figure 2.32: Velocity-density fundamental diagram: Decrease of the pedestrian local velocity $\vec{v}(\vec{r},t)$ in the passage area as a function of the local density $\rho(\vec{r},t)$. The measured data are represented by crosses, they are consistent with the empirical data of Predtetschenski and Milinski [1] represented by the solid line.

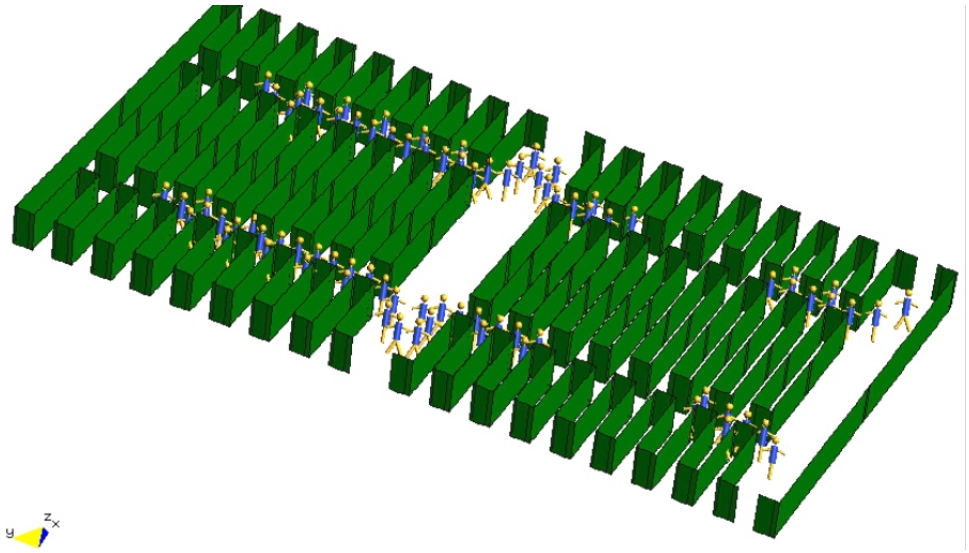

Figure 2.33: Examples: Evacuation of aircraft [21].

2.10 PRESSURE FORCES

2.10.1 Introduction

In the last decade many crowd disasters happened in different parts of the world. This chapter illustrates the crowd force which is responsible for the death of hundreds of people around the world every year. With the following research we intend to study the riot situations in the case of high density crowd dynamics and provide empirical data about crowd disasters, enabling one to understand what happens in the real world. Further we bring an overview of the huge physical interaction forces between individuals in case of stampedes or crowd disasters and how casualties or injuries occur in such situations, by registration of pedestrian activities in the real physics world.

Moreover we want to study in a constructive way how pressure will be built if a stampede occurs in a high density crowds, and how the victim's bodies will be affected in dangerous situations. To prevent more fatal situations in the future, as well as for better understanding of the circumstances of stampedes, several experiments were conducted.

Unfortunately we know from an long lasting experience that there is a lack in the data concerning panic situations in crowd dynamics. In the Hongik University Biomechanics Lab, Prof. Choi, decided to perform experiments of this kind. The main obstacle is often not the financial requirements of these experiments, but the technical know how of the (Human Pressure Build) experiment.

On this basis and with the cooperation of Hongik University Biomechanics Lab (one of the leading biomechanics institutes worldwide), Prof. Choi conducted these experiments. The first feasibility tests were made at Hongik University, Seoul, for the assessment of the danger of injury under inter-pedestrian pressure build-up. The SL-Rasch GmbH can offer a full report and PedFlow post-processing output interface for plotting Pedestrian Pressure Injury Scale values k_p:

- 0 = zero pressure
- 1 = light inconveniences
- 2 = moderate inconveniences
- 3 = breathing becomes difficult
- 4 = danger of suffocation; first injuries
- 5 = suffocation imminent; severe injuries

- 6 = lethal conditions

2.10.2 Classification of crowds and crowd accidents

The circumstances surrounding and environment play a key role on the formation of crowd type. From the literature survey we can determine two major types of high density crowds: "standing crowds" and "moving crowds" [5, 76, 83].

"Standing crowds" are observed in organized ways in many places such as elevators, vehicle queues, waiting lines, sport and music events etc., where people are waiting deliberately for the end of a specific task. In this situation, the contact forces between the members of the crowd are negligible and not directional, because there exists no reason for aggressive movement or pushing. In the case of undesired situations, due to unpredictable violence in the movement of the crowd participants in different directions, this may cause extra forces e.g friction and push forces.

"Moving crowds" happens if many people try to reach a common target e.g exit and entrance of specific places, or passing through a common path e.g. tunnel, and bridge as shown in the figure 2.34. An increase in the number of people may cause high density concentration which slows down the movement in the area. At this moment the free movement disappears. Push and pressure contact between the crowd can begin to be risky for instance in the case of a panic situation. The contact forces were uniform in the case of standing crowds, whereas in the current case they are not uniform anymore, nevertheless the pushes applied in the aimed direction by the individuals cause a new force component in the direction of the target in addition to an increase in average force level.

Crowd accidents occur in moving crowds, or in degenerate standing crowds, both of them have the same fatal consequences for the pedestrians [84].

2.10.3 Crowd forces

When people crushing or trampling in extremely critical overcrowding places, the high crowd pressure induced by the crowd forces rises (within the crowd member) and can reach an irresistible value to some crowd participants, causing victims from compressive asphyxia (people will be killed or injured) [76]. Many studies analyzing several fatal crowd accidents and crowd disasters show that forces of more than 4500 N per meter of barrier have been applied [85]. The deformation in the thorax induced by horizontal crushing force acting on standing people is the main reason for the death by asphyxiation. Human bodies react differently on this forces, depending on many parameters such as age, physical fitness.

Figure 2.34: High density crowd on the love parade in Duisburg Germany. People try to escape the dangerous area to protect themselves.

The components of the force driving the pedestrian to reach a certain place within a dense area (responsible for friction and pushing between the member of a crowd) are expressed in two main parts: the "self-driven" force, which is defined as internal force using body muscle action allowing the human body to move forward, and the other is the "leaning force", generated by body weight.

According to Zhen et al. the mean value of the lean force is about 260 N/person. Mean value of self-driven force is about 200 N/person. The crucial factor is the force between people which results in crashes [86].

2.10.4 Value of crush force and lasting time

The magnitude of the crush force and the acting time duration have a significant consequence on the deformation or compression of human bodies. The sensible part of the human body in case of crowd pressures is the thorax. When the pressure force exceeds an average values of 400 N (depending on the weight carrying capacity of the human being) most people will feel discomfort. The magnitude of this force can take minimum of 116 N and a maximum 774 N and when the human bodies are exposed to this force for more than 30 s, the pressure becomes intolerable. If the applied loading force magnitude reached an average of about 600 N the maximum lasting time is about 40 min [87]

Tests on live subjects conducted by [88] found that the tolerable force was typ-

ically 623 N for men when pushed against a 100 mm wide flat horizontal barrier. This force increased to typically 800 N when the subject was allowed to push against the barrier to reduce loading on the rib cage.

Suffocation can occur in a short time of 15 sec after a load of 6227 N. It was estimated that death occurred after 4 to 6 min after applying a load of 1112 N [89].

2.10.5 Comfortable space in crowds

Fruin researched crowds in the early 1970's. His book Pedestrian Planning and Design has been cited in many of the present guidelines for pedestrian planning [8]. He has defined the criteria for safety standards in places of public assembly. He defined the level of service concept where the density and speed relationship are stated as guidelines for comfort and safety. Below table indicates the square meters per person related to this Level of Service category and Figure 6 illustrates each Fruin Level of Service with overweight persons. As shown in figure 2.35, Fruin data appear to be too generous.

Level of service	A	B	C	D	E	F
Walk ways	> 3.25	3.25 to 2.32	2.32 to 1.39	1.39 to 0.93	0.93 to 0.46	< 0.46

Table 2.3: Fruin Level of Service (unit:m^2): A = Free flowing, B = Minor conflicts, C = Some restrictions to speed, D = Restricted movement for most, E = Restricted movement for all, F = Shuffling movements for all.

It is important to note that Fruin made his measurements in a pedestrian street environment. Crowd behaviour on a city street with its many distractions is quite different from a stadium behaviour, and very different to emergency egress behaviour. The modern stadium has crowd densities in excess of the Fruin observation and therefore the application of Level of Service needs to be examined.

2.10.6 Pushing mechanisms

A simple experiment was conducted by Hyung Yun Choi Professor at HongIk University, Research Institute of Science and Technology, (see fig. 2.36) where the leaning force magnitude was determined for different leaning angles θ. The experiment consisted of pushing against a vertical rigid wall and a force plate. In the first part of the experiment the leaning force for a small leaning angle was determined. In the second part the leaning force for large angles was investigated. In the first part an individual was asked to lean on the force plate using the own weight without pushing, this behavior is called passive pushing. In the second

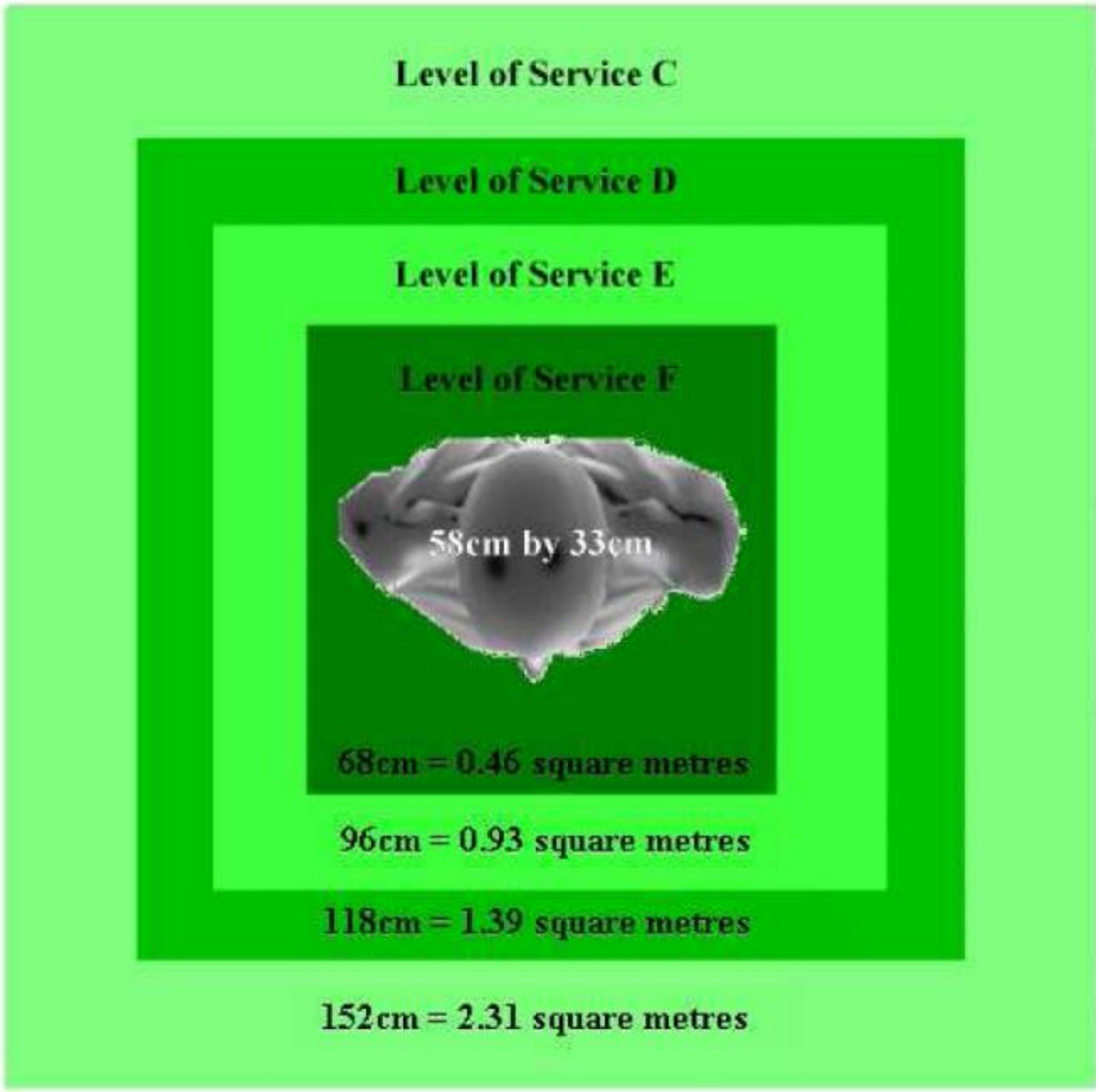

Figure 2.35: A single individual private sphere: Fruin Level of Service area per person [90].

part, an individual was asked to use muscle power to push against the load plate, which is known as active pushing.

The results of this experiment revealed a total force of 70 N and 140 N for passive leaning at the small and large inclination angle, respectively, 160 and 230 N for active pushing at the small and large inclination.

The differential horizontal component of the leaning force in passive pushing with respect to angle limit in small and large inclination was 70 N. A small angle induced a small force and vice versa. The difference between the force magnitude can be attributed to the weight of the person and the area of contact between the feet and the ground.

With respect to different angle of inclination the resulting tests of passive and active leaning force differ by an amount of 90 N. This force is an additional force released by muscle power of individual and will be added to the "self-driven" force component in case of forward pushing in high density crowds.

This result reveals a plausible and creditable basis to understand the phenomena and effects that influence the movement of an individual in a dense area. Moreover the active and passive pushing forces affect the crowd pressure in case of crowd crush which can be used in the conceptual model.

2.10.7 Contact pressure measurement of in-line pushing

As one can see in figure 2.37 the leaning angle decreases from the end to the front of the pushing line and take the minimum value at the barriers. This helps to understand the crowd pressure building between the individuals: The higher the pressure, the less the individuals can lean forward. Only the pushers at the end of the queue can lean forward, while they have relative free space. It is clear that the person near the wall would be squeezed into the inclination angle of the wall.

2.10.8 Leaning victim/pushers and no-leaning victim/pushers

This extreme scenario is illustrated in figure 2.38.

With the evidence that crowd forces are propagated with body contact, both cases leaning victim/pushers and no-leaning victim/pushers, can be very clearly seen in this figure, especially if pushing process is in one line. In the red zone on the picture people cannot lean because they are compressed if the line-up in the crowd is in front of a vertical wall. This is a dangerous area subjected to a very high crowd pressure. In this zone so called no-leaning victims reside, where the self-driven force is reduced to zero. In the blue sector the persons still have a weak self-driven force and they can for a while push forward. The pushing force

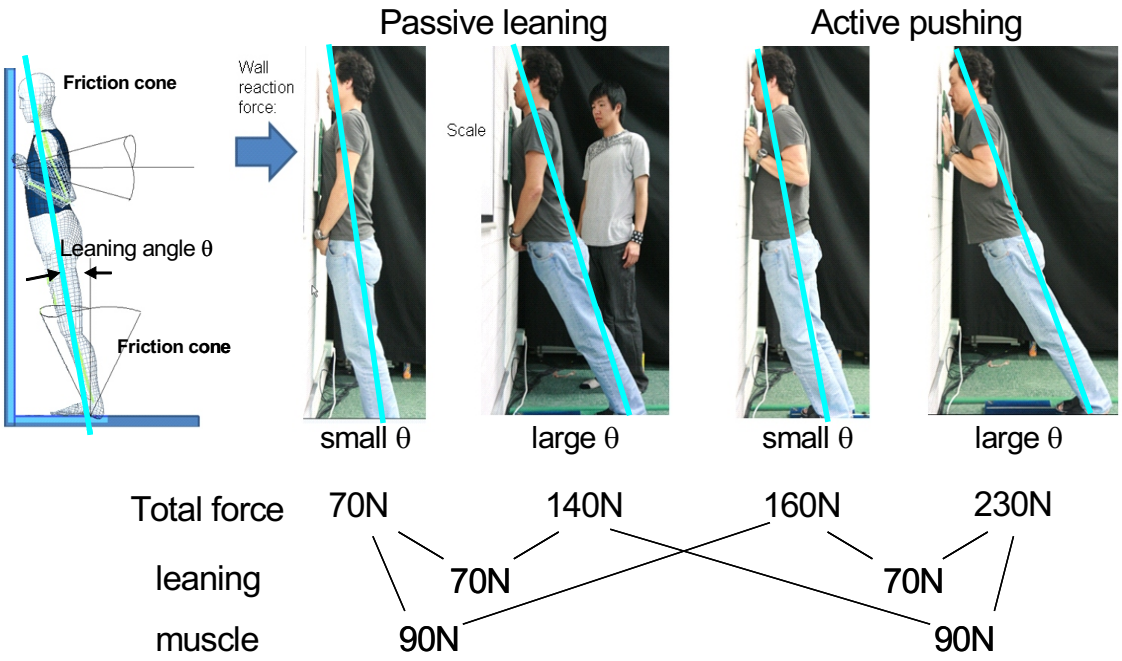

Figure 2.36: Single individual pilot test results performed by Hongik University Biomechanics Lab, Prof. Choi. We distinguish two types of pushing: passive and active. The differential force between the tests with passive leaning and active pushing, considering both conditions with small and large angle of inclination, was found 90 N, which corresponds to the added "self-driven" force component generated by muscle action. The pushing load is influenced by the individual parameters (fitness, sex, age...) and the environment (floor surfaces that are clean and dry can influence the force needed to move a load, confined spaces and narrow passages/doorways could provoke a tripping/trapping/abrasions injury) [91].

Figure 2.37: Contact pressure measurement of in-line pushing. People push in a particular direction when they want to move in that direction and are prevented from doing so. Also, people push when they want to keep their personal space in a crowd. This picture illustrates examples of the typical pressure levels. The contact forces between wall and the individual were measured on dependence of increasing numbers of pushers. One clearly recognizes the increase of leaning angles θ with growing number of pushers [91].

can be generated in one direction if all people move to the same exit for example or in any direction in case of crowd panic and turbulence.

In the pushing case the human body is subjected to two main forces: the self-driven force and the lean force. Self-driven forces exerted by subjects are applied at the hand locations. Firstly, pushing height H' of this force will be measured as normalized height, depending on the subject's preference, at about the subject's height. If the measured normalized height shows reliability and has statistical meaning, the mean measured normalized height will be used. If not, the height will be found by optimization to fit experimental data and numerical model data for force propagation.

The height of the center of mass h in a subject can be derived from segment mass-centers and segment weights, based on the segment link length. Because all subjects cannot have the same anthropometry, the mean height and weight in all subjects will be used to calculate the height of the center of mass to be applied on the leaning crowd model.

It is not easy to calculate the pushing height H of the supporting and reaction forces, because these forces are distributed and not regular. So, the value of pushing height H will be calculated by optimization to fit experimental data and numerical model data for force propagation.

2.10.9 Conclusion

According to a number of publications reported about crowd injuries and fatalities in the last years we can deduce that crowd accident can be classified in two types, trample and crush, both of them can be lead to fatal implications. This study and realized experiments, focused and investigated the crush incident. The majority of people were killed or injured in a crowd disaster from the asphyxia or crowd pressure, that reported [92]. Experiments to determine concentrated forces on guardrails due to leaning and pushing have shown that force of 30% to 75% of participant weight can occur. In a US National Bureau of Standards study of guardrails, three persons exerted a leaning force of 792 N and 609 N pushing [93]. In high density crowd individuals lose self-control and become a part of a fluid mass, where the crowd force reaches unbearable values for the crowd participants. The pressure load induced by forward pushing exerted on the people staying in the front of the crowd can be deadly. This pushing force can be resolved into two components, self-driven force and leaning force. The mean value of the leaning force is about 260 N/person and of self-driven force is about 200 N/person (not experimentally measured but roughly estimated from the observation). Most victims die from crowd compression or so called horizontal forces

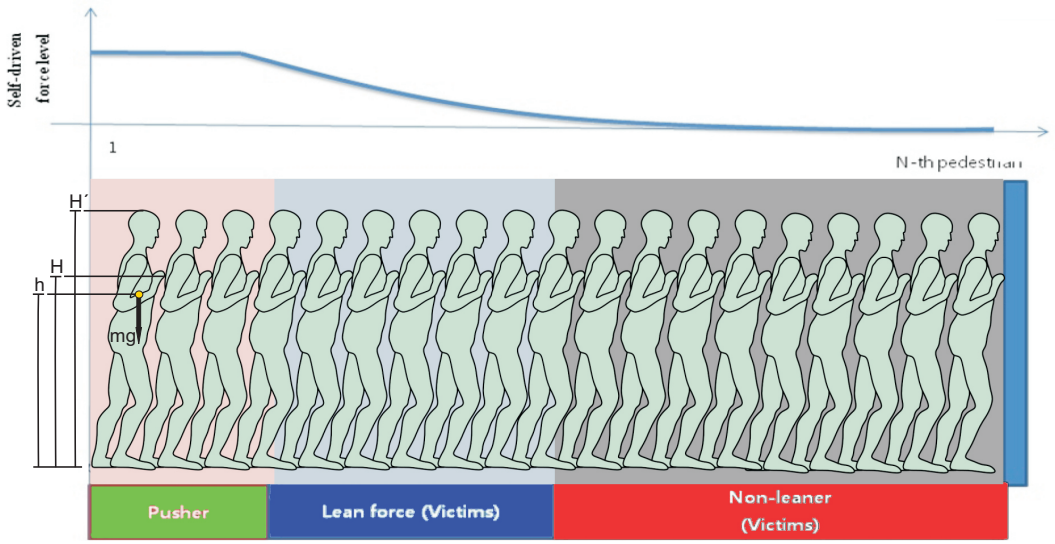

Figure 2.38: Self-driven force in dependence on the position of an individual in the pushing line. Note, that if the leaning force exceeds critical value the human body will be deformed or compressed.

rising from people pushing each other and applied on the upper part of the human body in the thorax region. Safe crowd conditions assume densities below 2-3 persons/m^2. Up to density of 5 persons/m^2 people cannot move freely and are squeezed between others and people begin to push around. The critical crowd density with body contact resulting in injuries occurs at 7.13 person/m^2, according to Fruin's study. The leaning angle in case of crowd disasters is estimated between 8 and 10 degrees according to observation of many accidents.

All this information about self-driven forces and leaning forces can be used advantageously for optimization and calibration of the PedFlow simulation model e.g. the value of the self-driven force, $F_{self-driven}$, is about 200N/person according to literature and about 90 N/person by previous pilot tests performed on one subject. The difference between the already existing values in the literature and the experimental values can be traced back to the individual loading height H', individual degree of muscle power and individual leaning angle θ. To calculate the maximum and mean values of the self-driven force a statistical method has been used in the experiment shown in figure 2.36, repeated many times with different volunteers.

CHAPTER 3

LIST OF PARAMETERS INFLUENCING THE PEDESTRIAN MOVEMENT

3.1 INTRODUCTION

Today's crowd simulation technology is not well adapted or compatible to the real world. Unfortunately, very little is known about the characteristics and behaviour of pedestrians in cases of high density crowd dynamics. There are a various parameters and factors affecting the behaviour of individuals, these parameters must be considered in modelling the rules of interaction between the individual and their environment, as well as between the individual and other individuals.

Modelling crowd behaviour exhibits a great and important challenge for international recognized scientists. For more realistic crowd behaviour studies, scientists must pay attention to a lot of parameters and factors (e.g. weather, age of the subjects, physical fitness,...) affecting the movement of the pedestrians when creating their models. The movement of a single individual at any time is a result of a long list of possible (and very likely conflicting) forces and circumstances. Among these, we mention the motivation to reach a certain place at a certain time. This depends on the will force of the person and the surrounding conditions in the field of movement. The will force can be affected by many parameters, such as the fitness condition of the pedestrian. The parameters influencing the desired velocity and the relaxation time of an individual (e.g. the environmental factors and the age of the person) have a significant effect on the time needed for the individual to reach a certain place (a young pedestrian reaches his point of interest faster than an older pedestrian). Time constraints, the importance of punctuality, location constraints and the importance of reaching a certain place are the results of an individual's inner and outer factors.

In the real world the pedestrian walking speeds are influenced by many physical and psychological factors e.g. environmental surrounding, traffic flow, and

pedestrian characteristics. Walking speeds can be affected by the terrain condition, although it can be expected that old walkers would be influenced more when walking up or down a stairs than the young walkers. Similarly, it can be expected that the older persons would be more careful in case of higher crowd densities and traffic speeds out of fear of traffic. Finally, pedestrian speeds on pavements and cross ways are strongly related to the number of pedestrians in the flow. The relationship between speed, flow, and space occupied (i.e. density) for a representative population group has been examined by Predtetschenski [1], Fruin [94], Seyfried [95] and others.

The new simulation model will consider individual behaviour and independent characteristics (age, sex, size, health, body language, ethnic origin, psychic state of the individual, psycho social interaction) while also taking into account crowd-level features (e.g. panic), and characteristics of the environment (e.g. safety levels). The simulations performed will model motion and emotion.

3.2 Conditions

In the simulation input we must consider at least two simulation conditions. The first is the normal condition and the second is the emergency condition or panic situation. In panic situations most parameters will be changed and the time factor becomes very important. Typical questions in pedestrian motion planning and design are: How many minutes would be needed to evacuate a football stadium or a pop concert arena? Where is the best place for a pedestrian information point or a poster wall to be placed? How many exit signs should be distributed over the area and where should they be placed? How many minutes does a pedestrian need to get from point A to point B in a restraint place? Are transfer times still realistic when the pedestrians are not familiar with the layout? These questions arise while planning for pedestrians, especially with the increasing number of events occurring and their accompanying pedestrian masses. One way to gain a better understanding of human behaviour in this area is to enrich the tools available for planning, such as pedestrian micro simulation in case of panic situations and emergency conditions.

3.2.1 Panic condition (emergency)

Panic situations are one of the most studied and investigated phenomena in collective behaviors [96, 97, 98, 99], as they often lead to panic attacks and hence are responsible for the deaths of many people. This effect is caused by natural catastrophes (earthquakes, fires,...) or by humans themselves (emotional instability,

fear, spatial limitations, demographic factors,...). Fire can be very dangerous or deadly and if the evacuation plan in the workplaces or generally in closed areas are not easy to follow, panic is inevitable. People are emotional, their emotion depends on factors, such as culture and weather. Another important panic parameter is fear. The fear of hazard or damage can evolve from emotions related to panic and may have deadly consequences. Act of violence propagate in a crowd when people feel anger or highly stressed. Spatial limitations can have dramatic consequences in panic situations. In an attempt to escape a dangerous area, there must be an available amount of space for every pedestrian to exit the facility safely. Many studies show that the demographic problems can be dangerous for crowd populations. Specific locations or groups of people cause crisis events. Depending on the nature of the event, it can create an environment for possible aggressive behavior, such as demonstrations (e.g. anti-war or anti-abortion) that the emotional surrounding of the protesters can developing disorder and violent situations. Another example which occurs frequently are fights between fans of rivaling soccer clubs after a match. Unfortunately, the number of such disasters increased worldwide over recent years (Love Parade, Pilgrimage places, soccer arenas,....). The growing population density, and therefore increased huge evolution of transport systems, leads to bigger mass events like pop concerts, sport events, and demonstrations.

Some characteristics of panic, according to Helbing et al. [22] are described in the following paragraph. In dangerous situations, individuals are excited and everybody gets nervous, i. e. they tend to develop inconvenient actions. People try to move considerably faster than normal [1]. Individuals start pushing and interactions between people become physical in nature. However, movements through bottlenecks frequently become uncoordinated, often this leads to blockade of the passage [100]. Jams occur at exits [100]. Sometimes, clogging effects are observed in intermittent flows [1], see figure 2.34. Crowd force can be fatal and can reach a high dangerous level, it rises with accumulate number of pedestrians in jammed crowds and can cause dangerous pressures of up to 4,500 Newtons per meter [101, 102], which can built steel barriers that nobody can escape. The magnitude and direction of interaction forces between members of a large crowd can suddenly change [5], caused throwing people around in all directions which may cause trampling of people. Trampling or falling people on the ground become a gravely "obstacle" and slow down the movement of the rest of the pedestrians. Usually in such situations people tend to show herding behaviour, i.e. to do what other people do [103, 98]. Shocked by the panic behaviour individuals can easily overlook alternative exits or forget the escape plan [103, 102].

3.2.2 Causes of panic

Crowd panic can be very dangerous and can have fatal consequences. Analysing many deadly situation one can assert the causes leading to crowd panic. Some of the main triggers include:

- Fire – Fire accidents rise the relative risk of dying or being injured, where people die from trampling or from asphyxia on oxygen deficiency in rooms.
- Emotional Instability – If a fight gets out of control this can lead to insecurity between the members of a crowd within a specific area.
- Fear – Fear of danger or harm can be caused by emotions related to panic and may lead to fatal consequences.
- Anger/Violence – Anger can lead to action or even violence. Violence is conceivable when feelings of rage or aggression take over in a crowd.
- Spatial limitations – In case of escaping emergency, there must be sufficient space for every person to escape the establishment safely. Otherwise, people may be injured or suffer from suffocation.
- Demographics – Where people come together in large numbers, the behaviour can be violent, e.g. soccer matches or demonstrations.

The above mentioned items are often a result of poor management and a deficiency of preparation for the events. In contrast, effective security measures and sufficient crowd management strategy may improve safety at a wide range of events and can help to control panic situations before they get out of control. These specifications about crowd panic was published by the International Foundation for Protection Officers [104].

3.3 Types of crowds

In real life, concerning the behaviour of human beings at any time, we can distinguish different types of crowds; every type of crowd has a specific property that must be considered in the simulation model.

- Ambulatory Crowd – People walk in and out or to and from a point of interest to accomplish their daily duties e.g. working and shopping. (Example: normal streets and public places, traffic stations).

- Crowd of Spectators – People attending a game/event. One distinguishes two type of spectators: first type not communicating with each other (example: Cinema, Theater),the other type of spectators interacting with other (example: soccer game or concert);
- Participatory Crowds – People participate in a common task (example: ritual activities).
- Expressive or Reveling Crowds – People let out their emotions (example: demonstrations).
- Panic Crowd – Evacuations from air planes, ships and trains.
- Special case Crowd – Huge people gathering in the same place at the same time (Hajj: places of pilgrimage and worship with up to 3.5 Million pilgrims in Mecca and the Love Parade as a very famous example with up to 1.5 million people).

These crowd classifications were published by the International Foundation for Protection Officers [104].

3.4 Ethnic groups and culture parameters

Ethnic descent and cultural origins intensively affect human behaviour, especially in the case of collective games such as soccer or street demonstrations. Different cultures mean different social norms what can be identified as normal behaviour in one culture may be regarded undesirable by another [105]. Although since the old civilizations the world has a wide diversity of cultural traditions, that are accomplishing or fighting against each other, there are some kinds of behaviour (such as incest, violence against clans, theft and rape) that are considered inadmissible in almost all of them. There are, however, considerable analogies in how individuals will be influenced by the same pattern or lifestyle i.e. growing up in the same culture. Furthermore, culturally induced behaviour patterns can influence the movement of people in celebration places where people from different countries and cultural origins meet (like the Hajj event in Mecca).

The personality and behaviour of each individual is a results of genetic inheritance and the accumulate experience in the society. Moreover the characteristics of each person is affected by a list of social and cultural circumstances (e.g. language, religion and school). Although the most social connections of persons can be traced back to their social rank [105].

These facts about the social behaviour of individuals in their social environment motivated scientists to perform experiments on the behaviour of people of different cultural origins in crowded places. Chattaraj et. al. [106] studied walking speeds of pedestrians with different cultural backgrounds in a corridor. The walking speed of Indian test persons is less related to the density then for German test persons. Surprisingly the disorganized behaviour of Indians is more effective than the ordered behaviour of Germans. By statistical measurements and quantitative comparison it is confirmed that these differences exist and can be traced back to the cultural differences in the fundamental diagram of the pedestrians [106]. Till this moment the relation between pedestrian walking speed and density are not clearly understood neither the parameters influencing the pedestrian dynamics. Even in case of a simple pedestrian flow (walking a corridor) this fundamental relation is not completely agreed. For this sake we were working to better understand the characteristics of the pedestrian movement and how, for example cultural attributes influence the fundamental diagrams.

We consider the above-mentioned results as very important to simulate, as people with different ethnics and cultural origin are found in crowds everywhere like in Hajj in Saudi Arabia or at soccer matches. The pilgrims arrive from more than 100 different countries (Africa, Americas, Asia and Europe). Hundreds of thousands of them are illiterate, and they speak dozens of different languages. In some of their countries, the custom is to walk on the right side of the street; in others, the custom is to walk on the left. The situation involves "many uncontrollable variables" which were noted by Dirk Helbing [5].

For this reason we mention that the ethic cultural parameter is very important to be considered in simulating more realistic crowd behaviour.

3.5 Age parameter and subject selection

Many investigations and studies on the walking speeds of young and old pedestrians, at different locations and under several different environmental conditions, indicate that the mean walking speed is affected by the age parameter. Richard L. Knoblauch in his field studies of pedestrian walking speed and start-up time [69], shows that location and environmental factors collected indicate a significant effect caused by age. Many observations carried out in different sites or locations showed a significant interaction between pedestrian age and the location factor. The causes of slow movement by older people have been attributed to muscle weakness among other factors.

Our database contained different data concerning the pedestrian walking speed, taking sex and age into account and whether the pedestrians were walking alone

or in groups. Data were collected respecting different kinds of pedestrian ages and sex. The following individuals were specifically interesting for our investigation on pilgrimage places:

- Pedestrians carrying children, heavy bags, or suitcases.
- Pedestrians pushing wheelchairs; (Hajj crowd).
- Pedestrians holding hands to stay closer or assisting others across the roadway; (group behaviour in Hajj).

All the data concerning pedestrian walking speeds are illustrated in chapter 4 with other data taken from the literature, which are entered into a pedestrian database called PedGui.

3.6 Physical fitness (or level of exhaustion)

The individual fitness or level of exhaustion can be affected by many internal factors (like sickness, disabilities, age, ...) and external factors (like weather, activities, surrounding conditions,...). For example fatigue is an important indication for the level of fitness of individuals and appears more often among older people than younger people. But the mechanisms describing this association in detail are not fully understood [107]. Decreasing habitual walking speed in older men and women is related to many factors that need to be examined. Many investigations from different science fields were conducted to quantify the walking speed and relaxation time of pedestrians of several ages under different conditions. The result of these studies indicates clearly that the individual walking speed is affected by the physiology and psychology of the individual.

In daily life, individual psychology will be affected by different kinds of stress. People become stressed when they feel that they are challenged or they need to cope with the current situation. In a broad sense, stress can be defined as any change caused by interactions between the environment and individuals. Generally, stress is caused by a discrepancy between environmental demands and the abilities of individuals [108]. Stressors are what causes the stress, which can be a situation, an object or even another individual. There are a number of sources that cause stress. In this paragraph, we focus on the following types of stressors:

- The stress caused by solving deep structural problems in working life (challenge to manage difficult situations and problems in a short time). E.g. time constraints associated with the goal of each agent (people feel stressed when

they believe to have not much time to manage a situation). Stress is therefore a negative experience. It depends on a lot on people's attitude, the situation and the ability to deal with it.

- Detected threats, e.g. fire, threatening animals or objects;

- Annoying events, e.g. heat, noise, air pollution (bad environmental conditions and over-crowding).

Investigations reveal that stress is made up of multiple things. Different people experience different aspects and identify with different definitions. The emotional or behavioural effect of stress is generally associated with increased aggression. This link can be found in both psychological models of emotion [109] and empirical studies of human behaviour. However, the result of stress is not always negative. In some situations increased aggression can have positive effects, and can improve performance up to a specific point [110]. By measuring the connection between how people act (measured through recorded observations) and how people feel (measured indirectly via heart rate, skin temperature and self reporting) psychologists have established a consequent relationship between increased stress and increased aggressive and agitated melancholia behaviour [111]. This result has held across various stressors, different settings, cultures, and genders [112]. Our approach to simulate high density crowd dynamics was inspired by the results mentioned in this paragraph and take advantage of these empirical studies considering various stressors which affect the movement of pedestrians.

3.7 Pedestrian radius parameters

The individual's projected area on the ground is often referred to as the pedestrian radius in crowd movement. This radius denoted by R is a very important input in the simulation. The pedestrian radius depends on the weather factor. The radius of the individual in summer will be smaller as in winter, see table: 2.1 and fig: 2.1. Some empirical data were collected by Predtetschenski-Milinski [1]. Table 2.1 illustrates the projected area of different types of pedestrians. Many measurements on people of different age and different clothes influenced the average values demonstrated in that table. The size of the individual corresponds to the size of the individual at breast (thorax) height.

3.8 Climatic parameters (weather conditions)

Man is not able to control the forces of nature, however, they can control and affect man. The forces of the nature are powerful and are able to influence people's behaviours. People prefer certain kinds of weather over others. For this reason and for the achievement of more realistic simulations, we must consider at least three different types of weather conditions that affect indirectly the pedestrian walking speed:

- Dry: clear (no precipitation), with dry roads and dry pavements.
- Rain: any type of rain from mist to moderate rain is not comfortable for walking people. During heavy rain pedestrians tend to go faster inside.
- Snow: when there is snow or ice in the atmosphere, on the road or pavement, or both, pedestrians take care and walk slowly to prevent slipping.

The weather parameter influences the velocity and the fitness (physical condition) of the individual. Richard L. Knoblauch [69] found relevant results about the functional relation between the pedestrian walking speed and weather condition. The data was collected on weekdays during daylight conditions. Surface conditions, weather conditions and the estimated wind intensity were recorded for each observation.

The analysis of the collected data showed that the mean walking speed was strongly affected by the weather and environmental factors. The collected data indicated also a relevant effect of age and of each the weather and environmental characteristics. This confirmed that weather plays a significant role in pedestrian movement in open air, hence the weather parameter must be considered in order to achieve more realistic simulations.

3.9 Psychology parameters

Till this moment the psychological factors affecting the behaviour of pedestrians are not completely understood. The decision making in human behaviour at any time is affected by the psychology of the individual, therefore it is very important to consider the psychology factors in the simulation model [113]. Psychologists have extensively studied human characteristics and behaviours. Many investigations and researches show that differences in human behaviours are influenced by many factors, including differences in stimuli, physiological and cognitive state, social and cultural environment, previous life experiences and individual characteristics [114]. Despite this diversity, factors influencing direct human behaviours

can be classified into some basic variations. In the case of panic conditions or dangerous situations, the physiological state of individuals becomes very important in making decisions in a short time. Until now, it has been very difficult to describe and model the psychological state of pedestrians in normal and dangerous situations and to establish a quantitative relation between the walking speed and the mental state of individual. We will include these factors in our simulation.

Figure 3.1: Crowd gathering to the Al-Tahrir place in Cairo (Arabic spring revolution). This crowd is referred to as an emotional crowd. A lot of physical and psychological parameters affecting the behaviour of the individuals within the crowd.

3.10 Illustration

The motion of a single pedestrian at any time is governed by several parameters. The direction and speed will be the result of a long list of possible (and very likely conflicting) forces and circumstances. We mention in particular the motivation to reach a certain place at a certain time (often referred to as will-force), time constraints, importance of punctuality, location constraints, importance of reaching a place and staying there long enough, etc.

Changes in the desired velocity of a single pedestrian have been attributed to a number of factors, including body composition and functional capacity. The most important parameters and circumstances influencing the pedestrian's movement in emergent or normal behaviour are demonstrated in the following graph, (see

fig. 3.2).

In figure: 3.2 illustrates how the measurable quantities of pedestrian motion, will force ($\vec{f}_w$), desired velocity ($\vec{v}_d$), and relaxation time (τ) are interrelated with the external and internal circumstances. They all have to be considered in realistic simulations, in which one calculates the average local density $\rho(\vec{r}, t)$, average local speed $\vec{v}(\vec{r}, t)$ and the average local flow $\vec{q}(\vec{r}, t) = \rho(\vec{r}, t)\vec{v}(\vec{r}, t)$.

3.11 PEDESTRIAN DATABASE

The evolution and design of pedestrian simulation models requires a lot of information and data. All these parameters (e.g. velocities and physical characteristics,...) are taken from observations of real pedestrian movement and their interactions at different events and places. The pedestrian parameters are taken from image data, so called empirical data. These data are obtained using a video camera or human detectors. The parameters are derived from real-world observations. They are very important in understanding the factors influencing how to alter crowd dynamics in different situations. The simulation input takes advantage of these parameters to achieve a certain realism in the simulation.

3.11.1 Data management

The management of the huge amount of information and parameters concerning pedestrians requires the set-up of computer databases and test systems.

Fig: 3.3 shows an example of the input of the simulation. These simulations represent complex interactions between individuals and their physical environment. For this reason considering all the parameters illustrated in the PedGUI can be advantageous for more realistic simulations. These factors attempt to predict pedestrian movement in both normal and panic situations, and in the PedGUI these options will be considered. The percentage of men and women, old and young people, and the ethnic origin of the pedestrians can be considered in the crowd simulation input. With the help of this system we can achieve, firstly more realism in the simulation and secondly a database of different ethnic groups that can be used for other purposes and studies.

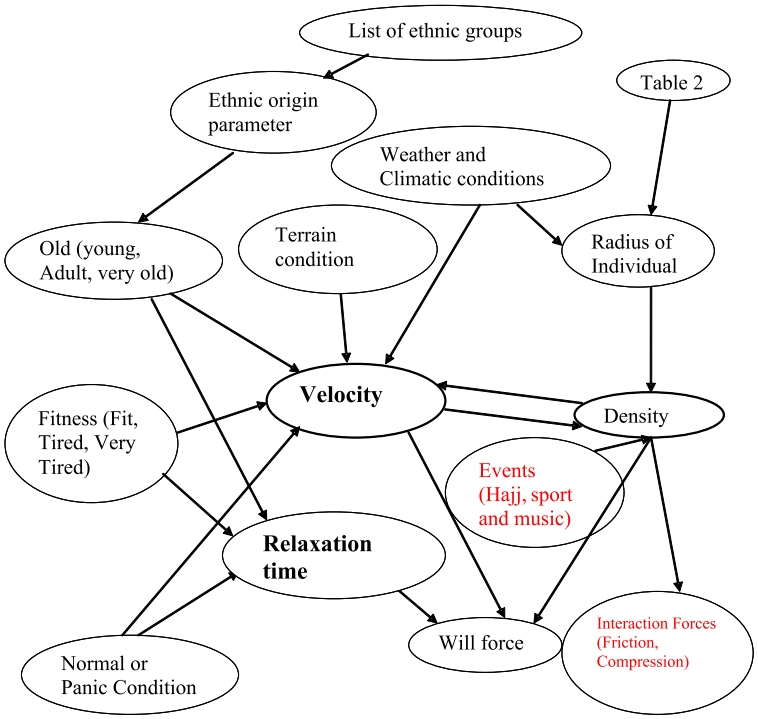

Figure 3.2: Graphical illustration of the list of circumstances influencing pedestrian movements.

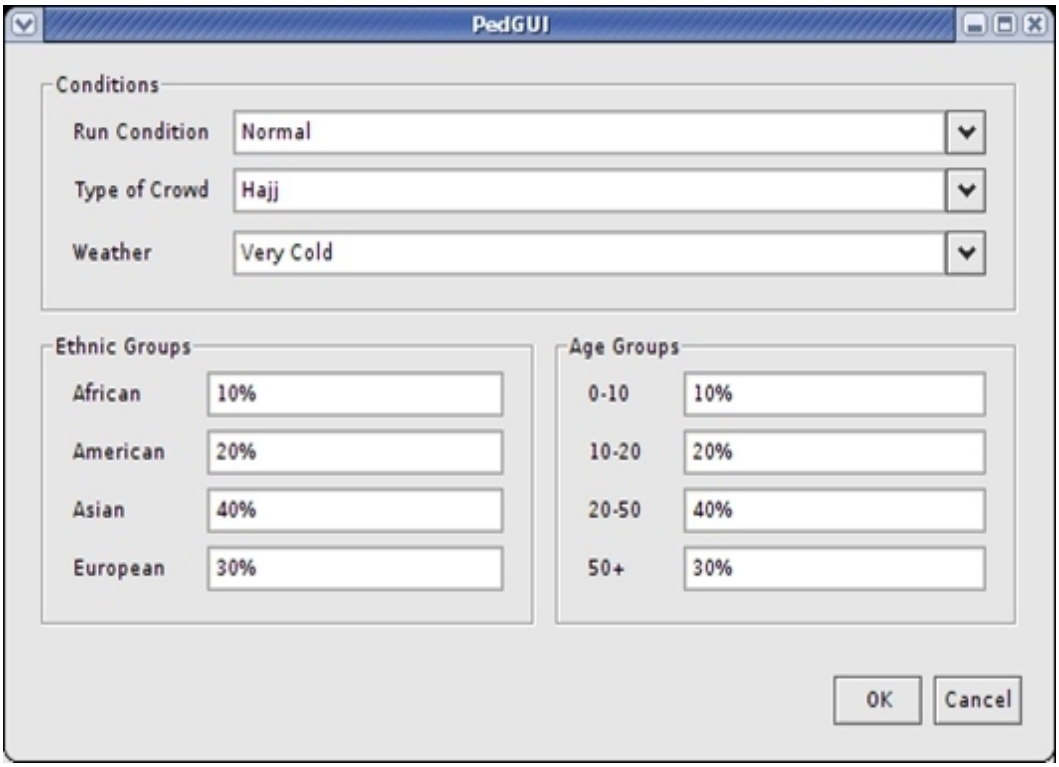

Figure 3.3: PedGUI user interface.

CHAPTER 4

ANALYSIS OF THE VIDEO RECORDING IN HAJJ 2009 (MATAF AREA)

4.1 INTRODUCTION

The electronic and digital revolution in video techniques during recent years has made it possible to gather detailed data concerning pedestrian behaviour, both in experiments and in real life situations [115, 116, 117]. The big challenge is to develop a new efficient method of defining and measuring basic quantities like density, flow and speed. Basic quantities of pedestrian dynamics are the density ρ [1/m^2] in an area A and the velocity $\vec{v}$ [m/s] of persons or a group of persons, and the flow through a door or across a specific line $\vec{Q} = \vec{v}(r,\vec{t})\rho(\vec{r},t)$ [1/s]. The measurements also yield mean values of these quantities. The task is to improve the given methods such that they allow to go fairly close to the real data of the crowd quantities. The methods presented here are based on video tracking of the head from above. Note that tracking of e.g. a shoulder or the chest might be even better, though more difficult to obtain.

The density distribution knowledge in a very crowded area allows us to draw a so called density map to show us congestion directly as regions of high density. The relationship between the pedestrian density ρ and the pedestrian maximum walking speed v_{max} are formalized into a graph known as the fundamental diagram $v_{max} = f(\rho)$ [8]. Since pedestrians move slower in a region of high density, the simulated particles should update their speed with the surrounding circumstances to maximize their rate of progress towards their goals.

4.1.1 Data collection and type of observation

Tawaf observations at the Haram mosque in Mecca were made during Hajj 2009 by Mr. Faruk Oksay. The Mataf area has 10 entrances / exits. The flow of the Tawaf is controlled. All pilgrims begin and end their Tawaf at the same place, (see fig.4.1). The number of pilgrims during this period is sufficient to observe

the behaviour of high density crowd dynamics.

Figure 4.1. shows the main gate doors, side entrances, stairs to the Mataf open air of the Haram.

All observations took place on Friday November 27th 2009 corresponding to 10th of Dhu al-Hijjah 1430 Hijri in the afternoon. During the total observation period of three hours, three prayers (Midday, Asr and Maghreb (sunset-prayer)) were performed, where in this time the Mataf area comes to a standstill, (see fig. 4.2). Our video observations show that the pilgrims have the desire to be near the Kaaba. Therefore approximately 70 percent (visually detected on video) of the pilgrims perform their Tawaf movement near the Kaaba wall, which causes a high density in this area.

In Figure 4.2, one can see all of the pilgrims perform the prayer ritual in the holy mosque in Mecca.

The Tawaf around the Kaaba is a periodic movement for the time between two prayers. The observed number of pilgrims performing their Tawaf ritual at the Mataf area increases slowly after every prayer until the Mataf attains it's maximum capacity, (see fig. 4.3).

Figure 4.3 shows a typical pedestrian movement in the Mataf area over daytime. During prayer times individuals stand still and therefore movement equals approximately zero. The fluctuations in the velocity flow are created by the turbulence in the pedestrian flux. Note that the average local density in a specific location in the Mataf area exceeded 8 persons/m^2 during the Hajj periods, (see fig.4.7).

4.1.2 Goals

Our first goal is to identify new methods and create a test system capable of extracting pedestrian movement information from video, similar to that collected by our HD-Cameras in the Hajj-2009, such that any movement can be analysed to spot suspicious activity. This task to collect pedestrian data and extract pedestrian motion from video sequences required an involvement and development of appropriate methods, followed by further analysis of this data to identify emergent motion or crossing trajectories.

The secondary goal is to identify the limitations of the approach including the system and data requirements for the techniques to work more effectively. More specific, the project goals are:

- Develop a framework for video and image analysis,
- Develop an approach and relevant diagnostic software to collect movement

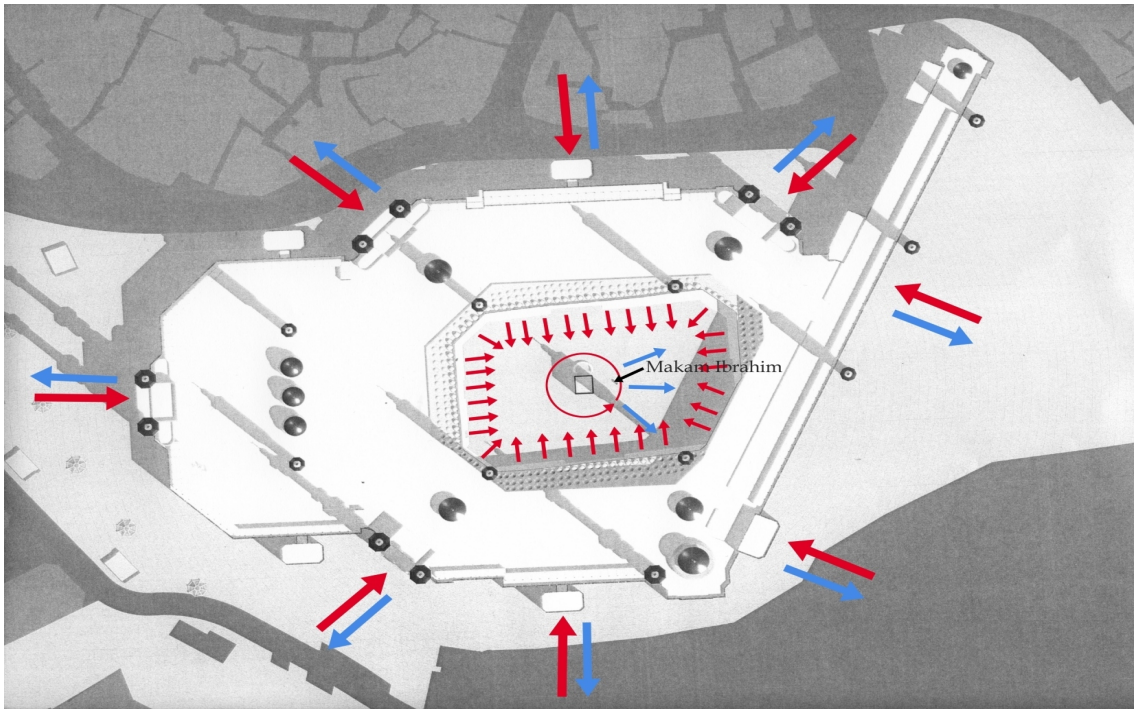

Figure 4.1: Overview of the Mosque with entrance doors.

data from video,

- Identify the requirements for such methods to work effectively, such as image quality, resolution and orientation,
- Identify how to interpret movement information,
- Interpret the movement data and examine abnormal behaviour,
- Design and produce a working implementation that demonstrates the above goals,
- Identify approaches that could further improve the system.

4.2 Estimation of crowd density

There are different techniques developed to extract information describing the position of pedestrians in a location, but not all of them are appropriate for detecting and pursuing pedestrian movement under different and extreme weather conditions. In their published work [118], Papageurgiou and Poggio developed a system attempting to recognize human figures based on pixel similarities through a large training set of figures under various light and weather conditions. To

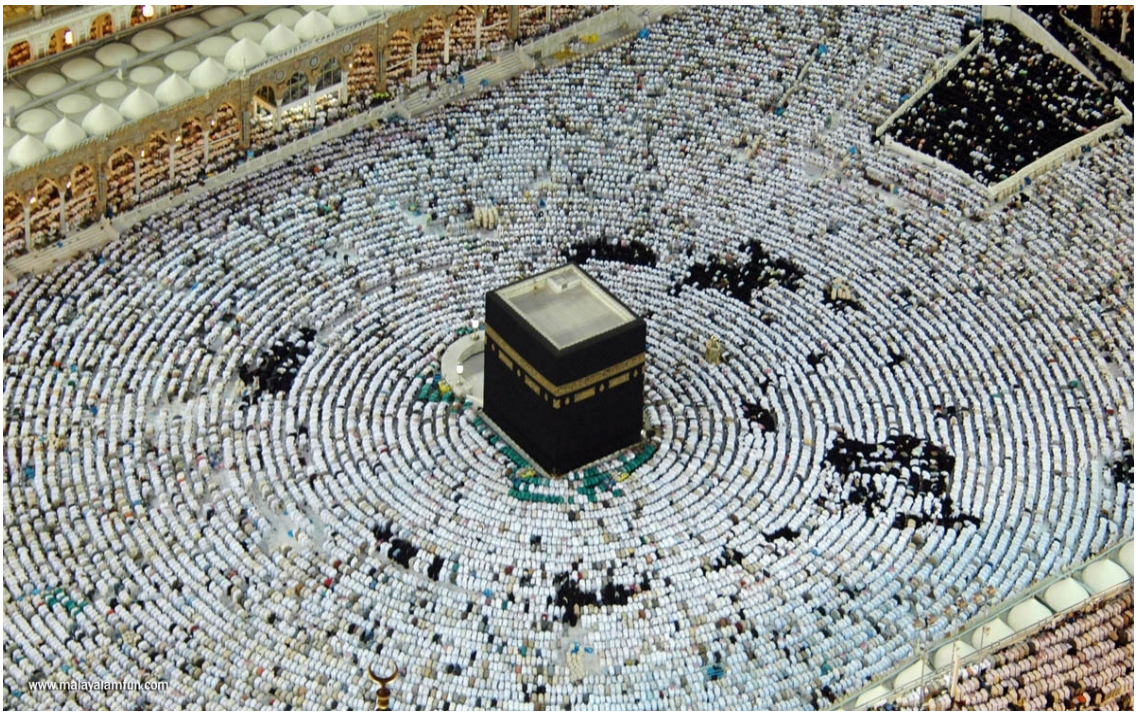

Figure 4.2: Pilgrims performing the prayer ritual in the Mosque in Mecca. During performance of prayer the Tawaf comes to a standstill, there is no movement around the Kaaba.

identify the movement of the figures, the system analyses the similarity between matches of consecutive frames. This method works quite well when the training set is large, but requires a high computational efficiency which achieves processing rates of 10 Hz [118]. The study shows that accurate recognition can be done with coarse image data.

Another approach to estimate crowd density is based on texture analysis. Velastin et al. [119] assumed that crowds with high density possess texture properties. The proposed method, texture features were computed for the whole image and applied to crowd density estimation [120]. In particular, all displayed textures, like wavelets [121, 122] and the gray level dependence matrix [123, 124], were used to estimate crowd density. The results exhibit, how effective statistical analysis of texture display is compared to neural networks when measuring crowd density. Unfortunately, this system examines only static images and cannot cover crowd motion, but the techniques can be used to track pedestrian movements.

Other strategies based on image segmentation were pursued by Heisele and Woehler [125], where raw data is filtered to split the image into segments, which are then analysed. Those images that match particular shapes are analysed further. This approach allows to distinguish different images with common color

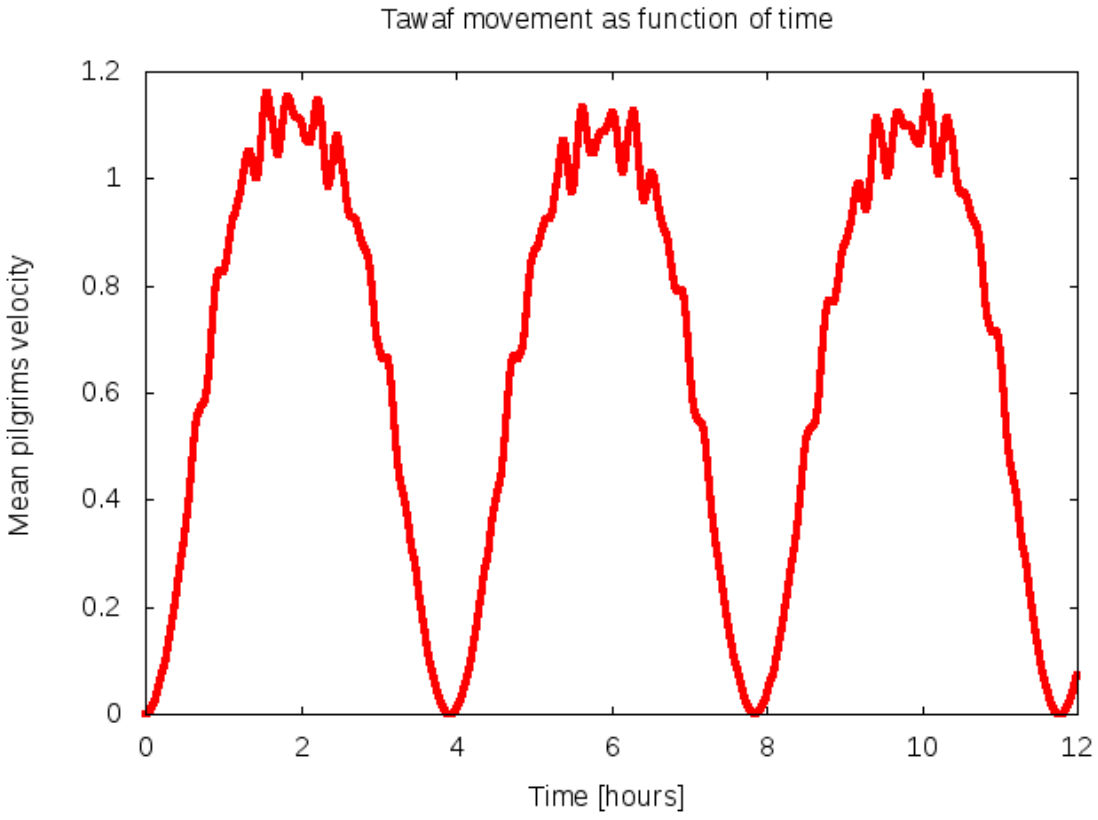

Figure 4.3: Mean velocity of pilgrims in the Mataf area as a function of time over 12 hours.

and luminescence.

4.2.1 Data

The required data on pedestrian behaviour (e.g. density-effect, shock-waves-effect,...) in the Haram can be done from our video recordings. All observed effects can be analysed by simply watching the recorded videos. But if we want to extract data like walking speeds from such observations we have to examine the videos frame by frame. This is very time consuming. As a result of this, and the need for more efficient data, the idea arose to use an automatic detection system. At that time no sufficient system was available for the detection of human bodies, therefore some essential requirements were formulated. From the requirements we derived an idea to formulate an image processing system with the help of other programs, such as Optical Flow with OpenCV (http://opencv.org/) and Quest3D (http://www.quest3d.com/). The materials used for this test are videos recorded at an outdoor piazza of the Haram mosque in Mecca where people congregated at different times during one day, simulating a surveillance application.

The data content had a wide range of crowd densities, from very low to very high. Three different data-sets, labelled morning observation, afternoon observation and combined observation (before and after the prayer times) were used. Each data set had 20 selected images with high resolution. Examples of images are shown in figure 4.4 and 4.12. In order to collect pedestrian data and to study pedestrian traffic flow operations on a platform in detail, observations were also made from a platform of the Haram Mosque in Mecca. These observations concerned pilgrim walking speeds and density distributions on the Mataf area and (individual) walking times as functions of the distance from the Kaaba wall.

4.2.2 Methods

Manual estimation of crowd density

The estimation of crowd density is an important criterion for the validation of our simulation tools. Processing is done in three levels.

- Existing footage is loaded on a 3D program as a backplate.
- From several provided 2D- architectural drawings we build a 3D model of the mosque.
- A virtual camera has to be matched in position, rotation and focal length to the original camera so that the features of the 3D-model match the features of the filmed mosque. As the dimensions of the mosque are known, we then establish a grid of regular cells on the Mataf area, each one of which has a size of 5mx5m, (see fig.4.5). Through image editing software, we start a manual counting process. This regular grid is used to observe the density behaviour over all of the Mataf area, from the nearest range to the Kaaba wall up to outside of the Mataf and the accumulation process (by the Black Stone and Maquam Ibrahim). The results of this investigation are shown in figures 4.6 (a), (b), (c) and (d) and illustrate us the behaviour of the pilgrim density on the Mataf area at different times during the day.

With a new computer algorithm developed within this investigation, where the Mataf area is divided in regular cells. The number of pedestrians in every cell as function of time is determined through repeating the counting process many times. The average value is identified as local density $\rho(\vec{r}, t)$. The data extracted from the videos allowed us to determine not only densities in larger areas, but also local densities, speeds and flows. As an example the density distribution on the Mataf area is shown in figure: 4.6. The data was obtained by semi-manual evaluation.

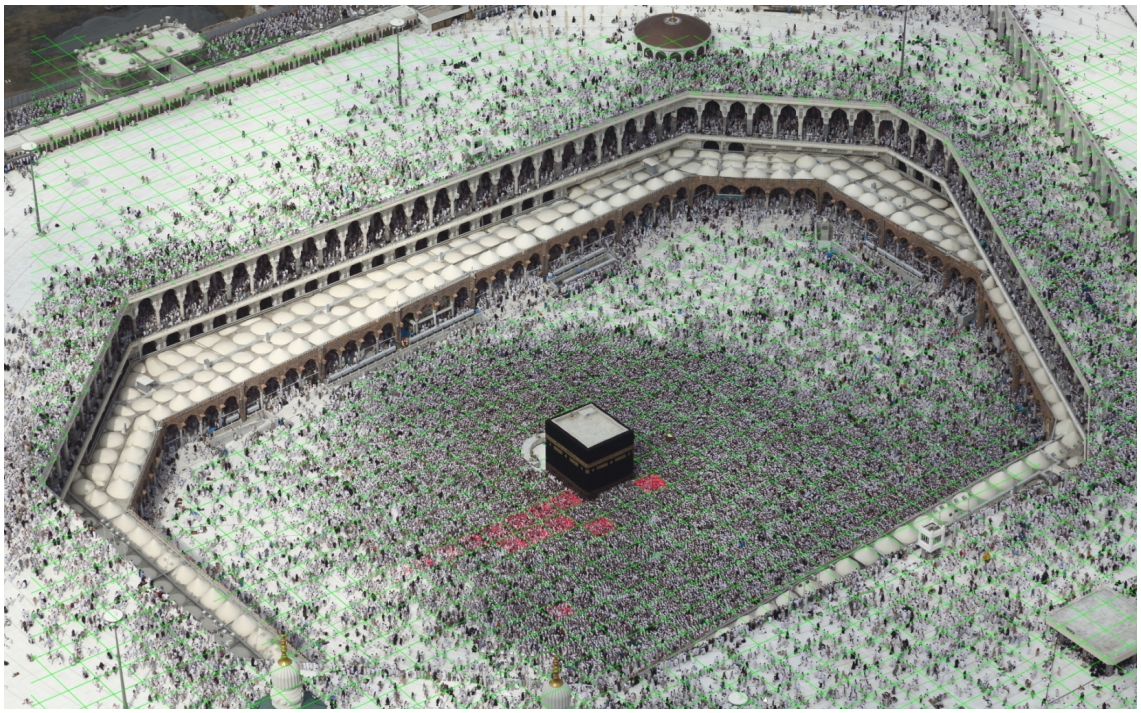

Figure 4.4: The Haram piazza top view (observation area).

The results of the estimation based on the statistical method, presented in tables 4.1, 4.2 and 4.3, reached a mean of 92 percent correct estimations. Table 4.1 shows the results obtained by the counting method of three different persons, which reached a mean of approximately 97 percent correct estimations (average deviation of 3%).

Distance from the Kabaa (m)	Density (p/m^2)
0	6,32
5	6,16
10	5,72
15	4,92
20	3,88
25	3,44
30	2,64
35	1,68
40	1,32

Table 4.1: The density distribution on the Mataf before Mid-Day Prayer.

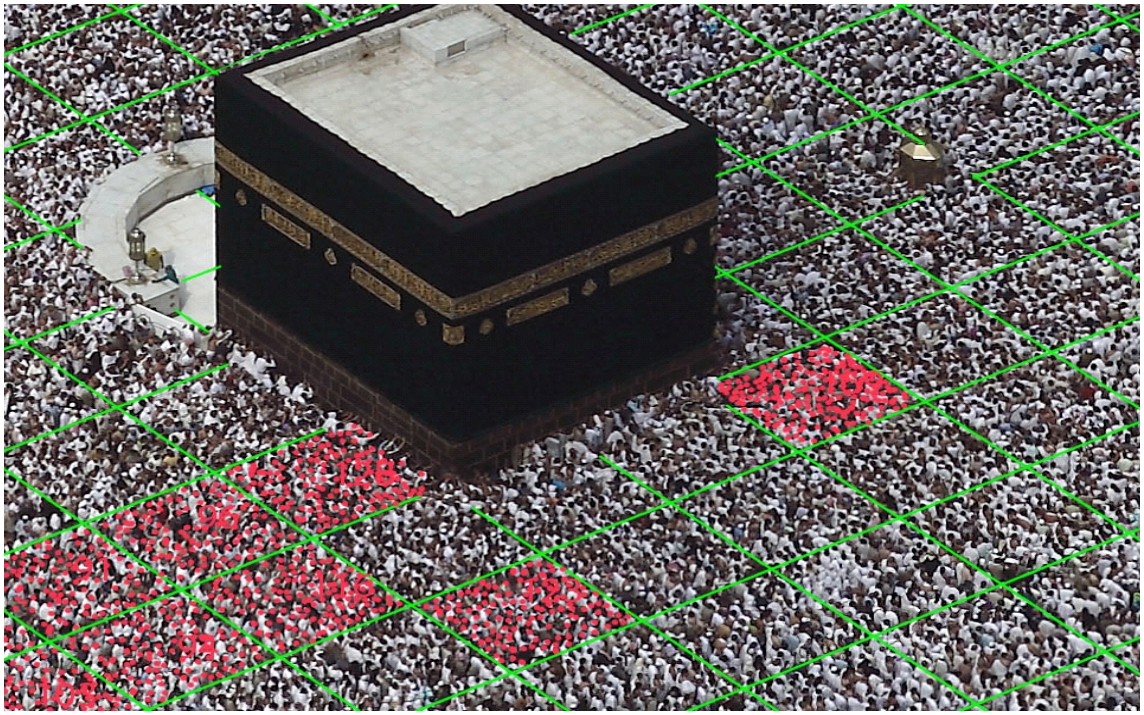

Figure 4.5: Grid of regular cells with dimension of 5m×5m.

Dependence of the density distribution on the Mataf as function of time

Figure 4.6 shows density decline curves for different distances from the Kabaa in a specific time. The curves indicate that the local density amount vary strongly over the (0 < x < 40 m) range.

Figure:4.7 shows the pedestrian density distribution on the Mataf area as a function of the position $\vec{r}$ and time t. One clearly recognizes density waves, with maximum density package near the Kaaba wall. There the average local density can reach a critical value of 7 to 8 persons/m^2. The congested area increases the local density to a critical and dangerous amount. As a consequence the pedestrians begin to push to increase their personal space and create shock-waves propagating through the crowd, which can be seen as density waves, or density packages.

The Density map illustrates how the pedestrian density decreases from the inside to outside of the Mataf area, (see fig. 4.8). As we have mentioned that in the Mataf area pedestrians move in the restricted space, the layout is gradually painted in different colors. The color of every point of the space corresponds to the current density in this particular area. The density map is constantly repainted according to the actual values: when the density changes in some point, the color changes dynamically to reflect this change. In case of zero density the area is not painted at all, (see fig. 4.8 (a), (b), (c) and (d)).

Distance from the Kabaa (m)	Density (p/m^2)	Density (p/25m^2)
0	5,12	128
5	3,84	96
10	3,64	91
15	2,6	65
20	2,16	54
25	1,28	32
30	1,2	30
35	0,68	17

Table 4.2: The Density distribution on the Mataf shortly after Mid-Day Prayer.

Distance from the Kabaa (m)	Density (p/m^2)	Density (p/25m^2)
0	6,56	164
5	4,16	104
10	3,36	84
15	3,2	80
20	2,76	69
25	1,92	48
30	1,4	35
35	1,2	30
40	0,84	21

Table 4.3: The Density distribution on the Mataf half-hour after Mid-Day Prayer.

During the rush hour in a Hajj period the local density in the Mataf area reaches the maximum as we can see in the following figures 4.7 (d) and 4.8 (d). The local density can reach 8 to 9 persons/m^2 in a specific time during the day. The maximal density concentrates near the Kaaba wall.

Densities over time and space

We observe the density behaviour on the Mataf area at different times during the day, before and after the prayer, and we compare this density with the simulation density results. The maximum registered density was 7 to 8 persons/m^2 and this represents a high crowd density. The results of the estimation based on the statistical method, presented in figures 4.6, 4.7 and 4.8, reached a mean of 92 percent correct estimations. It is possible to verify that the results were quite good for all evaluated images except for the one made up of high density crowd images, which reached only 84 percent correct estimations. In the Mataf area, near the black stone, the pilgrim density reached over 9 persons/m^2. For this reason

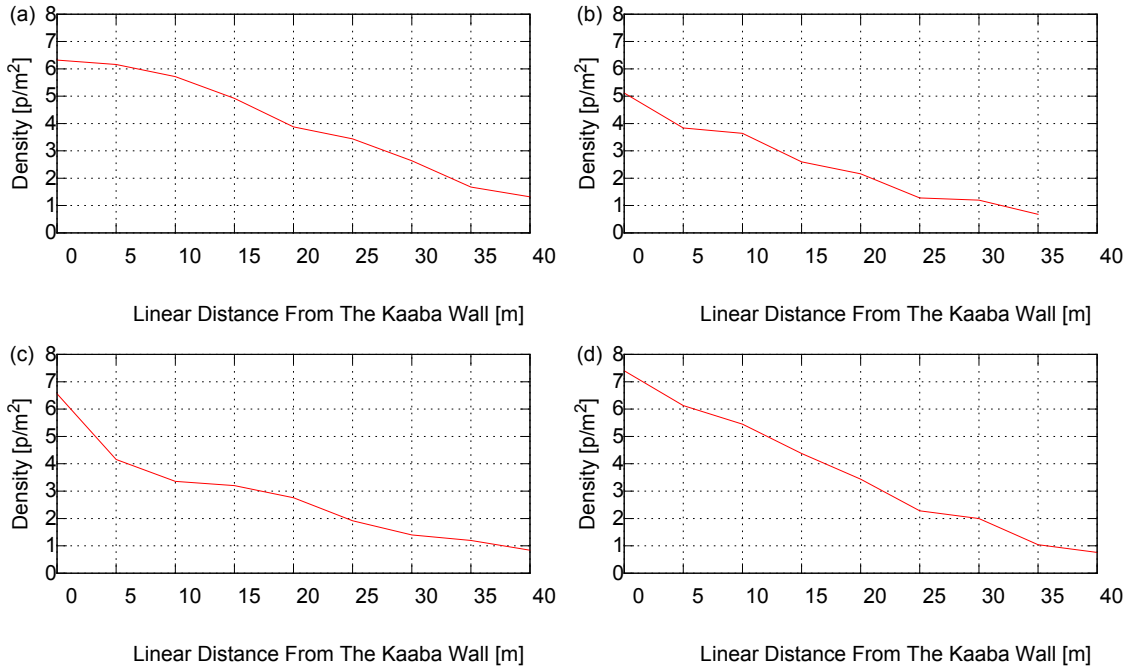

Figure 4.6: Decrease of pedestrian density on the Mataf Area as function of the distance from the Kaaba wall: (a) before Mid-Day prayer; (b) shortly after Mid-Day Prayer; (c) half-hour after Mid-Day Prayer; (d) Rush Hour.

it is very difficult to recognize and track every head and as a result, a 100 percent correct estimation would be very difficult. All statistical results illustrating the density distribution at the Mataf area at different time intervals are demonstrated in the Fig: 4.9.

4.2.3 Automatic estimation of crowd density

This part of the dissertation considers the role of automatic estimations of crowd density and their importance for the automatic monitoring of areas where crowds are expected to be present. A new technique is proposed which is able to estimate densities ranging from very low to very high concentrations of people. This technique is based on the differences of texture muster on the images of crowds. Images of low density crowds exhibits rough textures, while images with high densities tend to present finer textures. The image pixels are classified in different texture classes, and statistics of such classes are used to estimate the number of people. The texture classification and the crowd density estimation are based on self-organizing neural networks. Results obtained estimating the number of people in a specific area of the Haram Mosque in Mecca are presented in figure 4.10).

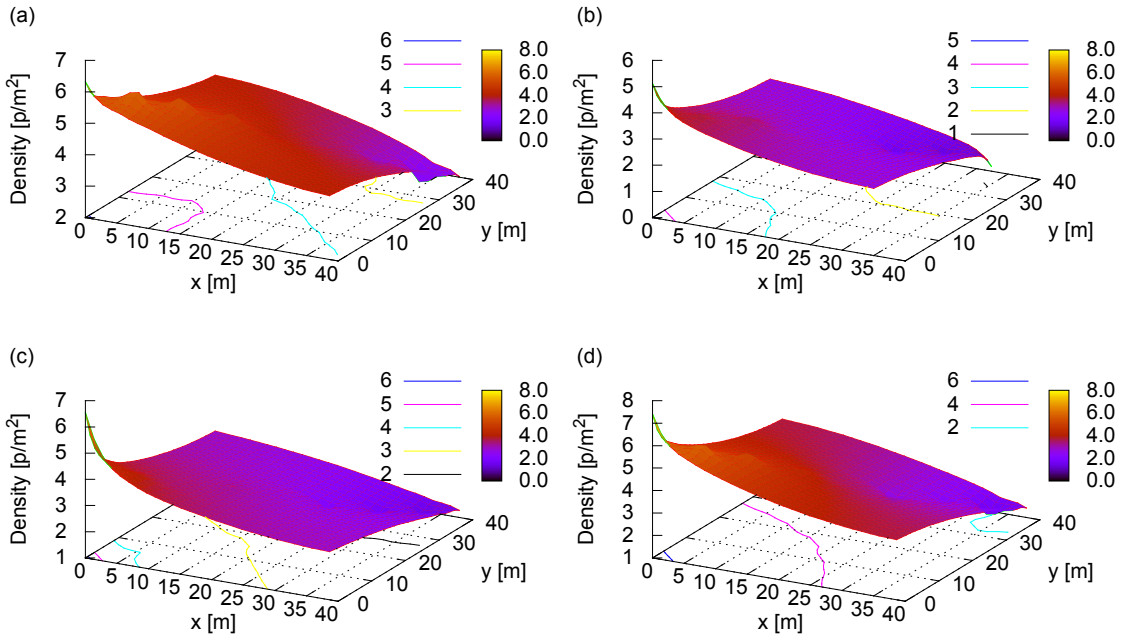

Figure 4.7: The Density Distribution on the Mataf Area $\rho(\vec{r}, t)$ with $\vec{r} = (x, y)$. The figure also shows the density index (persons/m^2). (a) before Mid-Day prayer (t = $t_{before\ Mid\text{-}Day}$); (b) shortly after Mid-Day Prayer (t = $t_{shortly\ after\ Mid\text{-}Day}$); (c) half-hour after Mid-Day Prayer (t = $t_{half\text{-}hour\ after\ Mid\text{-}Day}$); (d) Rush Hour (t = t_{Rush}).

4.2.4 Data analysis

In the latter paragraphs we focus on crowd density estimation for several reasons. According to the crowd disasters study by Helbing and Johansson [5], one of the most important aspects to keep a crowd safe is to predict and identify areas with high density crowds preventing large crowd pressures to be built up. Areas where crowds are likely to build up should be identified prior to the event or operation of the venue. This is important as crowds usually exist in certain areas or at particular times of the day. Places where crowd density rises up over time are likely to congest and need careful observations to ensure the crowd safety. Basically, crowd density surveillance and estimation can be a good solution for management and controlling the crowds safety.

The results of the estimations obtained during the tests allow us to consider both methods successfully. While the statistical method reached quite good estimation rates (around 92 percent) for most groups, the spectral method illustrated small deviations between the best and the worst estimations, reaching on average almost the same rates of correct estimation obtained by the statistical method.

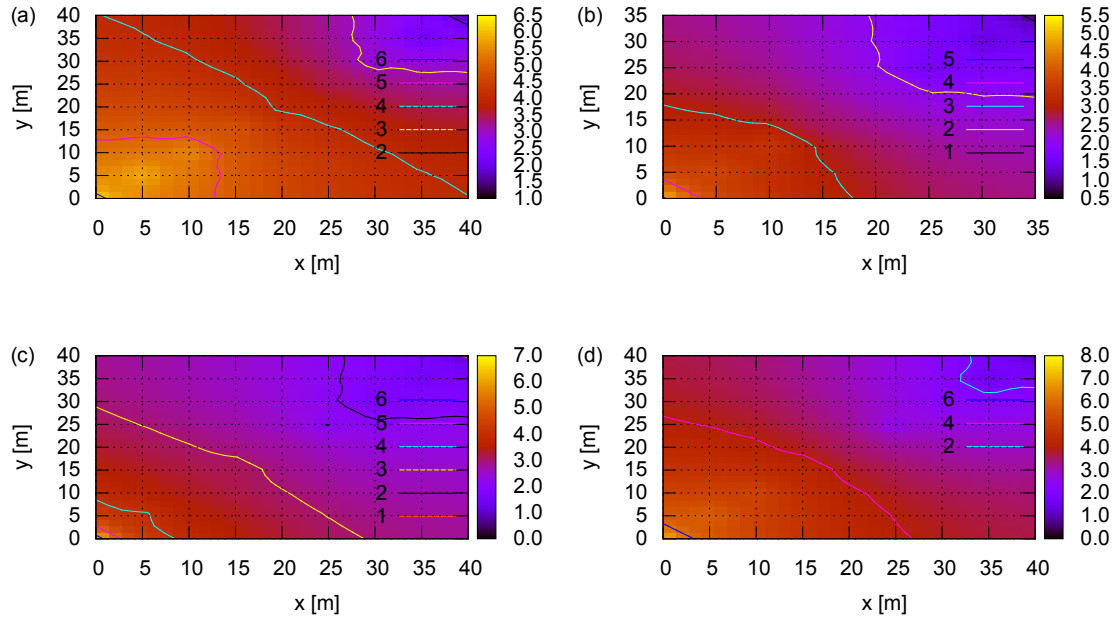

Figure 4.8: The Density map indicates that the highest pedestrian density in the area of the Kaaba: (a) before Mid-Day prayer; (b) shortly after Mid-Day Prayer; (c) half-hour after Mid-Day Prayer; (d) Rush Hour.

4.3 Method of determining the pedestrian speed

As speeds are hard to observe, walking times were measured, from which walking speeds were derived. In addition to walking times and pedestrian densities other variables needed to be considered to complete the input of the simulation model (such as the number of in and out going pilgrims and the configuration of the structure during the rush hour at the Hajj period). The observables are the walking time, velocities and the corresponding densities of the pilgrims performing their Tawaf and Sa'y. The movements of the pilgrims going in and out of the Haram give us data to calculate the flux related to the Tawaf. The distribution of both in and out going pilgrims over the Haram can be derived from this data. The second type of observation concerns individual walking times. In order to measure the pilgrims' walking times in and out of the Haram, pilgrims were recorded from the moment they started walking from one spot to another, either on the piazza or going up the stairs. The start and duration of activities, such as Tawaf or Sa'y, were measured also. Finally, locations of origin, destination and possible activities of the pilgrims were registered. To do this, the piazza is divided into small areas with a length of 5×5 meters. We also recorded the movements of the pilgrims at specific moments, such as prayer times when the

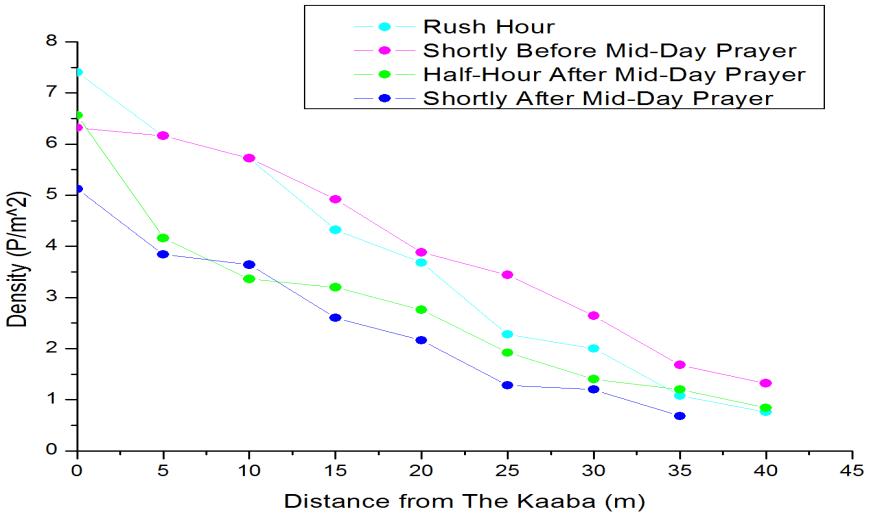

Figure 4.9: Crowd density on the Mataf area in different time intervals. Highest density in the area of the Kaaba.

number of pedestrians increases dramatically. Therefore, cumulative flow curves can be constructed, out of which densities can be derived. These curves can be compared with the reference curves of Predtetschenski-Milinski [1].

Subject selection

Data was collected on a specific subject group of pedestrians who appeared to be 40 years of age or older. On the roof of the Mataf area we selected our tracking subjects, consisting of adult men, women and people in wheelchairs. The following individuals were specifically not considered:

- Children under 13 years of age,
- Pedestrians carrying children, heavy bags, or suitcases,
- Pedestrians holding hands or assisting others across the Mataf,
- Pedestrians using a quad pod cane, walker, two canes, or crutches.

To accurately quantify the normal walking speeds of the various subject groups, pedestrians who exhibited any of the following behaviour were also not considered:

- Crossing of the Mataf path diagonally,
- Stopping or resting in the Mataf area,

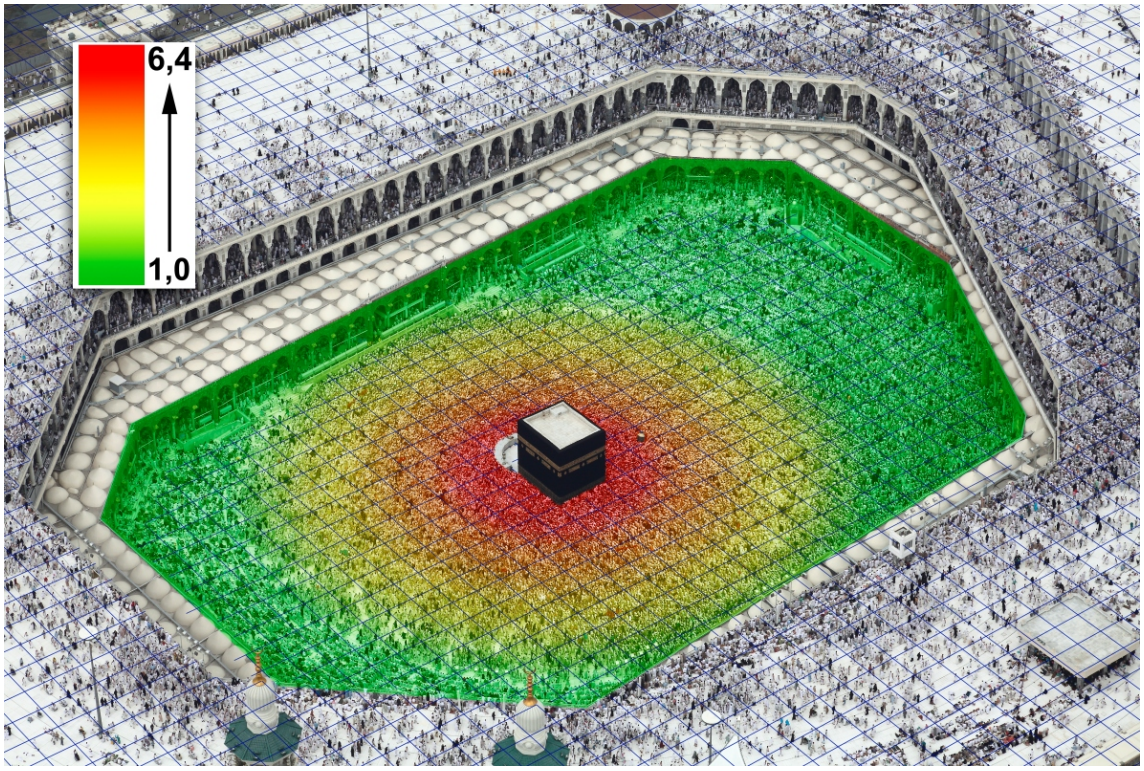

Figure 4.10: Density distribution in the Mataf area before Mid-Day prayer. Red color indicates high density, where green color indicates low pilgrims density.

- Entering the roadway running (anything faster than a fast walk),

The pedestrian sex (male or female) of each individual in the Mataf area was recorded, as well as whether he or she was walking alone or in a group. The group size was also noted when applicable. A group was defined by two or more pilgrims walking the Mataf trajectory at about the same time, regardless of whether or not they were apparently friends or associates. In the Mataf area, the pedestrian groups can reach 30 pilgrims walking together in the pedestrian stream. In addition, subjects paths were monitored to determine when they started and ended their Tawaf. Being inside the Mataf was defined as being within or on the painted Tawaf walking lines. Other pedestrian behaviour was recorded when if occurred:

- Confusion (hesitation, sudden change in direction of travel or change of point of interest) exhibited before walking,
- Confusion exhibited after entering the Mataf trajectory,
- Cane use,
- Following the lead of other pedestrians,

- Stopping in the walking path during the Tawaf movement,
- Difficulty going into Mataf,
- Difficulty going out of the Mataf.

Several methods were developed to check the accuracy and performance of walking speed estimation abilities of the observers. First, the walking speed was measured at the same time by three observers, then correlations between the estimates of all observers were determined. In particular, the walking velocity of one pilgrim was measured by the three observers and the mean value was taken. The results of these verification procedures are discussed after the next section.

4.3.1 Methods

Manual

From our video recordings we chose places between two minarets as references, (see fig.4.11). As the dimensions of the mosque were known, we then established a grid of regular cells covering all of the Mataf area, each one having a size of 5mx5m, (see fig.4.12). The distance between the two minarets is known. Pedestrian crossing times were measured with a digital timer and an electronic stopwatch was implemented and synchronized with the timer of the video recorder. The watch was started as the subject stepped off the first minaret and stopped when the subject stepped out on the opposite minaret after crossing all the distance between the two minarets.

Verification of observer walk-speed estimates and start-up time measurement

From the roof of the Mosque every pedestrian can be identified. To establish the ability of the field observers to identify the fitness level or the age of pedestrians with high accuracy a simple verification procedure was performed. The age estimation and the level of fitness of the pedestrians was based on their walking speed. It is a physio-medical fact that older pedestrians walk more slowly than younger ones (this is easily supported by field data), however, the published or already existing data on walking speeds and start-up times (i.e. the time from the beginning of a Tawaf movement until the pedestrian steps off the Mataf) have many shortcomings. Here we consider the complicated movement of the Tawaf and the human error rate of the observer. The walking speed on the Mataf area can be affected by many factors, one of the relevant factors is the age of the pedestrian. This demonstrates that the observations were quite good at identifying older pedestrians or pedestrians with fitness deficiency or physical

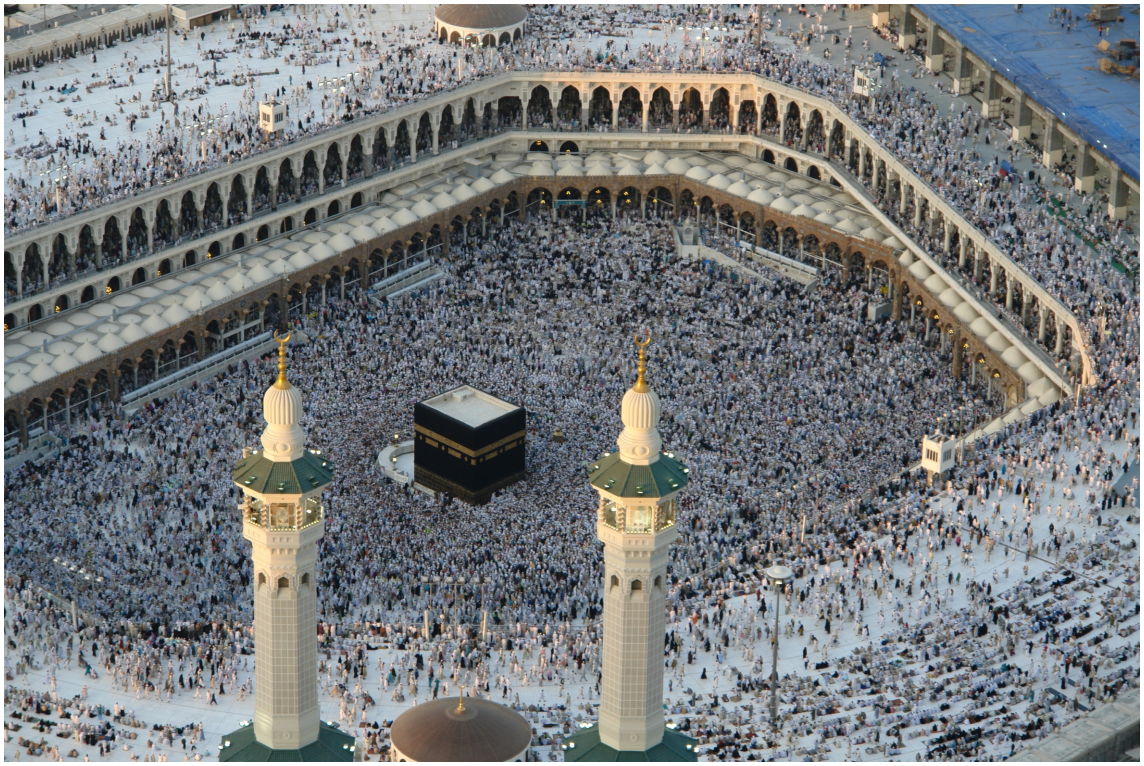

Figure 4.11: Overview of the piazza of the Haram, the place where our observations are made. With a digital clock the individual walking times t_p are measured. Since the distance between the two minarets is known from the architectural plan of the Haram, the average of the local pedestrian velocities $v(\vec{r},t) = \parallel \vec{v}(\vec{r},t) \parallel$ can be determined.

health problems. A digital stopwatch was integrated with the video recording sophisticated for the measurements of pedestrian crossing times. The crossing times of the same pilgrims were measured during five rounds of the Tawaf and the average value was determined.

Pedestrian walking speeds results

This research also examined the impact of the building layout on the pedestrian speed distribution and the pedestrian density of pilgrims performing the Tawaf movement around the Kaaba. The set of data of pedestrian walking speeds which were obtained through analysing video recording using a set of statistical techniques are displayed in figures 4.13 (a), (b) and (c). The results revealed that walking speed seems to be following a normal distribution no matter of male, female, older or younger. The average speed of young people is dramatically larger than that of older people, and the average speed of male is slightly larger than that of female. The width of the obtained curves is related to the different standard deviations.

The mean computed walking speed represents the speed that 85 percent of pedestrians did exceed. A total of 250 pedestrians were observed. Included were 100 male pedestrians of about 60 years of age, 100 women pedestrians and 50 wheelchair pedestrians. This data describes all of the pedestrians observed: those walking in the center of the stream and those walking by the edge of the Mataf trajectory. As is subsequently described, those who were walking by the edge of the Mataf tended to walk more quickly. All observed pedestrians moved in a rotational motion around the Kaaba counter-clockwise (Tawaf), in compliance with the pilgrim stream.

The mean walking speed for male pedestrians was 1.37 m/s and 1.22 m/s for female pedestrians. In conjunction with pilgrims old, the mean walking speed for younger pedestrians was 1.48 m/s and 1.20 m/s for older male pedestrians. The results revealed that the average walking speed for young women are 1.32 m/s and 1.12 m/s for old women. This means

- Young male pedestrians had the fastest mean walking speeds [1.48 m/s] and older females had the slowest [1.12 m/s]. The differences between young men and young women [0.16 m/s] and between older men and older women [0.1 m/s], this result shows a little deviation that can be traced back to the fitness level of pedestrian or other factors, in the normal condition are approximately the same. The mean walking speed for the younger pedestrians ranged from 1.37 to 1.57 m/s across all conditions, with an overall mean speed of 1.48 m/s. The means for the older pedestrians range from

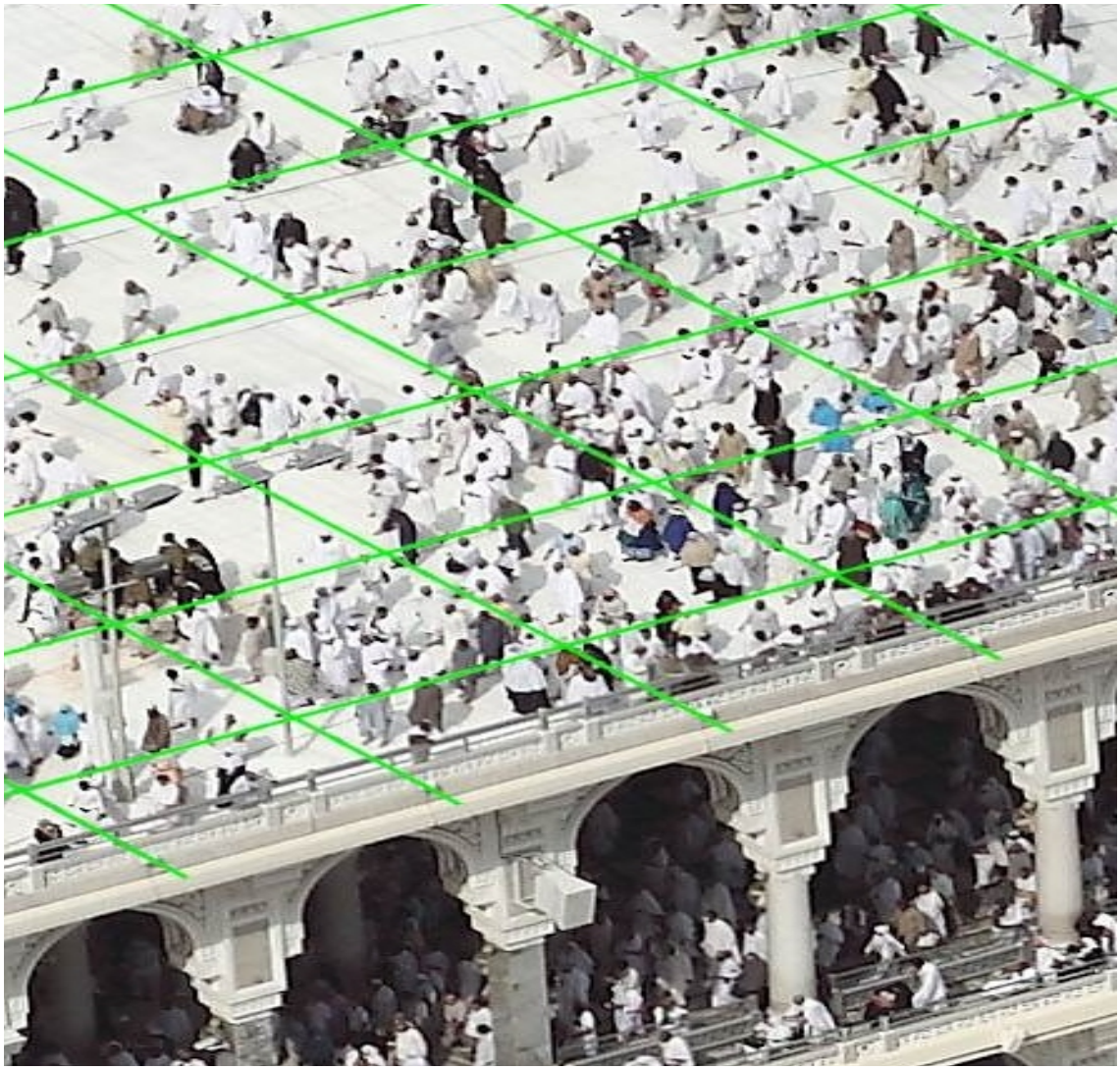

Figure 4.12: Grid of regular cells with dimension of 5m×5m. With the help of the regular cells and the distance between two minarets in the Haram, (see fig.4.11) the (individual) walking times t_p are determined and the average of the local speeds $v(\vec{r},t) = \parallel \vec{v}(\vec{r},t) \parallel$ is calculated. The average walking speed for male pedestrians is 1.37 m/s, female 1.22 m/s and for people moving on wheelchairs 1.534 m/s.

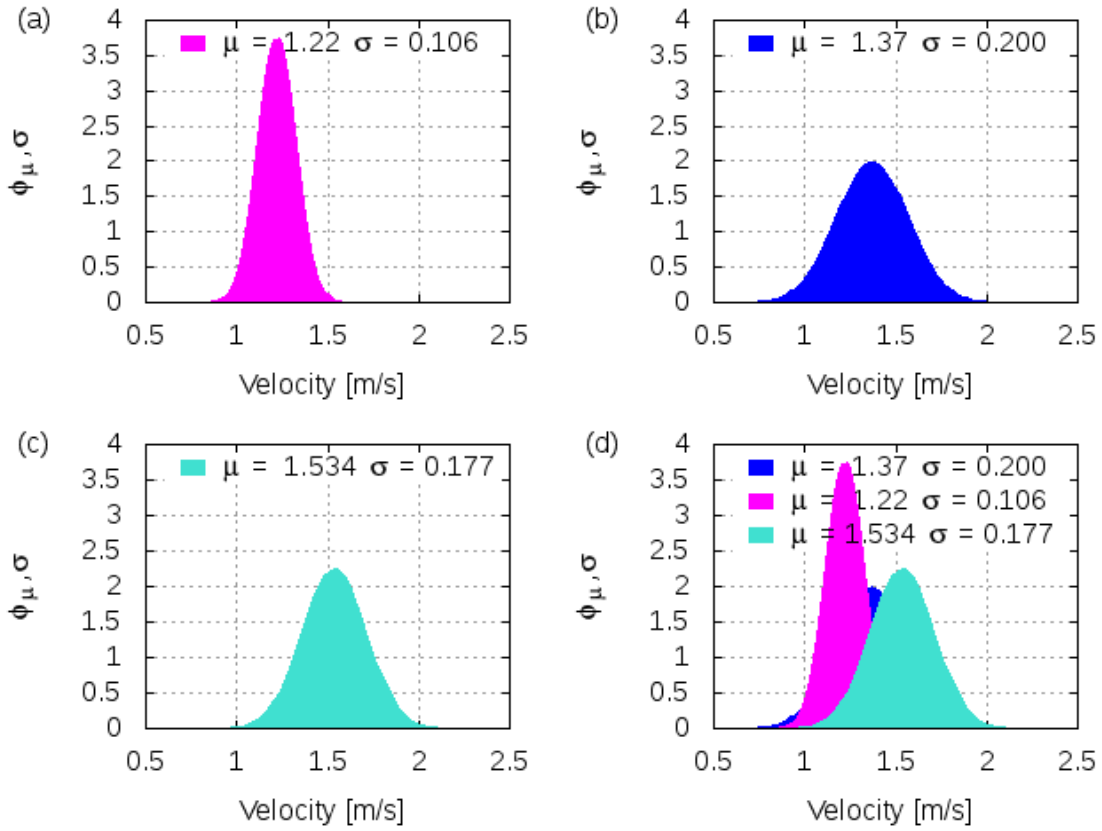

Figure 4.13: Walking speed distribution in Tawaf movement. (a) Women, (b) men, (c) wheelchairs and (d) shows a comparison of the three distributions. The average walking speed for female pedestrians is $\mu = 1.22$ m/s with a standard deviation of $\sigma = 0.106$ while for male pedestrians $\mu = 1.37$ m/s and $\sigma = 0.200$ and for pilgrims on wheelchairs $\mu = 1.534$ m/s and $\sigma = 0.177$.

Male Velocity (m/s)	Path Lenth (m)	Tawaf During Male in (min)
0,97	607	73
1,17	607	60,52
1,17	607	60,52
1,17	607	60,52
1,22	607	58,04
1,22	607	58,04
1,22	607	58,04
1,26	607	56,2
1,26	607	56,2
1,32	607	53,64
1,32	607	53,64
1,37	607	51,69
1,37	607	51,69
1,43	607	49,52
1,5	607	47,21
1,5	607	47,21
1,5	607	47,21
1,57	607	45,1
1,57	607	45,1
1,57	607	45,1
1,65	607	42,91
1,83	607	38,69
Average Velocity = 1,37		

Table 4.4: Male average walking speed in Tawaf movement.

0.97 m/s to 1.26 m/s, with an overall mean speed of 1.18 m/s. For design purposes a mean speed of 1.33 m/s appeared appropriate;

- Locations by the edge of the Mataf had faster walking speeds because such locations has a lower pedestrian density. It is clear that the pedestrians near the Kaaba had a short walk path but in this places densities of 7 to 8 persons/ m^2 can be exceeded, making the movement of pilgrims very slow and turbulent;

- Places situated further away from the Kaaba wall also tended to be associated with faster walking speeds. It is known from other fundamental diagrams, that pedestrians tend to walk faster along a free walkway. As might be expected the walking speeds associated with various factors. The motion of a single individual at any given time and the direction and speed result in

Female Velocities (m/s)	Path Lenth (m)	Tawaf During Female in (min)
1,06	607	66,8
1,06	607	66,8
1,1	607	64,37
1,1	607	64,37
1,13	607	62,66
1,13	607	62,66
1,17	607	60,25
1,17	607	60,52
1,17	607	60,52
1,22	607	58,04
1,22	607	58,04
1,22	607	58,04
1,26	607	56,2
1,26	607	56.2
1,32	607	53,64
1,32	607	53,64
1,32	607	53,64
1,37	607	51,69
1,37	607	51,69
1,37	607	51,69
1,37	607	51,69
Average Velocity = 1,22		

Table 4.5: Female average walking speed in Tawaf movement.

a long list of possible (and very likely conflicting) forces and circumstances.

The data taken show that each of the locations and surrounding factors have a significant effect on the behaviour and walking speed of the pilgrims on the Mataf area, not forgetting that the age of the pedestrians play a significant role on the Tawaf movement and density peaks and jams are caused by pilgrims of age 70 and more. For approximately one half of the location, the factors examined there also showed an important correlation between pedestrian age, the location and the mean walking speed of the pilgrims. This funding is consistent with results published by Knoblauch [69].

The walking speed of pilgrims shows statistically significant variations across a variety of sites, times and environmental conditions (pedestrian density on the Mataf area). On the roof of the Mosque the pilgrim density is low and every pedestrian can walk with his desired velocity. However, the mean walking speed data is explicit by clustered for both pedestrians sex, men and women, indepen-

Pilgrims moving on wheelchair (m/s)	Path Lenth (m)	Tawaf During Women in (min)
1,41	607	50,22
1,43	607	49,52
1,43	607	49,52
1,57	607	45,1
1,83	607	38,69
Average Velocity = 1,53		

Table 4.6: Wheelchair average speed in Tawaf movement.

dent of the age of the pilgrims are considered.

4.3.2 Automatic estimation of pedestrian walking speeds

There exist numerous methods that track the movement of single individuals by inspecting their orientation and limb positions.

This section highlights a real-time system for pedestrian tracking from sequences of high resolution images acquired by a stationary (high definition) camera. The objective was to estimate pedestrian velocities as a function of the local density. With this system the spatio-temporal coordinates of each pedestrian during the Tawaf ritual were established. Processing was done through the following steps (cf. also page 94):

- Existing footage was loaded onto a 3D program as a backplate.
- From several provided 2D- architectural drawings, a 3D model of the mosque was built.
- A virtual camera was matched in position, rotation and focal length to the original camera so that the features of the 3D-model matched the features positioned on the filmed mosque.
- Individual features were identified by eye, contrast is the criterion
- We do know that the pilgrims walk on a plane, and after matching the camera we also obtained the height of the plane in 3D-space from our 3D model.
- A point object was placed at the position of a selected pedestrian. During the animation we set multiple animation-keys (approx every 25 to 50 frames (equals 1 to 2 seconds)) for the position, so that the position of the point and the pedestrian overlay nearly all the time.

- By evolving the point with time we obtained the distance travelled, by measuring the distance from frame to frame. We also knew the time elapsed from the speed per frame, and hence the speed could be calculated.

Group tracking

Figure 4.16 shows the path of a pilgrim group in Tawaf movement around the Kaaba. The 5×5 m raster (grid) indicates the distance between the groups and the Kaaba wall. With help of this set-up, the path of this group can be defined.

As speeds are hard to observe, walking times are measured from which walking speeds are derived. For example a group of 30 pilgrims was followed to register individual walking times. This group consisted of about 30 pilgrims trying to keep together in the pedestrian stream, (see fig. 4.16).

Analysis

From Figures 4.14 and 4.15 we see that the edge of the Mataf moves faster than the center, this phenomenon being known as the Edge Effect. The Edge Effect occurs when the edges of a crowd move faster than the center of the crowd. The density becomes higher and higher as one moves from the edge of the Mataf towards the center. This phenomenon is explained by the fact that all pilgrims want to be near the Kaaba wall. As a result, we find the density near the Kaaba to be the maximum density. This data can be used in validating of simulation tools. The mean walking speed for a group of pedestrians moving in the pilgrim stream around the Kaaba was 1.0816 m/s at the edge of the Mataf and it was 0.3267 m/s for the same pedestrians groups moving inside the Mataf. These findings agree well with the statistical results discussed in a previous section.

4.4 Comparison of walking speeds

One of the must-have results is to compare the mean values and variances of walking speeds in both observations and simulation results. A distinction will be made for walking speeds inside and outside of the Mataf platforms. We made a comparison between our plots derived from the video observation and the fundamental diagrams of (cf. fig. 4.18):

- Walking speeds:
  - On the edge of the Mataf (free flow speed) where the pedestrian density is lower than 3 persons/m^2.

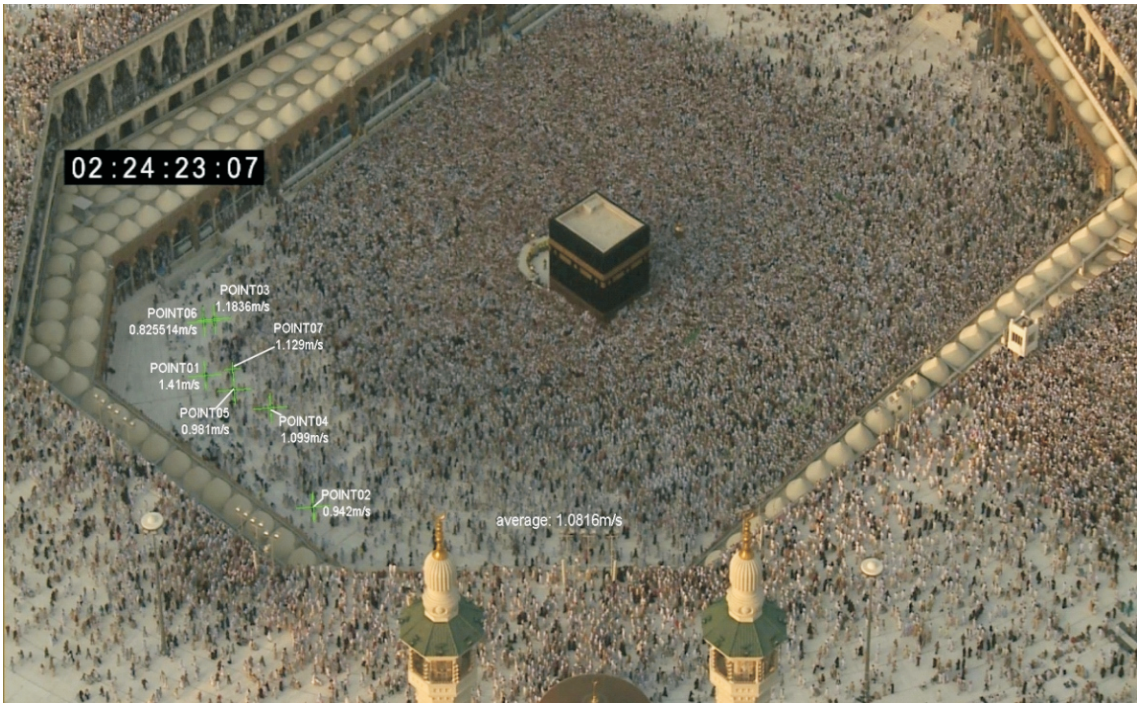

Figure 4.14: Pilgrims' walking speeds on the edge of the Mataf. The average walking speed is 1.0816 m/s.

- On the center of the Mataf.
- On the Mataf inside near the Kaaba wall where the pedestrian density attains extreme levels (8-9 persons/m^2).

All well-known fundamental diagrams predict the same behaviour and have the same properties: speed decreases with increasing density. So the discussion above indicates there are many possible reasons and causes for the speed reduction. For example there is a linear relationship between speed and the inverse of the density for pedestrians moving in a straight way [126]. However the pedestrian walking speed can be affected by internal and external factors (such as the amount of pedestrian inflow and outflow as well as the configuration of the infrastructure) not to forget the physiology of the human body. It is found that individuals walk faster in outdoor facilities than in corridors [127]. According to Predtechenskii and Milinskii (PM) the average walking speed depends on the the walking facility [1]. In other circumstances Weidmann confirmed a linear relationship between the step size length of walking pedestrians and the inverse of the density [74]. The small step size means low pedestrian velocity, caused by reduction of the available space with increasing density. The discussion above shows that there are many possible factors influencing the fundamental diagram. To identify these factors, it is necessary to exclude as many influences of mea-

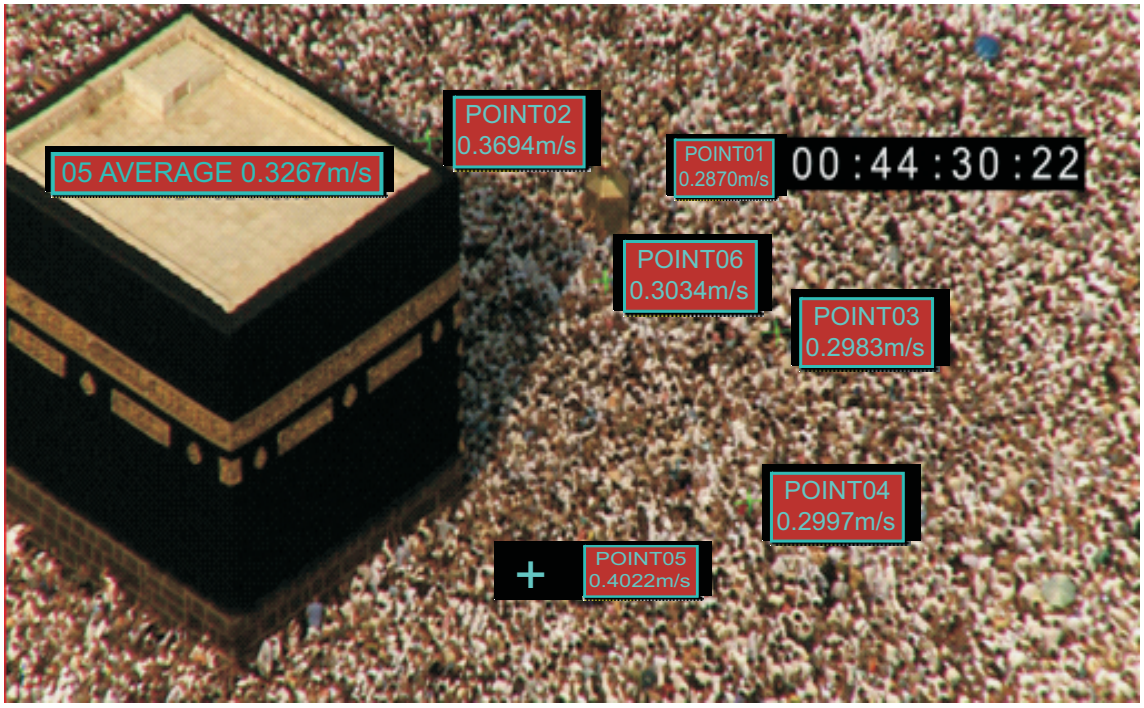

Figure 4.15: Pilgrims' walking speeds in the Mataf area (near the Kaaba wall). The average walking speed is 0.3267 m/s.

surement methodology and short range fluctuations from the data. Figure 4.18 shows the average local speed $\vec{v}(\vec{r},t)$ as a function of the local density $\rho(\vec{r},t)$ half-hour after Mid-Day Prayer (t = $t_{\textit{half-hour after Mid-Day}}$). Our own data is shown as red points. The blue points correspond to the Milinski fundamental diagram. Moreover investigation data analysing the Mataf area represented by blue points in figure 4.18 and showed that a reduction of the available navigation space illustrates the causes responsible for the speed reduction with density in pedestrian movement. The small deviation in pedestrian walking speed at lower density can be explained by the fitness level of the pedestrian.

Movement recognition

In the literature, there is a large number of approaches on detection and tracking of moving objects from video images. Spatio-temporal analysis has, in the past, been used to recognize walking persons, where subspaces in the video are treated as spatio-temporal volumes [128]. Application of a Fourier transform to this data can then identify data relating to movement across the volume. This approach allowed pedestrian trajectories to be reconstructed from video with high precision, taking advantage from the methods and the high developed computational technology. The common approach to detect movement is to produce

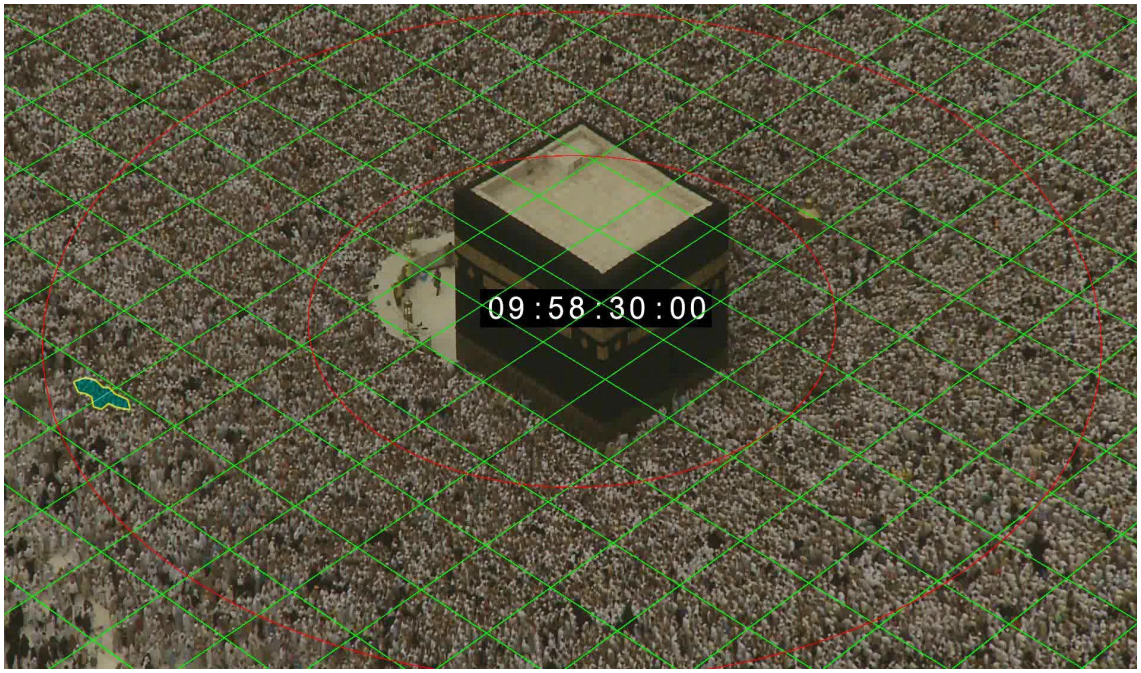

Figure 4.16: Group tracking video analysis.

comparison images (an image representing the different details between two images) since this is computationally efficient [129]. These comparison images can then be computed further to estimate movement vectors that describe the motion of drop-shaped objects captured in the respective images. Murakami and Wada demonstrate another method, filing the difference frame, and instead compare the properties of drops identified in consecutive frames [130]. A drop that is close to the position of a drop in a previous frame, and shares similar dimensions, is likely to refer to the same figure. Motion vectors are also used to find drop segmentation, which are subsequently merged or separated for the purpose of analysis. The same approach is applied to a 2D image to determine movement in 3D space. Extrapolating the movement of pedestrians in 3D space from a 2D image allows for a far greater understanding of the interactions between entities, but does require exceptional calibrations of equipment for complete accuracy. The Murakami and Wada approach can be used to analyse low-quality video streams due to the frame-differencing algorithm and some trigonometry. Determining 3D motion does require precise knowledge of the angle and position of the camera, in addition to the basic topology of the scene being analysed. But 2D paths are easy to identify without these details, (see fig.4.19).

In figure.4.19 we show the path of individuals within the crowd. One clearly recognizes to see that the movement around the Kaaba is not a circle movement. The tracking of a single individual in the pilgrims stream indicates some oscilla-

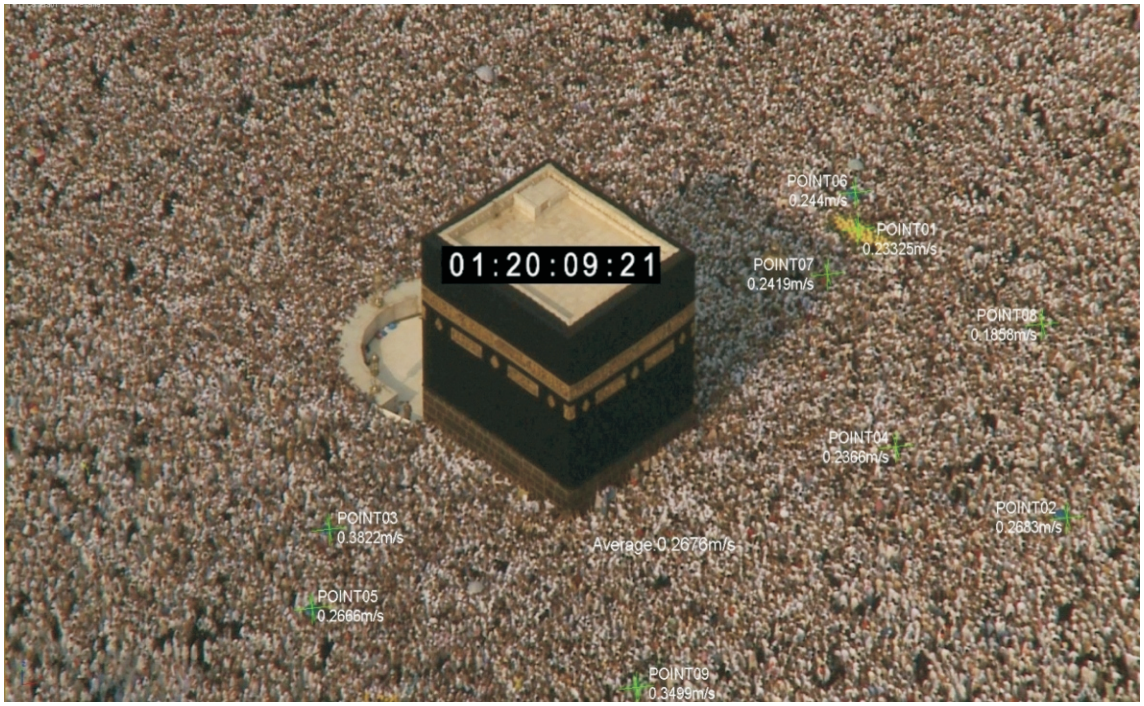

Figure 4.17: Mataf top view: Registration of individual walking speed through group tracking.

tion movement around the main path of the individual is caused by the physical repulsive and attractive forces acting on the individual. Physical forces become important when an individual comes into physical contact with another individual/obstacle. When a local density of 6 persons per square meter is exceeded, free movement is impeded and local flow decreases, causing the outflow to drop significantly below the inflow. This causes a higher and higher compression in the crowd, until the local densities become critical in specific places on the Mataf platform.

4.5 Analysis of the pilgrims movement on the Mataf

In the Mataf everything is dense and we have a compact state. The pilgrims have body contact in all directions and no influence on their movement; they float in the stream. This forms structures and turbulences in the flow. These turbulences can be well observed in our video recording. Density and velocity can also be seen. These observed Hajj rituals, especially the Mataf, showed some critical points in the motion of the pilgrims that we had not paid much attention to before. For example: the edge effect, density effect, shock-wave effect etc., and phenomena like these influence the restraint of the motion and are very important to be considered.

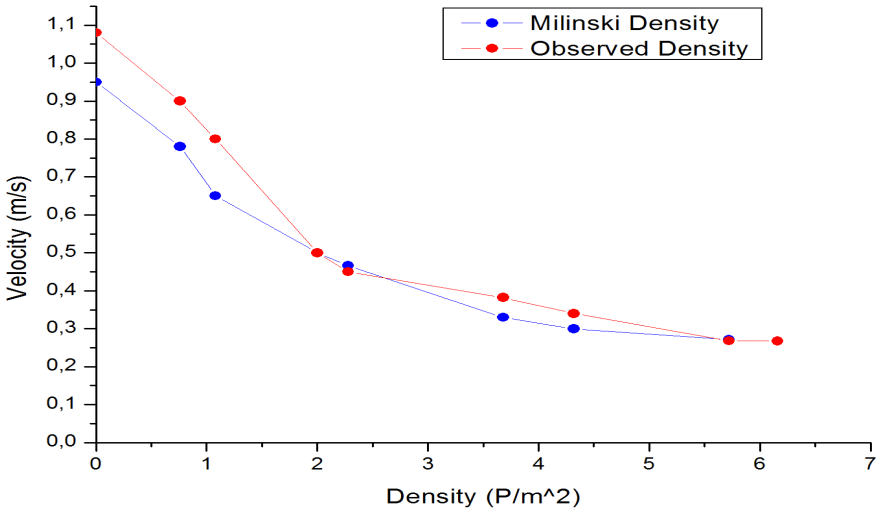

Figure 4.18: Velocity-density diagram half-hour after Mid-Day Prayer (t = $t_{half\text{-}hour\ after\ Mid\text{-}Day}$). Average of the local speeds $\vec{v}(\vec{r},t)$ as a function of the local density $\rho(\vec{r},t)$. Our own data are shown as red points. The blue points correspond to the data obtained by (PM) [1]. The difference in velocity at lower densities can be explained by the fitness level of pedestrians.

Our video analysis shows that the pedestrian density decreases with the distance from the Kaaba wall, cf. fig. 4.6, 4.7, and 4.8. It is the same as the real behaviour of pilgrims on the Mataf ritual (all pilgrims want to be near to the Kaaba wall). Our video analysis about the Mataf area indicates that, even at extreme densities, the average local speeds and flows stayed limited. This extremely high local density causes forward and backward moving shock-waves, which could be clearly observed in our video. We can see a kind of oscillation on the pilgrims paths around the Kaaba, this oscillation is caused by shock-waves and is affected by the repulsive forces between the pedestrians in high density crowds, (see fig.4.19).

4.5.1 Echo effect with 'Adobe After Effects' ®

'Adobe After Effects ®'[1] is a digital motion graphic and composition software published by Adobe Systems ®, used in the post-production process of film and television production. It is used for creating motion graphics and visual effects.

After Effects helps us to understand the fluidity of the pedestrian flow and the density waves observed in the video recording during the rush hour on the Haram. These density waves are generated by huge pedestrian forces that prop-

[1] http://www.adobe.com/de/products/aftereffects.html

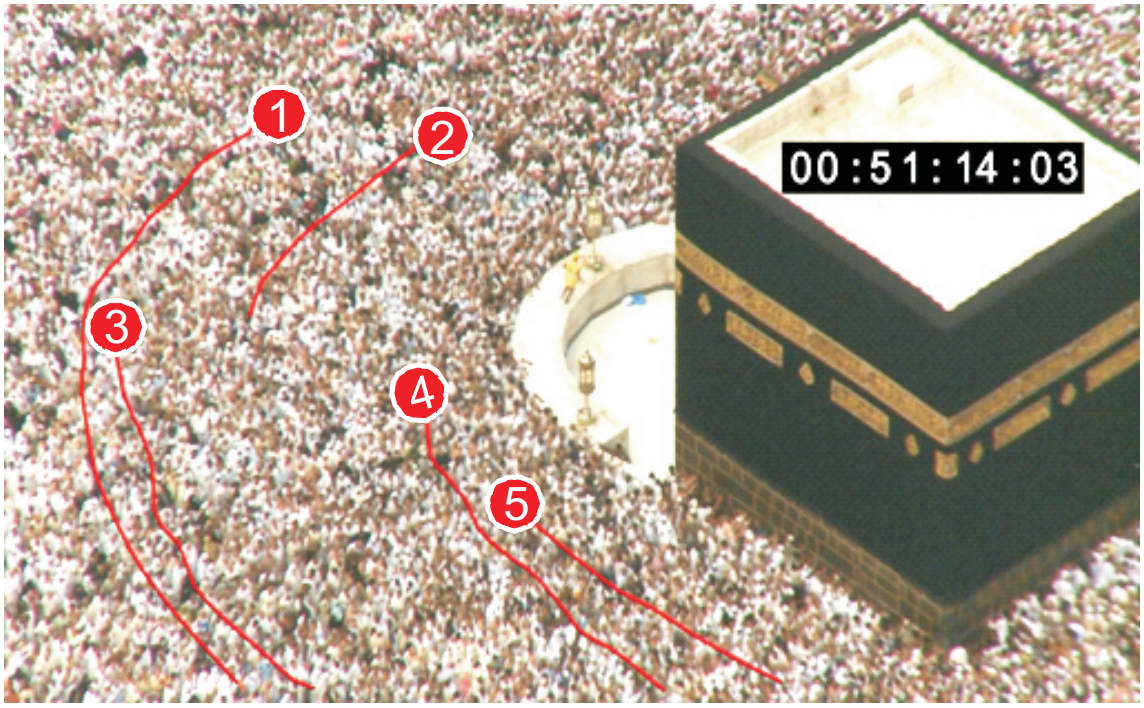

Figure 4.19: Pilgrims paths: With a new computer algorithm developed during this research, the trajectories or movements of pedestrians across the infrastructure over time are determined. Microscopic pedestrian fields require large amounts of trajectory data of individual pedestrians. Every red solid curve corresponds to one pedestrian trajectory. The oscillation in the pilgrims paths results from the huge pedestrian forces acting on every individual in the crowd.

agate with the help of body contact through a crowd.

4.5.2 Conclusion

One of the significant challenges in the planning, design and management of public facilities subject to high density crowd dynamics and pedestrian traffic are the shortcoming in the empirical data. The collected data concerning crowd behaviour using different techniques (image processing) and analysis of ordered image sequences obtained from video recording is increasingly desirable in the design of facilities and long-term site management. We have investigated the efficiency of a number of techniques developed for crowd density estimation, movement estimation, critical places and events detection using image processing. In the above sections and within this investigation we have presented techniques for background generation and calibration to improve the previously developed simulation model.

Even though extracting information about human characteristics from video recording may still be in its infancy, it is important to mention that the field of hu-

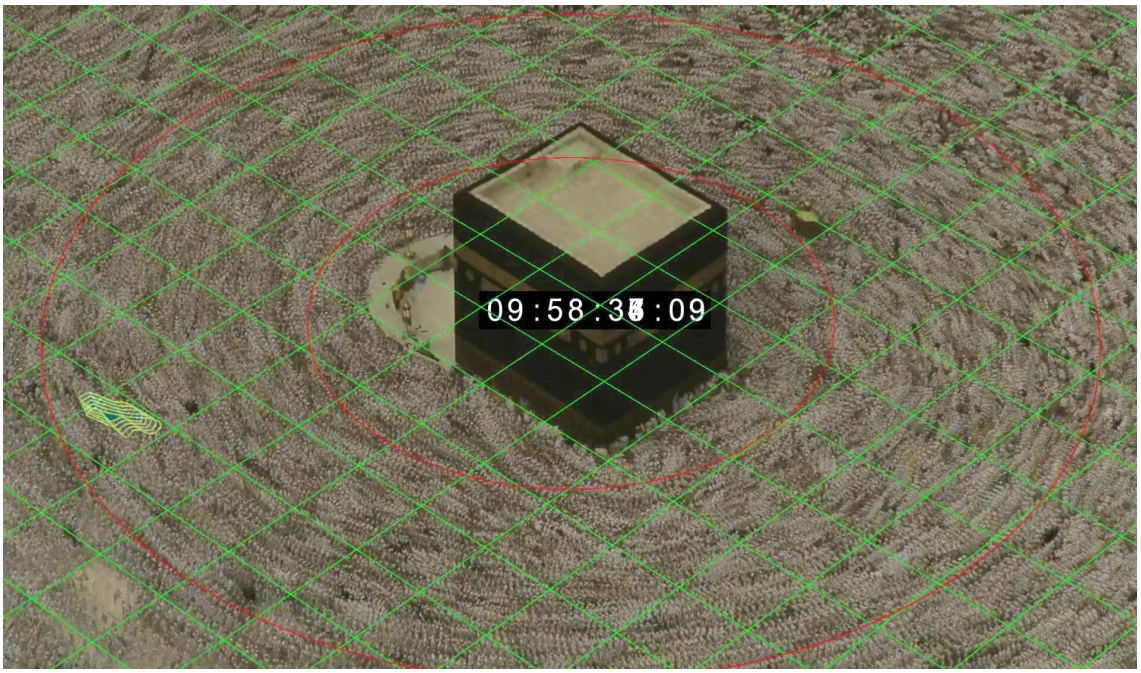

Figure 4.20: Density waves (echo-effect): gray cloud-like structures near the Kaaba.

man motion analysis is large and has a history traced back to the work of Hoffman and Flinchbaugh [131]. In the field of pedestrian detection techniques, moreover in the big area of computer vision, many problems have accumulated. In the human motion analysis, and also in the problem of the detection of moving objects, remain other problems, namely to recognize, categorize, or analyse the long-term pattern of motion. The inspection of the literature in the last decade indicates increasing interest in event detection, video tracking, object recognition, because of the clear application of these technologies to problems in surveillance. Recently many methods have been developed to extract information about moving object like speed and density. Almost all these systems require complex intermediate processes, such as reference points on the tracked objects or the image segmentation. One limitation of this current system is that the detection failures for these intermediates will lead to failure for the entire system.

Improvement of an algorithm to be able to reproduce traffic flow and to help in the microscopic pedestrian data collection is very essential. Moreover the automatic video data collection will highly enhance the achievement of a system for higher pedestrian traffic densities.

CHAPTER 5

MICROSCOPIC SIMULATION OF THE MATAF

5.1 INTRODUCTION

The pilgrimage (called Hajj in Arabic) is the most significant factor in the life and growth of the holy city Mecca. The number of pilgrims to Mecca increased in 2009 by 5 percent compared to 2008, official statistics said. In the last decade the number of pilgrims has been increasing dramatically, every year close to 4 million pilgrims arrive in the Saudi territory through Djedah airport, Djedah port by the Red Sea and through the high way connecting Saudi Arabia with neighbouring states. The arrival of the huge number of pilgrims each year during the last month of the Islamic calendar makes this event a grand human gathering in the world as well as one of the largest logistical and administrative undertakings [132]. The goal of pilgrims is to perform the Hajj ritual. Managing the flow of pilgrims to Mecca every year, posed various challenges to Saudi authorities [133].

Millions of believers perform the Hajj at the same time period, 4 specific days in the year. All pilgrims perform the same rituals, typically in same or concurrent time periods. The rituals are in specific points called points of interest, such as the Kaaba in Mecca, the mount Arafat etc. From the mountain Arafat, the pilgrims continue their course to Muzdalifah to throw stones at the pillars symbolizing the devil. Millions of believers live during the Hajj in tents in the Mina area (tent city). After that, millions of believers move towards Mecca to do their final Tawaf Al-Ifadah and to finish the Hajj ritual.

In this section we are concerned with Tawaf as an important pilgrims activity in Hajj period. The accurate prediction of pedestrian motion can be used to assess the potential safety hazards and operational performance at events where many individuals are gathered. The prediction of the pedestrian flow on the Mataf as permanent by overcrowded area and the investigation of the building facility through the simulation can be used to detect the critical points with high density in different regions of the Mataf. We attempt to determine the average capacity of the Mataf and we study the capacity of the mobile Mataf as possible solution

to reduce the pressure of pedestrian flow during the rush hour. As consequence of this solution we investigate how the columns of the mobile Mataf influence the fluidity of pilgrims stream on the ground Mataf. The columns serve as a support of the mobile Mataf. An understanding of how to alter crowd dynamics in Hajj activities would have a significant impact in a number of other scenarios, e.g. during riots or evacuations. Evacuation from dangerous zones, restrained places or overcrowded buildings, also represent cases where the prediction of pedestrian motion can be used advantageously.

5.1.1 Motivation

Now that the world population, particularly the Muslim population, is increasing, the number of pilgrims will also increase. With the huge development in the transportation technology in recent years the number of pilgrims arriving to Mecca grow systematically. It is a fact that the areas of Holy sites, such as Mina, Arafat, Muzdalifah and Mecca are fixed. This has motivated the Saudi government to find an effective and long-term solution. One of these solutions is to evaluate and build the mobile floor for Mataf expansion. The mobile Mataf has a lot of advantages, it can be built in a short time on the Mataf area during the Hajj period, after that it can be rapidly removed.

5.1.2 Observations in the simplified model

One of most important rituals in Hajj is the Tawaf, it consists of circling the Kaaba in the Holy Mosque seven times counter clockwise. Afterwards the Sa'y is performed, the walking between Safa and Marwa in an enclosed, air-conditioned structure. During Hajj seasons everything in the Mataf area is dense, and we have a compact state. The pilgrims have body contact in all directions and they have no influence on their movement, they are floated by the stream. This forms structures and turbulences in the flow. This turbulence is very well observable in our video recording see chapter 4. Density and velocity can also be seen. The following effects could also be observed during the Tawaf:

- Edge Effects: when the edges of a crowd move faster than the center of the crowd.
- Density Effects: crowd compression in local areas can imbalance the crowd flow.
- Shock Waves: propagation of some effects spreading throughout a densely packed crowd.

- Speed Effects: higher density causes lower walking speeds, with increasing contact area between pilgrims.
- Group Effects: groups of pilgrims move together and try to keep together all of the time.
- Break Out Effects: when pilgrims finish the Tawaf, they try to move directly to the edge of the Mataf. The movement of these pilgrims is normally spiral with increasing distance from the center of the Kaaba.
- Structure Effects: With higher density, turbulences and structures are created within the flow.
- The average time for Tawaf is ca. 1 hour.
- While praying in the Haram, there is no Tawaf at all. i.e. density decreases when praying is going to start and rises when praying has finished.

5.1.3 The Haram mosque building description

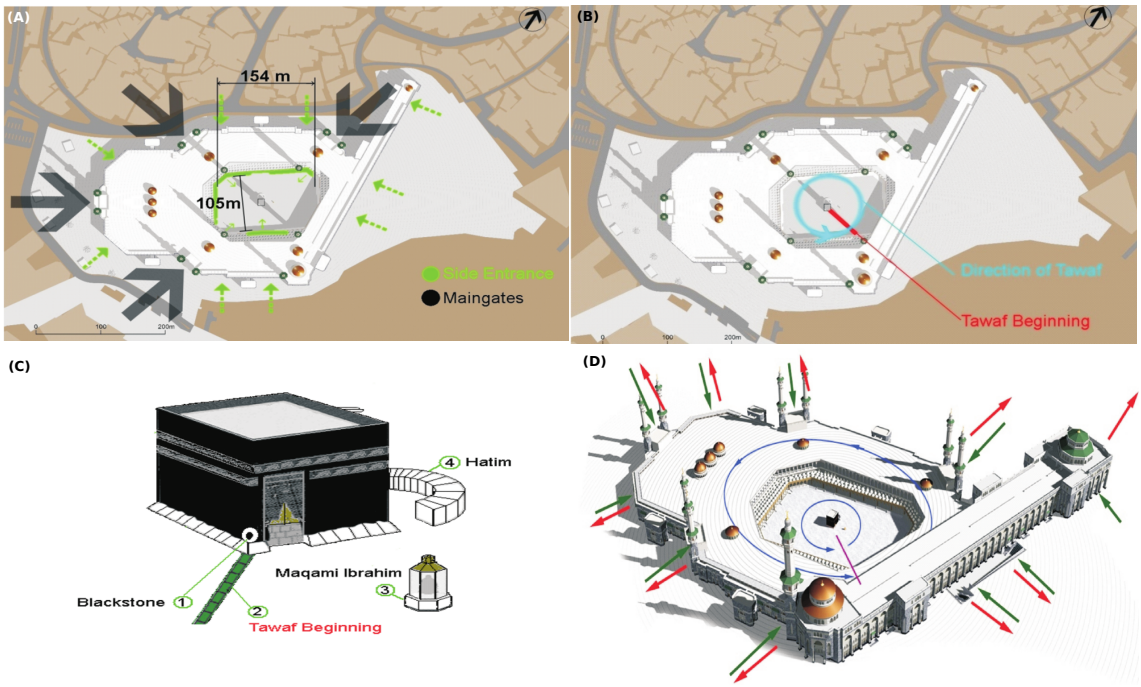

Figure 5.1: (A) Illustration of the Mataf dimension; (B) the direction of the Tawaf movement; (C) the Mataf description: (1) the black stone, one of the most overcrowded regions in the Haram, the measured local density $\rho(\vec{r}, t)$ in this place reached 9 persons/m^2, (2) the green strips on the ground indicate the begin and end of the Tawaf movement, (3) Maqam Ibrahim, hysterical monument near the Kaaba that must be considered in the simulation; (D) the gates and entrances to the Mataf.

The pilgrims stream into the Mataf from all gates of the Haram, (see fig. 5.1 (A)), but the beginning of Tawaf must start at a specific line (see red line in figure 5.1 (B)). As we can see in figure 5.1 (D), the Haram has 8 gates, stairs and an escalator. The gates are probably used by all pilgrims. Nearly (approximately 80 percent) of pilgrims make Sa'y after Tawaf, the rest (20 percent) of the pilgrims go out through any of the doors. For the simulation all doors are treated equally.

In Tawaf the pilgrims must circle the Kaaba seven times in a counter-clockwise direction. The black stone designates the beginning and end of the Tawaf (the pilgrims must stay 5-7 s in front of black stone to appreciate saying "Bismuallah Allahu Akbar" after every round). Before performing Tawaf, pilgrims try to reach the black stone. They queue around the Kaaba wall with some pilgrims not wanting to queue and trying to push through. After the Tawaf people try to pray between Maqami Ibrahim and the Kaaba, (see fig. 5.1 (C)) (The prayer is about 4 to 5 min).

In figure 5.1 (D) a 3D model of the Haram Mosque in Mecca is illustrated. This model shows the main gates, doors, side entrances, and stairs to the Mataf open air area of the Haram. The start/end of the Tawaf is indicated by the red line. The blue line indicates the Tawaf movement direction on the roof of the mosque or in the piazza of the Haram near the Kaaba.

5.1.4 Simulation of the simplified model

Our first set of simulations consisted of the pedestrian flow through the Mataf area without columns, (see fig. 5.2 (B)). The Mataf area was 105 m wide and 154 m long and in the center of the Mataf the Kaaba with 21.14 m long and 11.53 m wide is placed. The circumambulation area (ground floor) of Mataf is around 16 170 square meters. Each pedestrian's desired speed was set to a relatively high value of 1.2 m/s, the pedestrian radius R was 0.178 m to 0.2 m and the relaxation time τ was set in the range of 0.5 s to 1 s. After a pedestrian finishes the Tawaf (seven times circling around the Kaaba) they go in the direction of Sa'y. The measured densities are 5 - 6 persons/m^2 (measured in different part of the Mataf area with respect to the distance from the Kaaba). These results are consistent with those obtained by Predtetschenski and Milinski [1], who also found out that high density results in reduced velocities. The congested area increases the density sometimes up to 7 or 8 persons/m^2. In consequence the pedestrians begin to push to increase their personal space and create shock-waves propagating through the crowd.

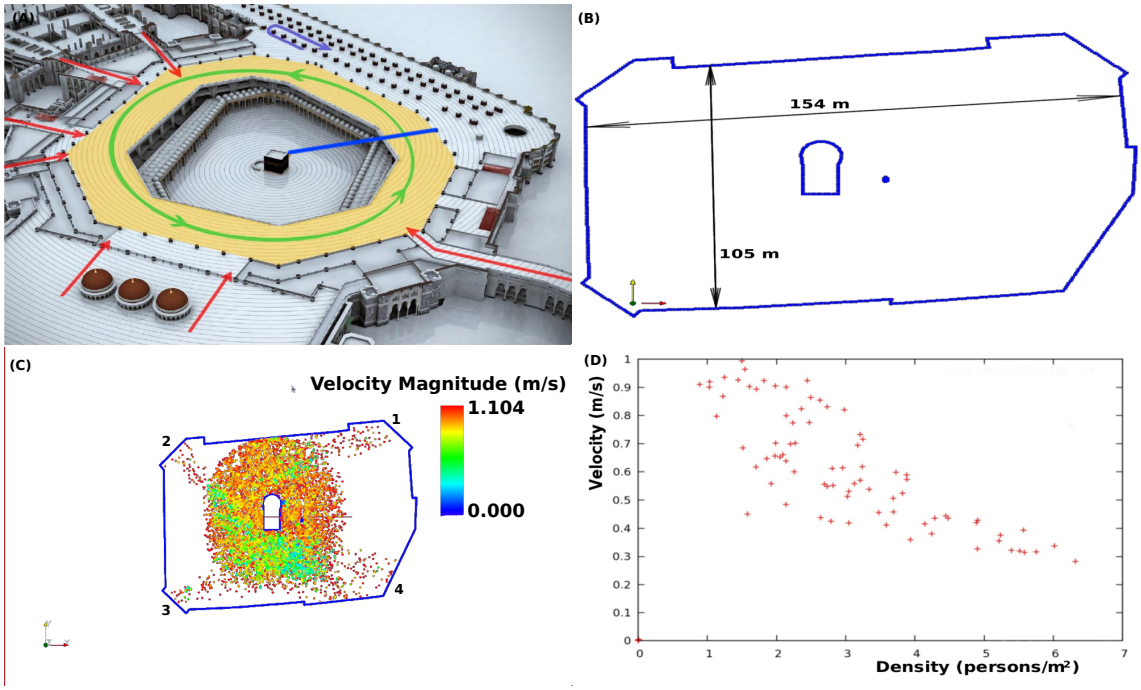

Figure 5.2: (A) 3D-Model of the mosque building in Mecca. Main gates and entrances are indicated through the red arrows, the green arrow indicates the direction of the Tawaf movement, the blue line indicates the beginning and the end of the Tawaf and the pink arrow indicates the Sa'y movement; (B) Mataf dimension; (C) PedFlow simulation snap-shot results, the numbers 1, 2, 3 indicate the entrances or particles streaming in the Mataf area and the number 4 particles streaming out of the Mataf or the exit from the Mataf toward the Sa'y area; (D) decrease of the pedestrian velocity in the Mataf area as a function of the local density, the measured data are represented by the crosses, they are consistent with the empirical data of Predtetschenski and Milinski [1].

Figure 5.2 (C) displays a pilgrims movement simulation within Mataf area. The entire influx consists of three uni-directional pedestrian flows coming from three entrances. The velocity indicator shows that the movement in the edges of the Mataf area is faster than in the area of the Kaaba. The picture shows a snapshot of the simulation at 38 s, which has a particularly high density of 6.5 persons/m^2. Also note that the pedestrian density is very high at the places where the Tawaf begins and ends. Note the clumping of pedestrians going in opposing directions, when the pilgrims finish the Tawaf. The average density for many runs was 5 to 6.5 persons/m^2, (see fig. 5.2 (D)).

5.1.5 Simulation of the enhanced model

The second set of simulations consisted of the pedestrian flow through the Mataf area with columns, (see fig. 5.3). The parameters are the same as in section 5.1.4. After pedestrians finish the Tawaf (seven times circling around the Kaaba) they are going in the direction of Sa'y. The measured densities are again 5 - 6

persons/m^2 with up to 7 or 8 persons/m^2 in the congested area. Thus, all results are identical with the simulation without the columns, cf. section 5.1.4. Obviously the columns do not influence the densities and velocities of the pilgrims in the congested area. The only observable difference are the vacant rings on the circles defined by the positions of the columns.

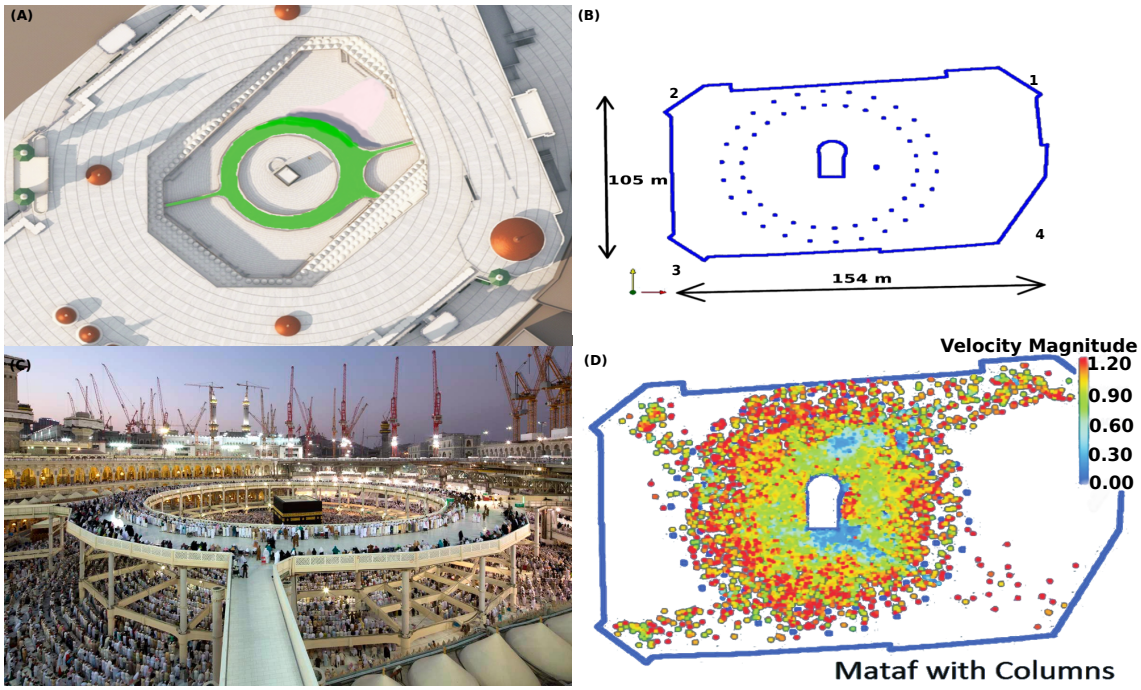

Figure 5.3: Snapshot 1: (A) 3D Model visualises one favourite concept for developing of the Mobile mataf (see green coloured area); (B) CAD drawing displaying the Mataf dimension area with columns; (C) mobile floor for the expansion of the Mataf area in Haram mosque, one can see the columns (pillars) bearing the mean structure of the temporary Mataf; (D) simulation result demonstrates how the pillars influence the movement of pilgrims on the Mataf ground. The colour coding represents the magnitude of the local velocity, PedFlow snapshot.

Figure 5.3 illustrates two simulation snap-shots with different entire influx. The pedestrian streaming the Mataf area from three entrances are indicated by the numbers 1, 2, 3 in figure 5.3 (B). The velocity indicator shows furthermore that the congested area still is in the interior zone near the Kaaba and at the area where the Tawaf begins and ends. The picture shows a snapshot of the simulation at 38 s, which has a particularly high density of 6.5 persons/m^2.

For the first moment one can not realise the difference to the results illustrated in figure 5.2 and figure 5.3, both pictures exhibit the same critical points. Note the clumping of pedestrians going in opposing directions, when the pilgrims finish the Tawaf. One may conclude that the columns have little influence on the movement of pilgrims but one can clearly see a vacant ring along the columns and this

results from repulsive interaction between the particles and the columns, this effect is better seen in case of lower crowd density. In case of high density crowd the pressure between the individuals is so huge that this vacant ring along the column disappears. This means that under the enormous surrounding pressure, people are forced to come near the pillar. Here we stress that the small size and smooth form of the column is very important to prevent people injury or dangerous situations.

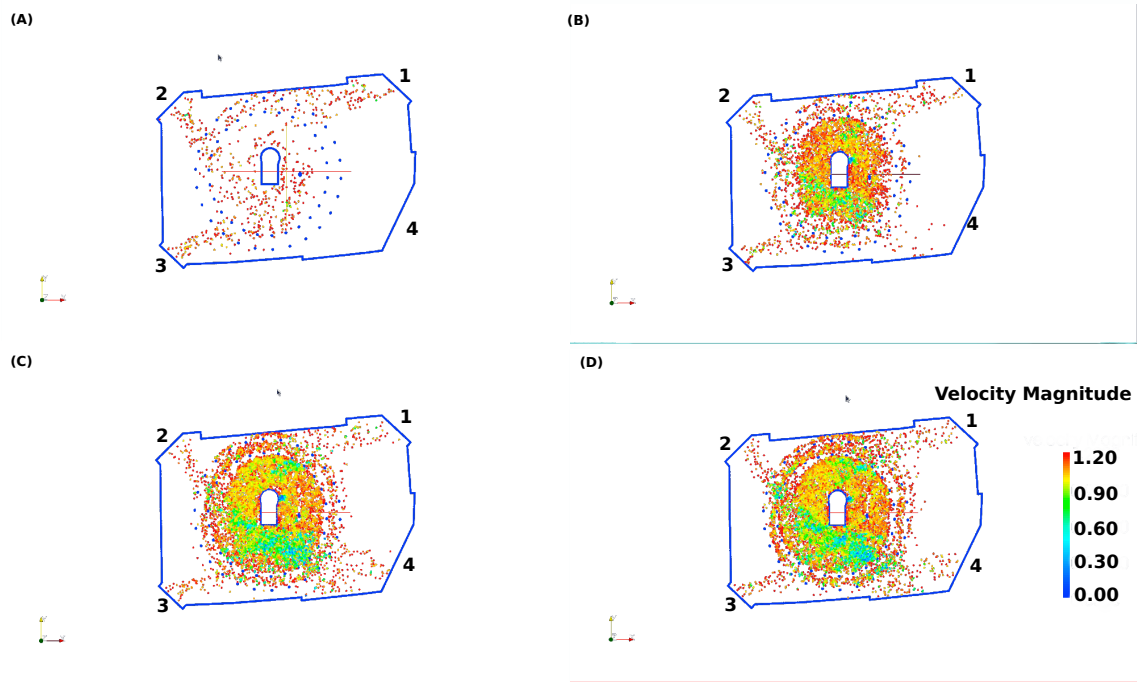

Figure 5.4: Pilgrims streaming the Mataf area through three different gates denoted by 1, 2, 3 and leaving the Mataf floor through gate 4. Step by step simulation of a pedestrian flow circling seven time the holy Kaaba ((A), (B), (C) and (D) illustrate time consecutive PedFlow animation snapshots). The impact of the columns on the pilgrims movement performing the Tawaf is demonstrated. The red colour indicates pedestrian walking with their desired velocities and the turquoise colour indicates pedestrian walking with lower velocities.

5.2 Mataf capacity estimation

5.2.1 Fundamental Diagram

Pedestrian distribution on the used surface must be identified with the fundamental diagrams, (see fig. 2.8).

5.2.2 Calculations

We divided the Mataf area into three parts according to the density distribution. The first part is the area near the Kaaba wall. The second part is the middle of the Mataf, the area between 10 m and 20 m from the Kaaba wall. The third part is the edge of the Mataf, the area between 20 m and 30 m.

- The first part of the Mataf area:
  - Usable Area = 820 m^2.
  - The mean pedestrian density = 6 pilgrims/m^2.
  - The total number of pilgrims = 4920 pilgrims.
  - The mean pedestrian path = 91 m.
  - The mean Tawaf path = 91 $\times$ 7 = 637 m.
  - The Tawaf lasts 39 min with average walking velocity of 0.266 m/s = 15,96 m/min.
  - The capacity is 7596 pilgrims Tawaf/hour
- The second part of the Mataf area
  - Usable Area = 1380 m^2.
  - The mean pedestrian density = 3,68 pilgrims/m^2.
  - The total number of pilgrims = 5078 pilgrims.
  - The mean pedestrian path = 151 m.
  - The mean Tawaf path = 151 $\times$ 7 = 1057 m.
  - The Tawaf takes 52,85 min with average walking velocity of 0,33 m/s = 20 m/min.
  - The capacity is 5859 pilgrims Tawaf/hour.
- The third part of the Mataf area
  - Usable Area = 1900 m^2.
  - The mean pedestrian density = 2 pilgrims/m^2 .
  - The total number of pedestrians = 3800 pilgrims.
  - The mean pedestrian path = 212 m.
  - The mean Tawaf path = 212 $\times$ 7 = 1484 m.

  - The Tawaf lasts 49,46 min with average walking velocity of 0.5 m/s = 30 m/min.
  - The capacity is 4653 pilgrims Tawaf/hour.

The total capacity of the Mataf is 18923 pilgrims Tawaf/hour.

According to several studies about the Haram, the actual capacity of the entire Mataf (ground, intermediate floors and the roof) are around 50,000 pilgrims/hour, but the capacity of the new Massaa is much higher than the capacity of the existing Mataf. During peak times worshippers are in danger of injuries due to extreme high density in the Mataf. To increase the capacity and improve the conditions for worshippers a new additional floor for the Mataf called temporary Mataf has been developed.

5.3 Mobile Mataf geometry

The new floor is based on a modules concept with fast assembly and disassembly without interruption of ongoing Tawaf. This light weight structure is designed to be integrated into the existing Haram Mosque. The outer diameter is about 94 m, the inside diameter is around 70 m and the width is around 12 m, (see fig. 5.6 (A)). An additional area of 3000 m^2 is added to the existing Mataf area. Access is achieved over several ramps. The clearance height is around 2.7 m leaving enough space for worshipper to pass underneath.

5.3.1 Concepts and evaluations

The idea to develop a new moving platform above the existing Mataf has the goal to take pedestrian pressure from the old Mataf. The design and evolution of this mobile area revealed a new concept concerning the safety and fluidity of pilgrims flow. In the next paragraphs we discuss two approaches with two different geometries and we present our analysis data.

- Mobile Mataf with extension: we shall discuss
  - Geometry
  - Simulation results
  - Capacity of the Mataf according to Predtetschenski and Milinski densities

5.3.2 Simulation

This set of simulations considers a unidirectional pedestrian flow circling the Holy Kaaba seven times. Different strengths of the influx of pilgrims were used, see table 5.2.The walking pedestrian area named mobile floor for the expansion of the Mataf contains two exits and one emergency exit. The design of the Mobile Mataf allows one-directional pedestrian flow, (see fig. 5.6 (A)). The parameters used in the simulations were the desired velocity of the individual v_d, the individual radius R and the relaxation time τ. The size or radius of particles are given in Table 5.1 and according to Predtetschenski and Milinski [1]. For simplicity, all parameters are identical for each person.

Type of Person	Projected area (m^2)
Children	0.04 –0.06
Adolescent	0.06 –0.09
Grown-up in summer clothes	0.100
Grown-up in interseason	0.113
Grown-up in winter clothes	0.125
Grown-up in interseason clothes with briefcase	0.180
Grown-up in interseason clothes with light luggage	0.240
Grown-up in interseason clothes with heavy luggage	0.390

Table 5.1: Set of different individual sizes [1].

Parameters

- Individual Parameters.
  - Desired velocity: v_d = 1.2 $\pm$ 0.2 m/s.
  - Individual Radius: R = 0.178 $\pm$ 0.02 m (Milinski).
  - Relaxation Time: τ = 0.5 $\pm$ 0.1 s.
- Geometry Parameters.
  - Usable Area: A = 3540 m^2.
  - The mean Radius of the Mataf: R_M = 42 m.
  - The mean pedestrian path: $L_{Path} = 2\pi R_M$ = 263.76 m.
  - The mean Tawaf path: L_{Tawaf} = 263.7 $\times$ 7 = 1846.32 m.
  - The Tawaf time: t_{Tawaf} = 43.35 min with average walking velocity $\bar{v}$ = 0.7 m/s = 42 m/min.

Results

In table 5.2 the maximum number of pedestrians on the Mataf without clogging is 8404 with a density of 2.37 persons/m^2. The optimal capacity without clogging is 11726 pilgrims per hour completing the Tawaf, calculated with an average Tawaf duration of 43 min.

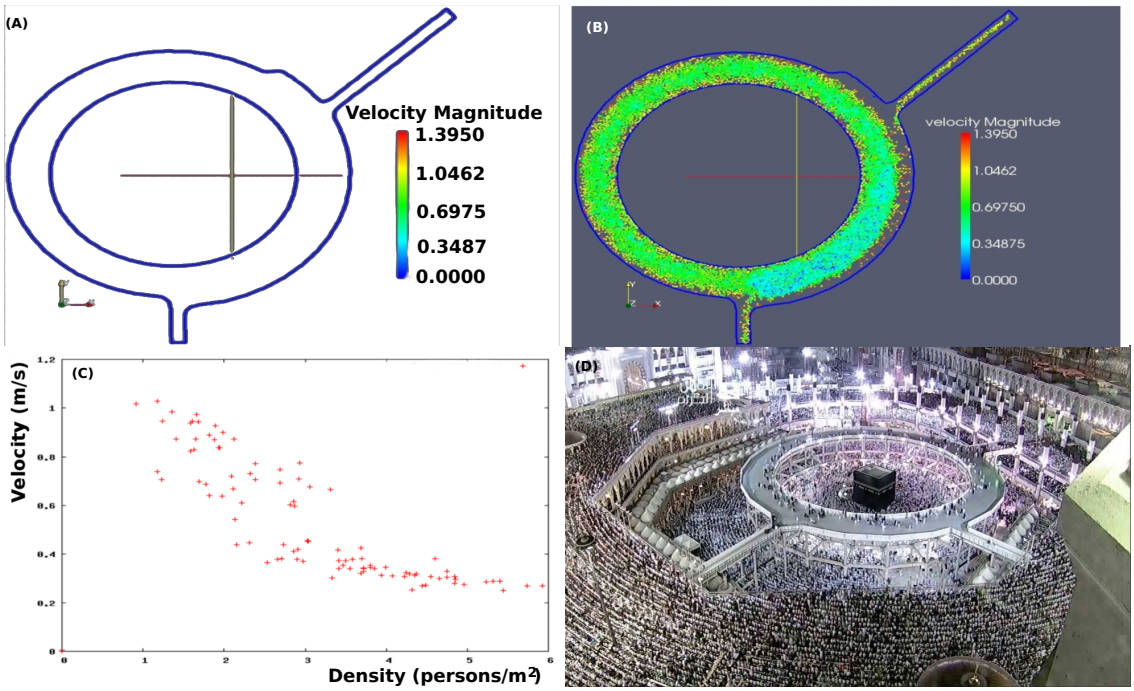

.

Figure 5.5: (A) CAD drawing displaying one of many geometry concepts developed for evaluation of the mobile Mataf; (B) simulation results (new geometry concept); (C) velocity density diagram (PedFlow simulation); (D) the actual mobile floor facility top view.

The maximum number of pedestrians on the Mataf was 11629 with a density of 2.79 persons/m^2. The optimal capacity without clogging was 16226 Tawaf/hour, calculated with an average Tawaf duration of 43 minutes. If one Tawaf is 50 minutes then the capacity of the Mataf will be 13954 Tawaf/hour.

5.4 Mataf capacities estimation

According to the Predtetschenski and Milinski fundamental diagram figure 2.8, the capacity of the mobile Mataf was determined. The results of this investigation are illustrated in Table 5.3. The capacities of the mobile floor were computed with respect to different pedestrian densities. Every density in the fundamental diagram is related to a certain velocity. With help of these given velocities we

Influx (Persons/s)	Max Number of Ped	Density($1/m^2$)	Capacity(Tawaf/h)	Remarques
2,0	5032	1.42	7021	fluid
2,1	5338	1.50	7448	fluid
2,2	5796	1.63	8087	fluid
2,3	6147	1.73	8577	fluid
2,4	6691	1.89	9336	fluid
2,5	6955	1.96	9704	fluid
2,6	7443	2.10	10385	fluid
2,7	8106	2.28	11310	fluid
2,8	8519	2.40	11886	fluid
3,9	9236	2.60	12887	Slow Movement
3,0	10358	2.92	14453	Clogging effect

Table 5.2: The Mataf capacity at different simulation influxes.

tried to calculate the mean average time for one complete Tawaf. Afterwards we calculated the capacity of the Mataf. We can see that the optimal capacity is about 12000 Tawaf/hour, (see fig. 5.6 (C)). This result consistent with the simulation result which is about 13954 pilgrims per hour completing the Tawaf.

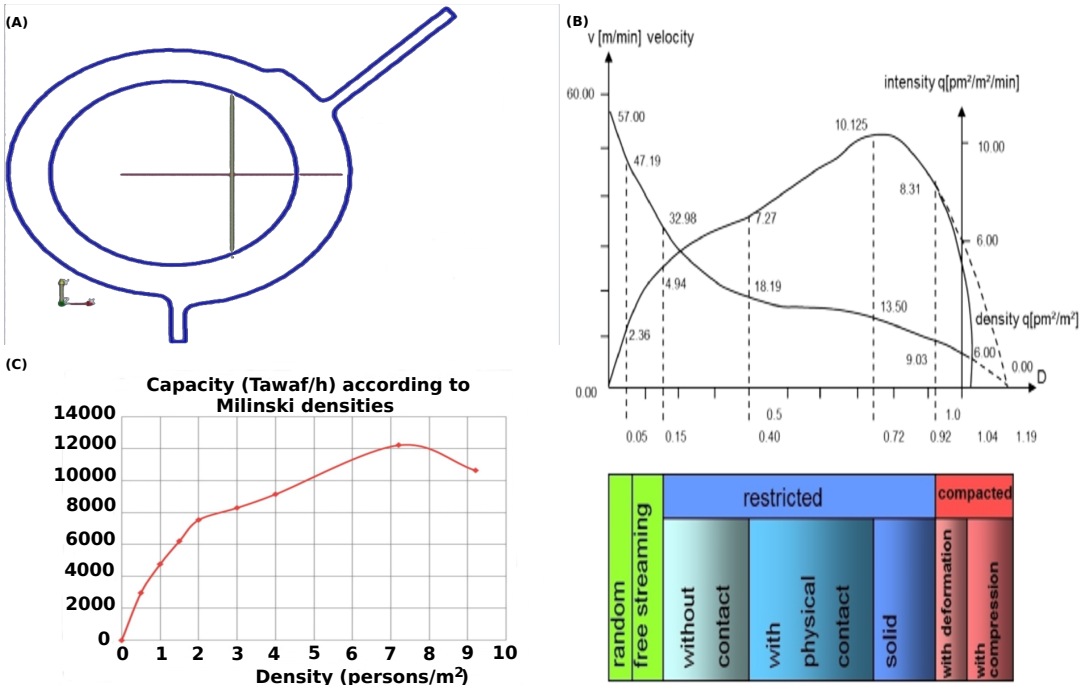

Figure 5.6: (A) CAD drawing displaying the geometry concept of the new walkway around the Kaaba; (B) Predtetschenski and Milinski fundamental diagram (cf. Fig. 2.8); (C) mobile floor capacity according to Predtetschenski and Milinski densities.

5.5 Conclusion

A newly developed simulation software for analysing pilgrim movement was used for the evaluation of the Tawaf capacity of the Mataf area and the new mobile floor. Different scenarios were analysed to find out the optimal capacity. With a flux of only 12 pilgrim/min entering the floor, much space was left unused. Pilgrims moved with their desired speed and the average time for completing a Tawaf took around 25 minutes. The second scenario showed 108 pilgrim/min entering the floor, causing the space to become fully occupied by pilgrims and the velocity to decrease, resulting in dangerous jams especially in the exit area. The third scenario showed the optimum steady state when about 125 pilgrim enter per minute and also exit the floor, with no jams. This results in an overall capacity of about 9000 finished Tawaf/hour and an average time of approximately 25 min to complete the Tawaf.

Density ($1/m^2$)	Velocities (m/min)	Path (m)	Tawaf during (min)	Usable Area (m^2)	Max Ped. number	Capacity (Tawaf/hour)
0	60	1846		3864	0	0
0.05	47.19	1846	39.11	3864	1932	2963
0.1	38	1846	48.57	3864	3864	4773
0.15	32.98	1846	55.97	3864	5796	6213
0.2	30	1846	61.53	3864	7728	7535
0.3	22	1846	83.90	3864	11592	8289
0.4	18.19	1846	101.48	3864	15456	9138
0.72	13.5	1846	136.74	3864	27820	12207
0.92	9.03	1846	200.65	3864	35548	10629

Table 5.3: Mataf capacities according to the Predtetschenski and Milinski fundamental diagram (New-concept).

CHAPTER 6

VALIDATION

6.1 VALIDATION AND VERIFICATION TECHNIQUES

6.1.1 A short overview

For the verification and validation of microscopic simulation models of pedestrian flow, we have performed experiments for different kind of facilities and sites where most conflicts and congestion happens e.g. corridors, narrow passages, and crosswalks. The validity of the model should compare the experimental conditions and simulation results with video recording carried out in the same condition like in real life e.g. pedestrian flux and density distributions. The strategy in this technique is to achieve a certain amount of accuracy required in the simulation model. This method is good at detecting the critical points in the pedestrians walking areas. For the calibration of suitable models we use the results obtained from analysing the video recordings in Hajj 2009 and these results can be used to check the design sections of pedestrian facilities and exits. As practical examples, we present the simulation of pilgrim streams on the Jamarat bridge, (see fig. 6.6).

The objectives of this study are twofold: first, to show through verification and validation that simulation tools can be used to reproduce realistic scenarios, and second, gather data for accurate predictions for designers and decision makers.

6.1.2 Introduction to crowd simulation tool validation

In this chapter we attempt to explore the methods that can be used to make the results made by a software or simulation tool more authentic or believable. A set of statistical data taken from real life experience can be used to check the output values created by the simulation tools to validate the simulation model. This method is referred to as statistical technique method and can be applied to simulation models, depending on which real-life data is available [134]. In general lack of empirical data makes the verification of any simulation model a

complicated task.

In case the real data are not available - the simulation data obtained by the simulation tools are still guided by the condition of a statistical theory and probability distributions on the design of experiments [135].

In case only output data is available - the values carried by the simulation model can be compared with well-known statistical data [135].

If data can be collected on both system input and output trace-driven simulation becomes possible, model validation can be done through comparing the collected data with the simulation results. In trace-driven simulation, the simulation input data are identified by the trace data collected by a myriad of instruments and methods [135].

What, however, does 'validation' mean? The term validation will be used to refer to various processes. The process of examining whether the acceptability and credibility of the conceptual model is referred to as validation, it is an accurate method to check the actual system being analysed. Validation can help to develop the right model. Verification is a process to check simulation output for acceptability and controlling whether the results made by the computer program are compatible with the real data collected about the same system [135].

Concerning this topic many books could be written to describe the philosophical and practical aspects involved in validation (see, the monograph by Knepell, and Arangno 1993) [135]. For this reason, I identify validation as systematic examination of the simulation model whether (if) it displays or illustrates the real world in a reasonable time, either as a procedure to check for correctness or meaningfulness of the resulting data. Validation is a process to check the ability of the model to reproduce the real system. In the next sections we will concentrate on validation that uses mathematical statistics and comparison with video recordings of real situations.

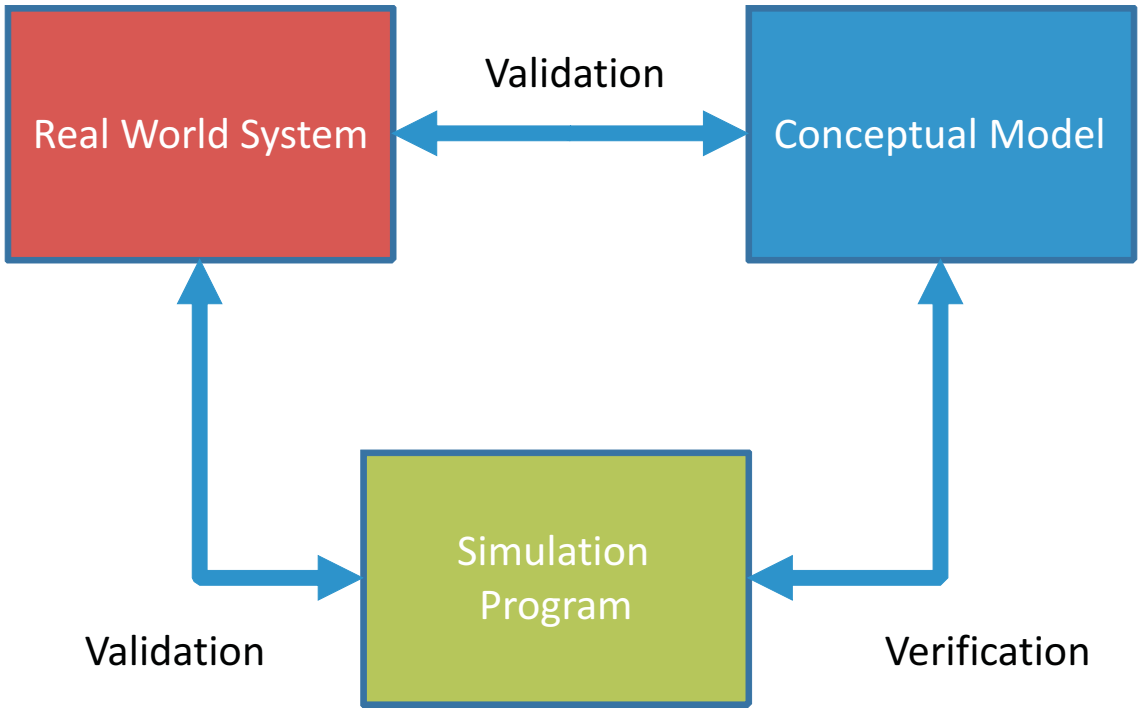

Figure 6.1: Validation procedure for a given simulation model.

Since modelling and simulating has become very important in many domains in modern science, much literature on verification and validation of a simulation models have appeared: see the web (http://manta.cs.vt.edu/biblio/), and the detailed surveys in Beck et al. (1997) [136], Kleijnen (1995b) [137], and Sargent (1996) [138]. Important work concerning the choice of statistical tests to validate a model was made by Kleijnen (1999) [139].

For the first step we try to compare our video taking with the simulation results. A lot of phenomena (like the lane formation, oscillation effect and edge effect) can be seen, to make sure if our simulation reproduces a part of the reality. For this investigation we need to make scenarios for the next video observation in the great mosque in Mecca.

Verification, validation and testing techniques

This paragraph describes different validation techniques and tests, used in model examination and validation. Most techniques described here are found in literature, although some may be described slightly differently. They can be used either subjectively or objectively. In the "objectively" case we attempt to implement mathematical methods using a kind of statistical test e.g. confidence intervals and hypothesis testing. A combination of techniques is generally used. These

techniques are used for the examination and validation of sub-models and the universal model [140].

- Comparison to other models: In a verification and validation of a simulation model process, different results (e.g. outputs) of the simulation model will be compared with the results of other models. For example, (1) comparison of a simple case of a simulation model with well-known results of empirical models, and (2) the comparison of the simulation model with other validated models with the same properties.

- Event validity: The appearance of events in a simulation model will be compared with those of the real system to determine if they are identical.

- Extreme condition tests: The model structure and outputs should be credible for any extreme and improbable combination of levels of factors in the system.

- Face validity: Experts or specialists in the system will be asked about the suitability of the model and its behaviour. For example, is the logic in the conceptual model true and are the model input-output relationships appropriate.

- Historical data validation: The system can take advantage of the historical collected data to calibrate itself, specifically the data collected on a system for building and examining the model, a part of the data can be used to establish the model and the remaining data is used to determine whether the model behaves as the system does. (This testing is led by driving the simulation model samples from the distributions or traces) [141, 142, 143].

- Multi stage validation: Another efficient method for validation a simulation tool was proposed by Naylor and Finger (1967) [144]. It consists in associating three well known methods of rationalism, empiricism, and positive economics into a multi-stage process of validation. This technique is based on (1) evaluation and development of the simulation model with respect to the theory, observations, and practical experience, (2) validating the model using possible existing empirical data, and (3) comparing the results (output) made by the simulation model with the real system.

- Operational graphics: Measured values of various performances e.g. using statistics for time series, are illustrated graphically while the model runs over time; i.e. a visual indicator of performance shows how the program

behaves during run time to ensure the correct performance of the simulation tools.

- Sensitivity analysis: A sensitivity analysis is a powerful technique for validating systems. This validation method consists in changing the input parameters of the simulation or internal parameters of the model to realize how the model's output will be affected. If the system does the right things, the same relationships resulting from the model should be visible in the real system. Using this technique both qualitative (directions only of outputs) and quantitative (both directions and exact amount of outputs) properties of the system can be verified. Parameters cause important changes in the behaviour of the model (sensitive parameters). These parameters have a high importance for the model and the simulation results (this may require iterations in model development).

6.2 Calibration and validation of the PedFlow model

In this section we present a variation of different techniques used to calibrate and validate the PedFlow simulation model. PedFlow is a microscopic simulation model, which was developed by Löhner Simulation Technologies International, Inc. (LSTI) [21]. For verification and validation, data was provided by the Institute of Hajj research and the Ministry of Hajj, consisting of layout information, pilgrim numbers, and Hajj schedules. We augmented this data with camera-based observations at several stairways, gates and the piazza inside and outside the Great Mosque in Mecca. This collected data can be used as input parameters of the simulation and improves the acceptability and accuracy of the data carried by the simulation.

PedFlow must model all processes that are related to pedestrians inside and outside the Haram at the normal and the busiest rush hours of the Hajj events such as: walking, performing activities, and route choice. In order to validate pedestrian flow modelling in PedFlow and to study pedestrian traffic flow movement during the Hajj in detail, observations were collected on the Haram in Mecca during the Hajj 2009. These observations concerned the Tawaf, Sa'y, (individual) walking times, and other sites such as the Haram gates before and after each prayer. These observations are very helpful in obtaining the data that will be used to verify our simulation tool PedFlow. This data concerns the numbers of pilgrims going in and out of the Haram and individual walking times and densities of pedestrians on the Mataf. Finally, a comparison is made between the observations and modelling results of PedFlow, in order to check the validity of

PedFlow with respect to pedestrian traffic flow operations.

Since this investigation is concerned with studying safety and fluidity of large scale pilgrim flows at pilgrimage places in Mecca, the validation of the simulation tool is mainly concentrated on pedestrian traffic flow at the holy places. The main variables to be observed and compared with the model predictions are:

- Walking speeds.
  - On the stairs (upward and downward directions).
  - On the piazza and the Mataf of the Haram.
- Densities over time and space.
  - Video recording.
  - Fundamental diagrams Predtechenski and Milinski [1].
- Layout information
  - Data about the boundary condition and environmental information.

6.2.1 Validation through comparison with other models

The credibility of the data produced by the pedestrian microscopic simulation model can be validated through comparing with results obtained by other models having the same characteristics, although we mention that the comparison with other simulation tools is necessary for the acceptance of the data but not sufficient. Different results (e.g. outputs) of the PedFlow simulation model, being validated, are compared with results of other models. For example, emergent lane formation generated by many simulation models, e.g. Blue [2], who used a cellular automata model. Lane formation in bidirectional flow and clogging effects at bottlenecks in case of emergency situation were realized by Helbing, Molnar, and Vicsek [4], who use a social force model. First a simple case of a simulation model is compared with known results of analytic models [1], and second the simulation model is compared with other simulation models that have been validated, such as social-force models (see [22] and the references therein) and cellular automata, e.g [23, 24].

Walking through narrow passage

Our first set of simulations consisted of pedestrian flow through a hallway with a narrow passage, (see fig. 6.2) (a). The hallway was 80 m wide and the narrow passage was 16 m long and 4 m at the narrowest point. Each pedestrian's

desired speed was set at a walking speed for adult pedestrians in normal conditions $v_d = 1 \pm 0.02$ m/s; relaxation time: $\tau = 0.50 \pm 0.1$ s; (smaller times $\rightarrow$ more aggressive) and pedestrian radius: $R = 0.2 \pm 0.02$ m; (smaller radius $\rightarrow$ smaller repulsive forces). Repulsive potentials were assumed to decrease exponentially. The relaxation time is the time needed to reach 90 percent of the desired velocity.

This experiment is realized with constant influx, that means if a pedestrian has passed through the passage, he will be replaced by a new pedestrian at a random starting location, i.e. at the entrance of the hallway to keep the number of people in the hallway constant. The mean velocities (measured in the passage area) for different pedestrian influxes and the results are illustrated in figure 6.2 (d). These results are consistent with those obtained by Predtetschenski and Milinski [1] and other fundamental diagrams, who also found out reduced velocities due to the tendency of pedestrians to converge at the same time in the direction of the passage area when the hallway is narrow. This caused blocking and the velocities to drop and the density to increase with time, creating bottlenecks and clogging, (see fig. 6.3).

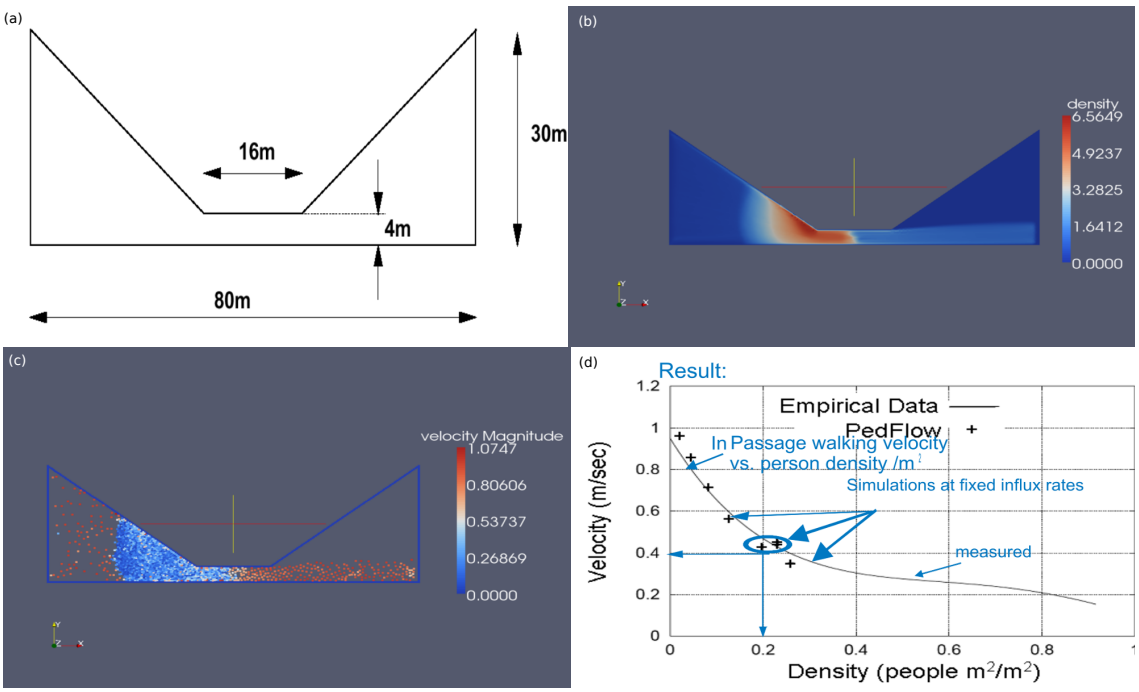

Figure 6.2: This figures illustrates a pedestrian flow walking through a narrow passage: (a) bottleneck geometry; (b) the density index; the density map illustrates how the pedestrian density rises in the congested area. Red color indicates high density which can reach 7 people/m^2, while blue color indicates low pedestrians density; (c) the velocity index, the blue color indicates the lowest velocity; (d) decrease of the pedestrian velocity in the passage area as a function of the local density, the measured data are represented by the crosses in the graph, they are consistent with the empirical data of Predtetschenski and Milinski [1] represented by the solid line.

Pedestrian motion in passages is one of the few cases where reliable empirical data exists. In order to assess the validity of the proposed pedestrian motion model, a typical passage flow was selected. The geometry of the problem is shown in figure 6.2 (a). Pedestrians enter the domain from the left and exit to the right. In this case, each pedestrian has the goal of first reaching the entrance of the passage, then traversing it to the other end, and finally to exit on the right. Typical snapshots during one of the simulations are shown in figure 6.3.

The resulting data of the simulation are shown as crosses in figure 6.2 (d). The data flows are shown in a graph besides the analytical data from Predtetschenski and Milinski. This graph corresponds to specific parameters and illustrates a defined simulation state, although they exhibit the relation between the input parameters and the simulation results. In the low density range the data are synchronized with a high accuracy. There are no deviations of the simulation values and the analytically data. The walking speed drops in dependency of density. The small deviation in the start-velocity, can be traced back to the input parameters.

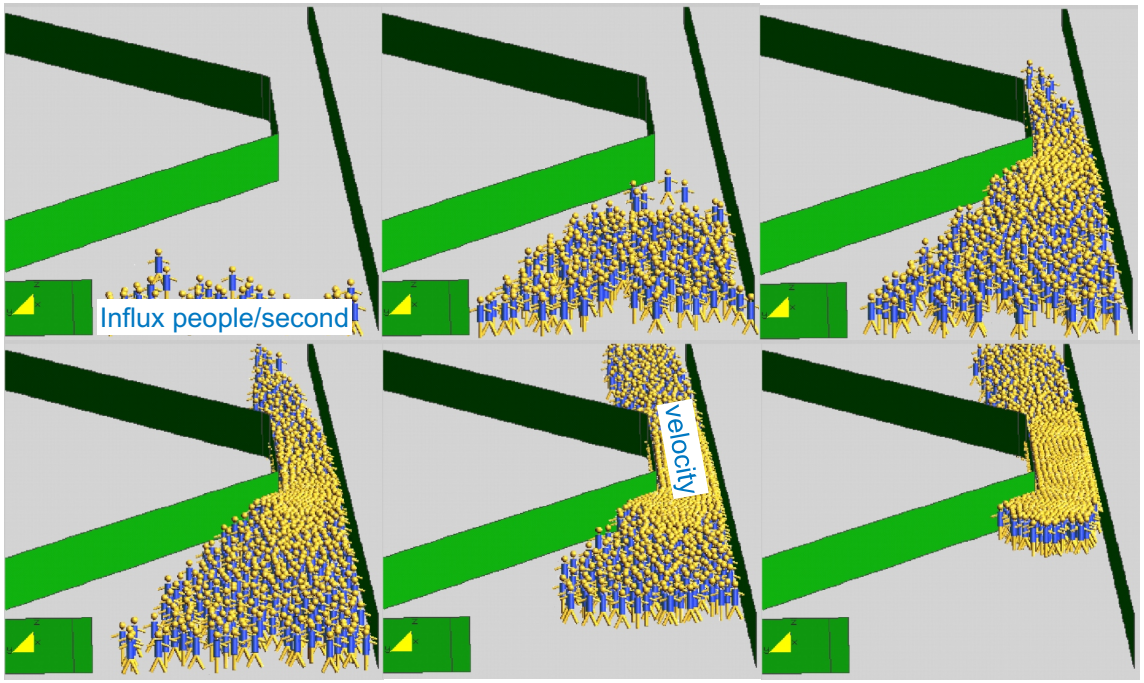

Figure 6.3: Step by step simulation of a pedestrian crowd walking through a passage (PedFlow animation results).

Comments

Through the simulation of pedestrian flow walking on a well known geometry called bottleneck or narrow passage, (see fig. 6.2) we attend to check simulation output for credibility. We performed different simulation runs for several input scenarios and tested to see if the output is reasonable. It is easy to compare certain performed measures with other computed results. Using animation is another method to improve the simulation model, (see fig. 6.3). The resulting data of the simulated system will be displayed in a dynamic or moving picture for the model users. Since the model developers and model users are familiar with the real system, they can ameliorate the performance of the program and detect programming and conceptual errors. With this tests we try to verify the simulation response by running a simplified version of the simulation program with a known analytical result. If the output data resulted by the simulation model do not exhibit a significant deviation from the known empirical data, this result can then be used to validate the model.

Example: Simulation of the Tawaf movement

In this test we try to verify the simulation response by running a simplified version of the simulation program with a known analytical result. If the output data resulting from the simulation model do not exhibit a significant deviation from the known empirical data, this result can then be used to validate the model.

Through the simulation of pedestrian flow on the well known geometry of the Mataf in the Haram Mosque, (see fig. 5.2) we intended to check simulation output for credibility. We performed different simulation runs for several input scenarios and tested whether the output is reasonable. It is easy to compare certain performed measurements with other computed results. Using animation is another method to improve the simulation model. The resulting data of the simulated system is displayed in a series of snapshots of the animation of the model users. Since the model developers and model users are familiar with the real system, they can ameliorate the performance of the program and detect programming and conceptual errors.

Figure 6.4 illustrates typical simulation results for Tawaf movement (circling the Kaaba seven times in a counter-clockwise direction). The entire influx consists of three one-directional pedestrian flows coming from three entrances. The velocity indicator shows that the movement in the edges of the Mataf area is faster than in the area of the Kaaba. The picture shows a snapshot of the simulation, which has a particularly high maximum density of 6.5 persons/m^2. Note that the pedestrian density is very high at the places where the Tawaf begins and ends,

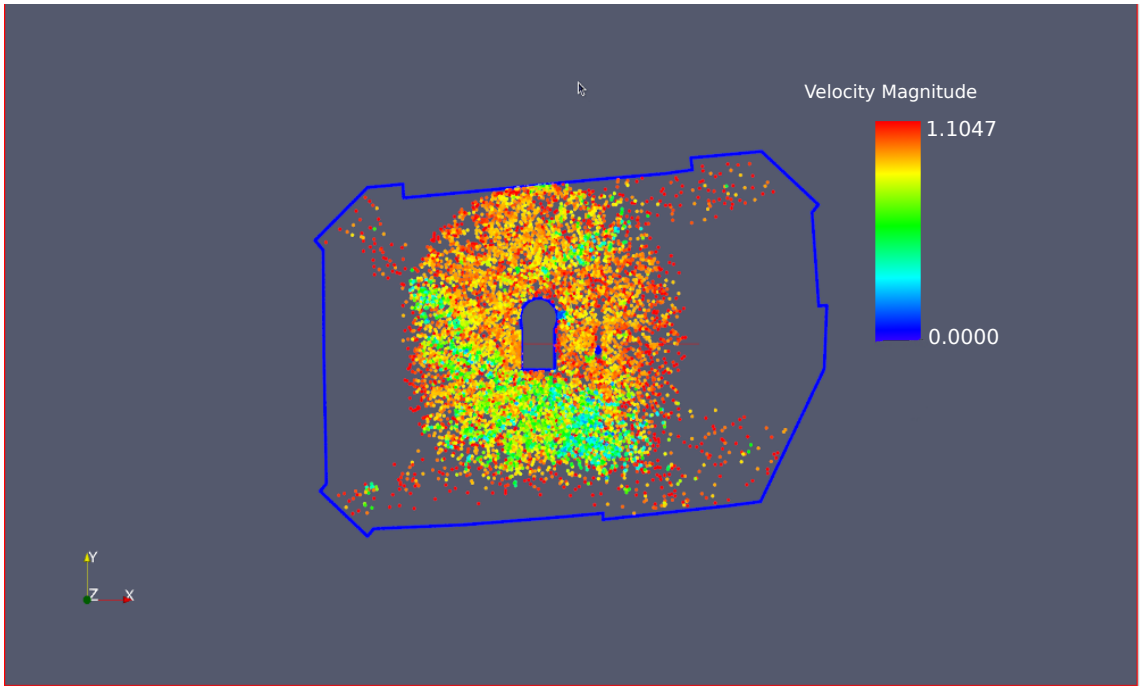

Figure 6.4: Tawaf movement simulation: Pilgrims movement simulation within the Mataf area, the red color indicates the desired velocity 0.9 to 1 m/s while turquoise color the lowest.

and the clumping of pedestrians going in opposite directions, when the pilgrims finish the Tawaf. The average density for many runs was 5 to 7 persons/m^2, see fig. 6.5 (b) and (d), while (a) and (c) illustrate the velocity-density distribution on the Mataf area during the rush hour calculated according to Predtetschenski and Milinski (see fig. 2.8).

Examples: Al-Jamarat bridge

The simulation of high density pedestrian flow streaming the Jamarat area during the rush hour of the Hajj period revealed a great technical progress in the modelling, simulation and better understanding of how large crowds alter. In the past many fatal accidents happened in this extremely dangerous area, where a large number of pilgrims stream through the site and try to stone the pillars in a relatively short period of time. Since the movement of pilgrims is very slow an accumulation effect on both sites of the pillars arises. This leads to physical jamming, pilgrims trampling, and in the worst situation to the death of pedestrians underfoot. To accomplish the safety of millions of pilgrims walking this overcrowded area every year and for better fluidity of pedestrian flow near the pillars, the proposal was made to build a bridge with a 5-level structure to ease the process of performing this ritual. The bridge was designed to satisfy the inter-

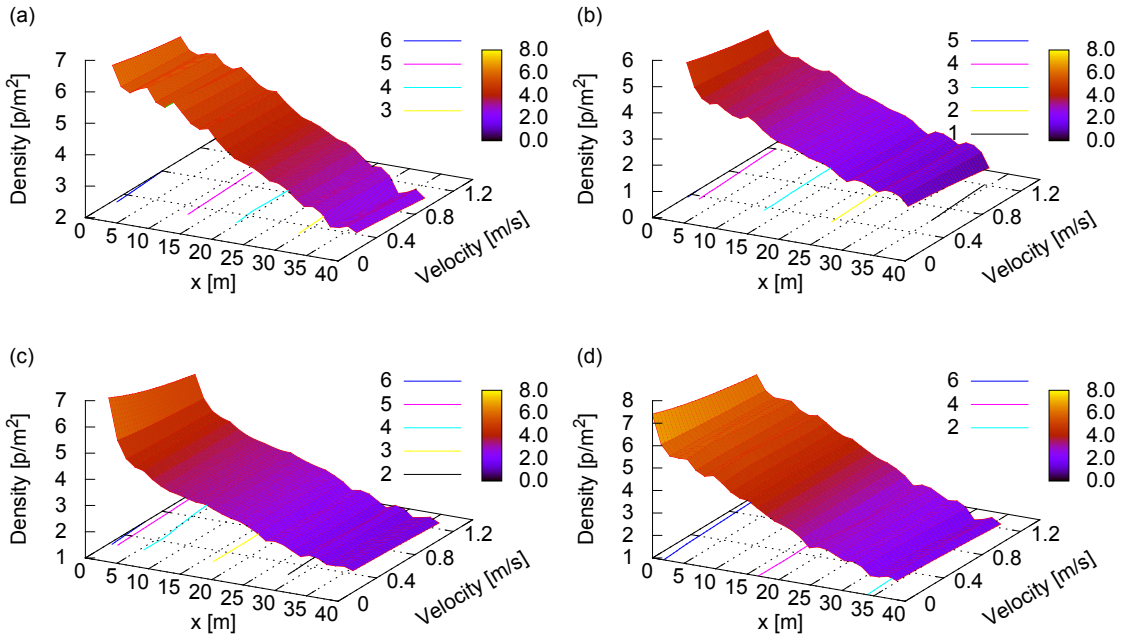

Figure 6.5: Tawaf movement simulation: Velocity-density distribution as a function of the distance from the Kabaa wall, the curves (b, d) illustrate the simulation results for two different initial velocities while the curves (a, c) show the results obtained by a calculation according to the Predtetschenski and Milinski fundamental diagram with the same velocities as in (b) and (d), respectively. The difference in velocity at lower densities can be explained by the fitness level of pedestrians.

national standard criterion of pedestrians safety, especially during overcrowding, and this concept arose from the idea to conduct the pilgrims flow in one direction without any counter flow. The Saudi government designated Professor Dr. Saad A. AlGadhi (expert in transportation management and design) and Dr. G. Keith Still (the crowd dynamics expert) to evaluate a model using crowd dynamic software tools to improve the conceptual design [145]. This study produced a lot of data and information about:

- Sufficient arrival capacity
- Sufficient throwing area
- Sufficient space (density $\leq$ 4 Hajjis per square meter)
- Sufficient passing area
- Sufficient egress capacity

in the Jamarat bridge area that can be used to validate other pedestrian simulation tools. For example, published data about the Jamarat bridge capacity,

in-flux and out-flux, demonstrate that the total available ingress width must be greater than 28 meters to allow 125,000 pilgrims per hour. This is a minimum requirement and provision for security forces/civil defence, bi-directional/counter flow and hesitation (pilgrims stopping to rest) where the longer ingress ramps have additional width requirements [145].

Figure 6.6 illustrates how a combination of microscopic and macroscopic techniques can assess the progression of queues approaching the Jamarat (above - Simulex/Myriad, below Myriad and site photograph) [146].

The other set of data about the Jamarat bridge was published by Helbing after the onset of the crush event of 2006 in his paper: The Dynamics of Crowd Disasters: An Empirical Study 2007 [5]. His video analysis revealed a lot of data and information about the average local speed, average local flows and the average local densities in the Jamarat area before and after the deathly crush accident. It was found that the pedestrian density near the pillars area can reach a huge value of 9 persons/m^2.

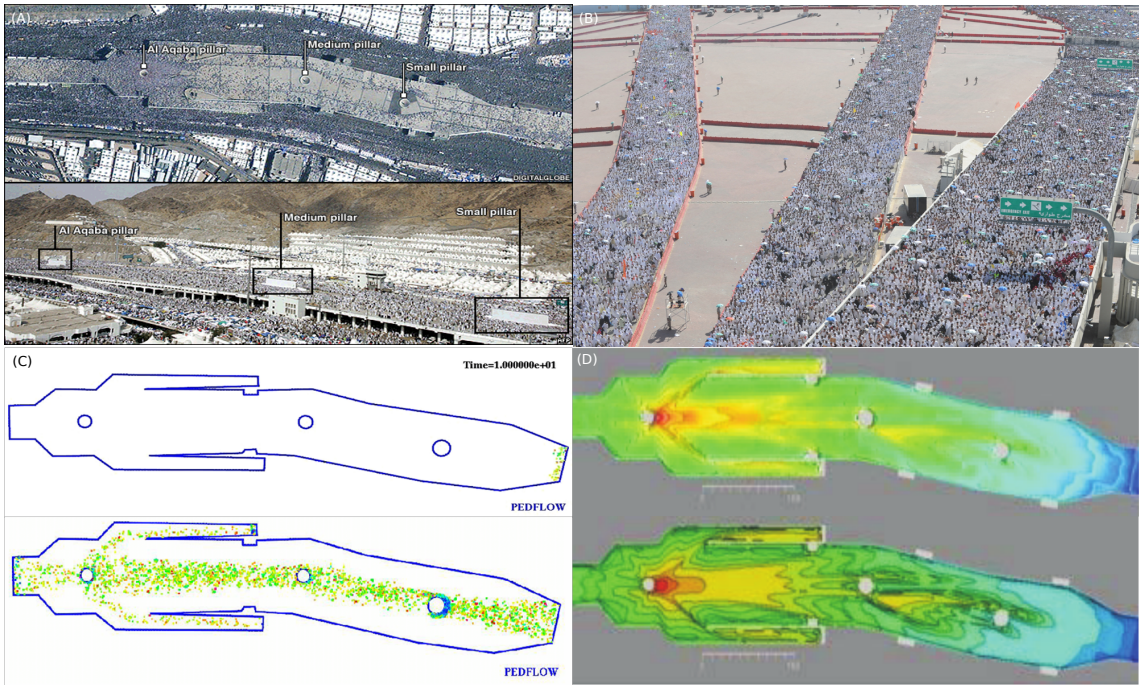

Figure 6.6: During Hajj, pilgrims flock to the Jamarat Bridge in Mina to cast stones at three pillars representing the devil. The cylindrical pillars (A)(top) were replaced by short walls (A)(bottom) after a previous fatal stampede in 2004. The idea was to improve crowd flow and reduce congestion. (A) shows the geometry and the location of the stoning pillars; (B) shows a huge number of pilgrims streaming toward the pillars; (C) Jamarat Bridge microscopic simulations/PedFlow and (D) Microscopic simulations/Myriad [146] (red color means high density; yellow color means middle density; green and blue color means low density).

To assess the validity of the PedFlow simulation model and for improvements of resulting data we apply analytical and comparative tests. These tests are used to compare the simulation output with the output from other simulation tools e.g. Simulex/Myriad [146]. Compared to other models PedFlow is more sophisticated to predict high density crowd dynamics. The simulation result is shown in figure 6.6. Of course the simulation input takes advantage of the published data to predict accurate results.

6.2.2 Validation through visualization and comparison with the real world

The aim of most procedures and methods testing model validity is to determine the similarity between the results carried out by the conceptual model and the collected data. The better the simulation output resembles the output from the real system the better the results in general. The animation and visualization of the output simulation data are necessary to prove the credibility of the system, moreover this test is very important to examine how close the data is to the real world.

Crowd visualization

A literature survey reveals several investigations and animation methods which have been proposed to provide more realism in the conceptual model simulating large scale pedestrian motion. Treuille and Shao [26, 34] suggested a method that increases the degree of accuracy and realism of crowd simulations. For example a realistic human like character is an essential role in the animation of high density crowd simulation. They illustrate the effects and interactions between the individuals itself within the crowd and the individuals and their environment. This yields a better prospect about the density distribution of pedestrians in a given site.

In the context of pedestrian animation we considered the technique of motion graphs [147] in order to provide advanced behavioural human characters. We attempted to modify the motion graph approach to associate an existing database of short MoCap (Motion Capture) animations into a larger clip of continuous motion. However, in our approach the pedestrian movements are expressed as paths or trajectories of the character extracted from unlabelled motion capture data. This technique modifies the character's position and orientation for the entire animation clip. The trajectory and orientation of a character in a BVH (Biovision Hierarchical data) MoCap animation is interconnected, and one cannot be modified without influencing the other, hence rendering the animation unrealistic. Our technique allowed us to produce a continuous and longer sequence of

animations using an existing database of MoCap animations and joining the animations together. Behaviour is closely related to the corresponding animation. It is this binding between behaviour and animation that we intended to utilize to validate our model.

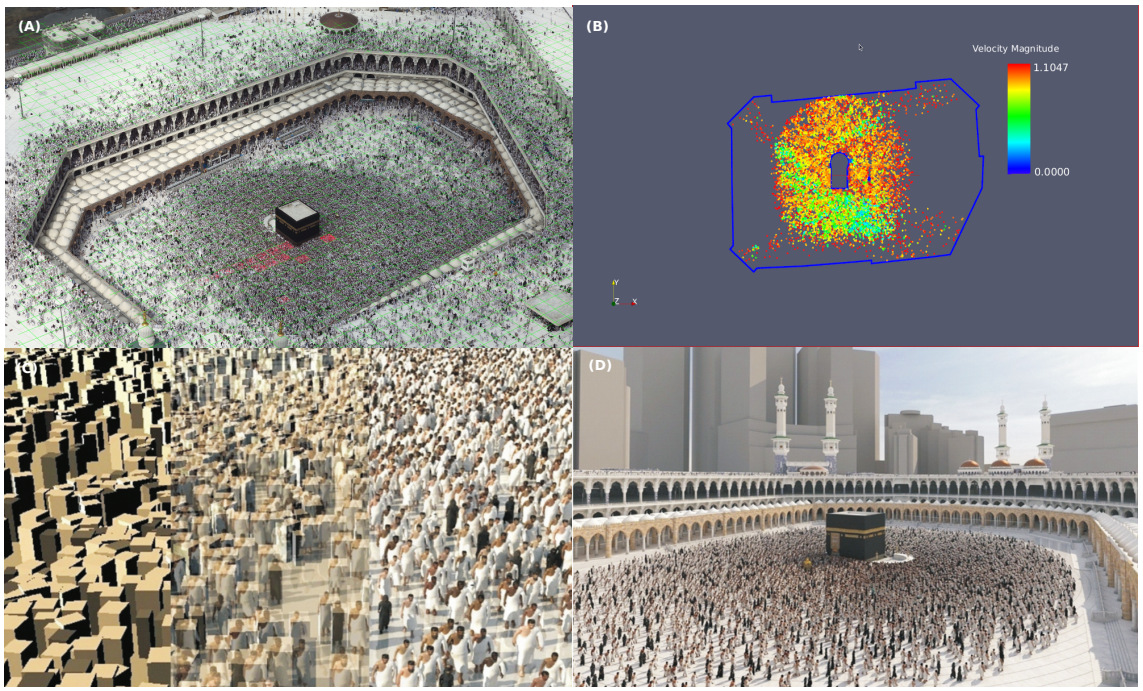

Figure 6.7: Crowd visualisation, real vs. virtual world: (A) The real world represented in the Mataf top view; (B) simulation snapshot of the Tawaf movement; (C) crowd visualisation (Characters Implementation); (D) illustrates the reproduced virtual world.

The processes used to describe animated movement of one or more objects or persons are presented in this paragraph. From tabular values carried by the microscopic simulation data results the path and velocity vectors of the agents are determined. The coordinates and velocity of every pedestrian at any time is given by the simulation data. The animation of the characters is designed in two steps: first we attach a polygon to every coordinate, and next we attach every polygon to a human character, (see fig. 6.7(C)). The motion tracking and motion animation is applied in many disciplines and scientific fields like entertainment, and medical applications, and for validation of computer vision [148]. However, we distinguish two types of animations: the film and game-makers, who take advantage from this technique to reproduce multitudinous number of avatars. The second type of animation is based on exact simulation results and illustrates more realism, which can be used to help the decision maker to manage huge crowds, detect critical points in a closed area and to help the architects and designer to establish the number of fire exits required for a building. This animation can

contribute to the validation of the simulation tools.

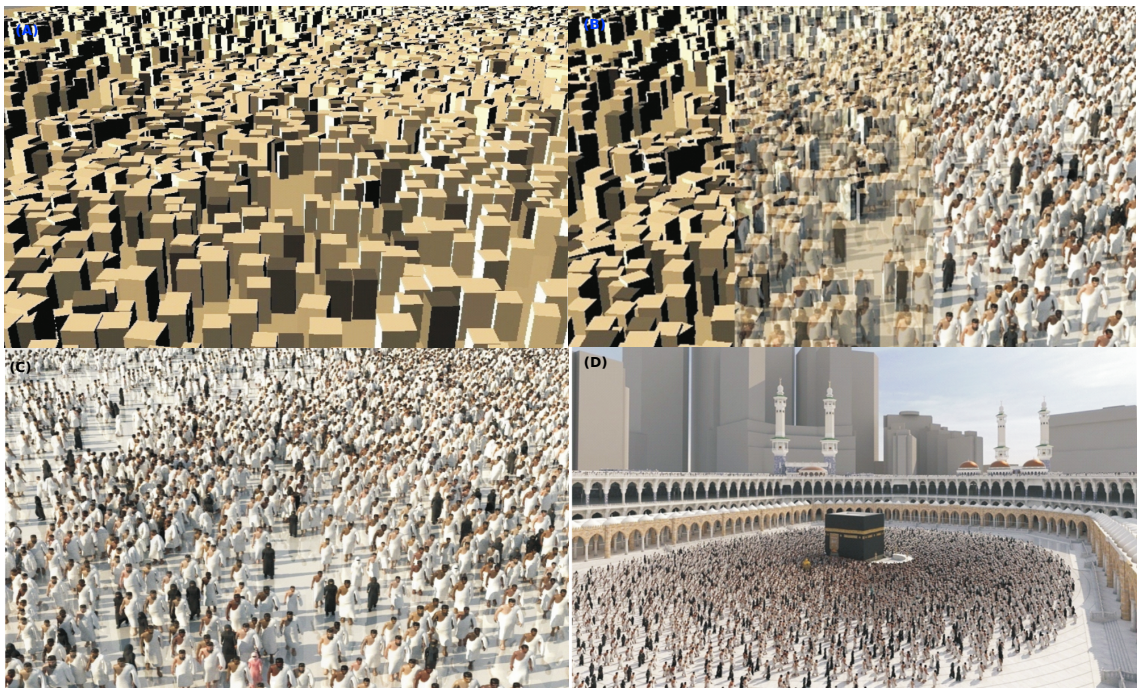

Figure 6.8: Crowd visualisation and illustration of the virtual world: (A) polygons generation from simulation data results e.g. pedestrian velocities and positions; (B) polygons vs. characters;(C) characters implementation; (D) illustrates the reproduced virtual world.

For validation of a simulation model, it is necessary to compare the simulation output with real-world data, such as video recordings representing the same circumstances of the simulation. This method can ascertain a lot of effects and behaviours that appear in crowds.

Through observation of pilgrim flow we attempt to validate and verify the crowd dynamic model tool PedFlow. The obtained real data presented in chapter 4 is used to verify a microscopic crowd dynamics model developed to solve complicated problems concerning high density crowd behaviours. The crowd dynamics model attempts to simulate the global movement of each individual influenced by the temporal circumstances and the surrounding crowd. A good agreement between the predictions and observations will validate the prediction model.

6.3 Validation of PedFlow using the optical flow method

Figure 6.9: Real vs. virtual world.

6.3.1 The optical flow method

In the last years optical flow is considered as one of the most important techniques concerning image processing and computer vision. Computing of optical flow vectors using consecutive image sequences is achieved in two different ways: gradient methods and correlation methods. Many studies show that optical flow techniques can be successfully used to identify or recognize moving objects, e.g. moving cars or walking person, [128]. Compared to other models this approach is able to operate with relatively low computational expenditure or visibility requirements on a diversity of entities, permitting reconstruction of object trajectories with high accuracy from video recordings. The detection of movement can be determined by the introduction of different sets of image sequences - by considering the different details between two images - since this is more accurate in computational calculation and prediction [129]. The difference in image brightness can then be analysed further to extract movement vectors that describe the motion of the drops (entity) captured in the respective images. This method is based on video segmentation and position identification, rather than motion recognition by analysing frame by frame sequences of ordered images.

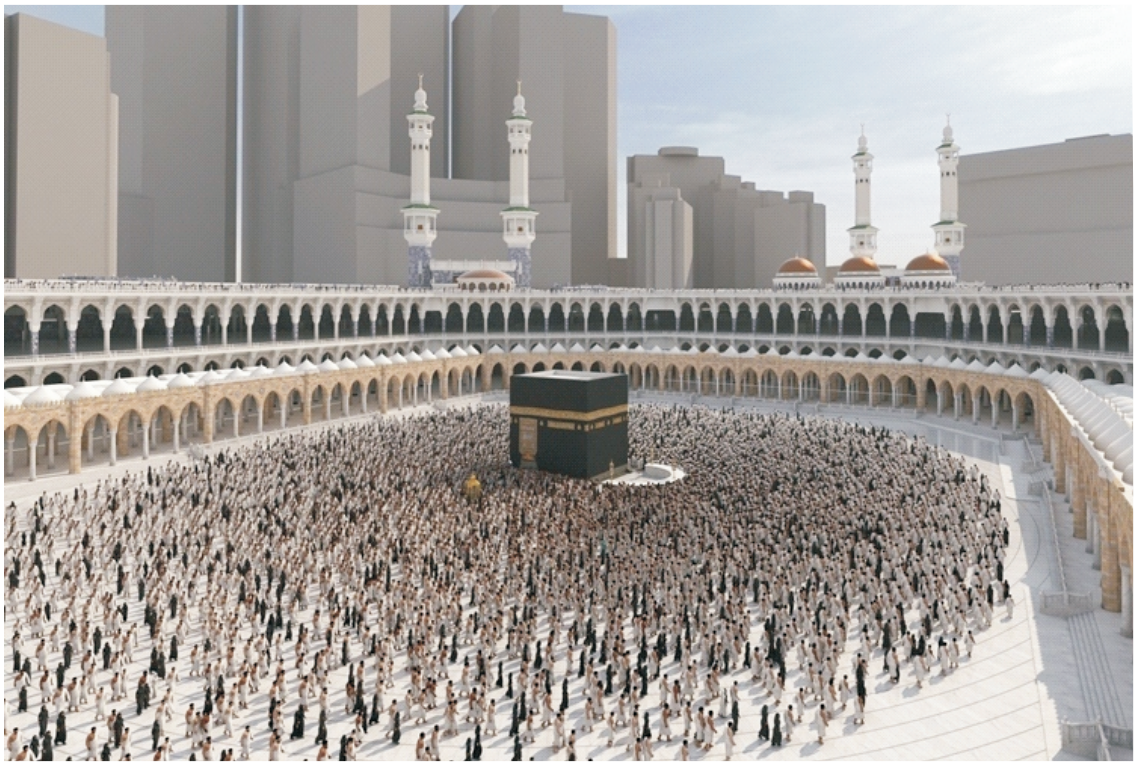

Figure 6.10: PedFlow simulation results. This figure illustrates a virtual reality based on exactly simulation results in order to give an indication of the functions of the Haram (Mataf) design to both designer and decision makers. Today simulation or computer aided engineering using finite element analysis is a method of virtually proving a product or design. Through multiphysics, and highly dynamic problems we get close to the limit of our solver's abilities. It make sense to run a complicated problem in a simulation programs in order to detect the critical points in this problem and to optimize them.

Over the last decades, computer scientists have worked in different ways to reconstruct the trajectory of moving objects. Many studies and investigations appearing in different scientific fields attempt to compute the optical flow given by a sequence of images (see the comprehensive surveys [149, 150]). The gradient and correlation methods are the mainly used techniques for computing and calculation of optical flows. In addition to these, there are other statistical methods which are able to estimate the motion parameters [151] and the use of phase information [152]. The approach proposed by Hayton establishes a relationship between optical flow and image registration techniques [153].

Let us denote by $I(x, y, t)$ the image intensity function associated with to the pixel grey value at location (x, y) of the image at time t. Gradient-based techniques are predicated on the intensity conservation assumption

$$I(x, y, t) = I(x + \delta x, y + \delta y, t + \delta t), \tag{6.1}$$

which can be expanded in a Taylor series neglecting higher order terms [154]. In general, gradient-based techniques are accurate only when the intensity is preserved, and the Taylor series approximation stays reasonable when frame-to-frame displacements due to subjects motion are a part of a pixel. To reduce the errors resulting from using this technique and to compute flow vectors over a larger image region an iteration method is deployed.

Correlation-based techniques will be useful if the image sequences do not meet the conditions required for gradient-based techniques, that means the brightness intensity is not preserved, for example in cloud [155] and combustion [156] images. Such techniques try to establish correspondences between invariant characteristics between frames. Typical features might be blobs, corners and edges [157].

6.3.2 Motion analysis and object tracking

As already mentioned optical flow is a method to estimate object motions through brightness intensity changes in sequences of consecutively ordered images. A brightness intensity region variation related to the average pixel intensity of each image in a sequence of crowd images is used to estimate the pedestrian density distribution at various sites.

The technique permitting pedestrian's movement capture e.g, extracting information about pedestrian speed, using video footage obtained from CCTV observation of urban crowd movement surveillance and image processing can be traced back to Velastin [158] and [159], who use algorithms operating on pixel intensities under a certain condition (such as a high frame rate) [160]. Other techniques and methods to compute the optical flow regarding changes in pixel intensities in a series of images sequences are developed by [161, 162, 129, 163].

Optical flow is defined as an apparent motion of image brightness. Let $I(x, y, t)$ be the image brightness that changes in time to provide an image sequence. Two main assumptions are made:

- Brightness $I(x, y, t)$ smoothly depends on coordinates x, y in a greater part of the image.
- Brightness of every point of a moving or static object does not change in time.

Let some object in the image, or some point of an object, move and denote the object displacement after time dt by (dx, dy). Using Taylor series expansion for brightness $I(x, y, t)$:

$$I(x + dx, y + dy, t + dt) = I(x, y, t) + \frac{\partial I}{\partial x}dx + \frac{\partial I}{\partial y}dy + \frac{\partial I}{\partial t}dt + ..., \quad (6.2)$$

where ..... are higher order terms, then, according to assumption 2:

$$I(x + dx, y + dy, t + dt) = I(x, y, t), \quad (6.3)$$

and

$$\frac{\partial I}{\partial x}dx + \frac{\partial I}{\partial y}dy + \frac{\partial I}{\partial t}dt + ... = 0, \quad (6.4)$$

Dividing (6.3) by dt and defining

$$\frac{dx}{dt} = u, \frac{dy}{dt} = v \quad (6.5)$$

results in

$$-\frac{\partial I}{\partial t} = \frac{\partial I}{\partial x}u + \frac{\partial I}{\partial y}v, \quad (6.6)$$

usually called the optical flow constraint equation, where (u, v) are components of the optical flow field vector in x and y coordinates respectively.

The movement recognition in this work is based on the optical flow method extracting data from picture sequences using the Lucas and Kanade algorithm [164]. It considers a group of adjacent pixels and supposes that all of them (the group of adjacent pixels) have the same velocity. It finds an approximate solution of the above equation (6.6) using the least-square method by solving a system of linear equations. The equations are usually weighted. Here the following 2×2 linear system is used:

$$\sum_{x,y} W(x, y)I_x I_y u + \sum_{x,y} W(x, y)I_y^2 v = -\sum_{x,y} W(x, y)I_y I_t, \quad (6.7)$$

$$\sum_{x,y} W(x, y)I_x^2 u + \sum_{x,y} W(x, y)I_y I_y v = -\sum_{x,y} W(x, y)I_x I_t, \quad (6.8)$$

where $W(x, y)$ is the Gaussian window and the subscripts denote derivatives. The Gaussian window may be a representation of a composition of two separable kernels with binomial coefficients. Iterating through the system can yield even better results. It means that the retrieved offset is used to determine a new window in the second image from which the window in the first image is subtracted, while I_t is calculated.

6.4 Pedestrian tracking using OpenCV software

To determine pedestrian dynamics in the mosque of Mecca, with millions of people performing their rituals, we chose to use the OpenCV tools from Intel.

This section describes the structure, operation, and functions of the open source computer vision library (OpenCV) for the Intel Corporation architecture [165]. The OpenCV library is mainly used for real time computer vision. Some example areas are human-computer interaction (HCI); object identification, segmentation, and recognition; face recognition; gesture recognition; motion tracking, ego motion, and motion understanding; structure from motion (SFM); and mobile robotics.

6.4.1 Results

Image sequences were obtained from videos collected by hd-cameras at the Hajj-2009.

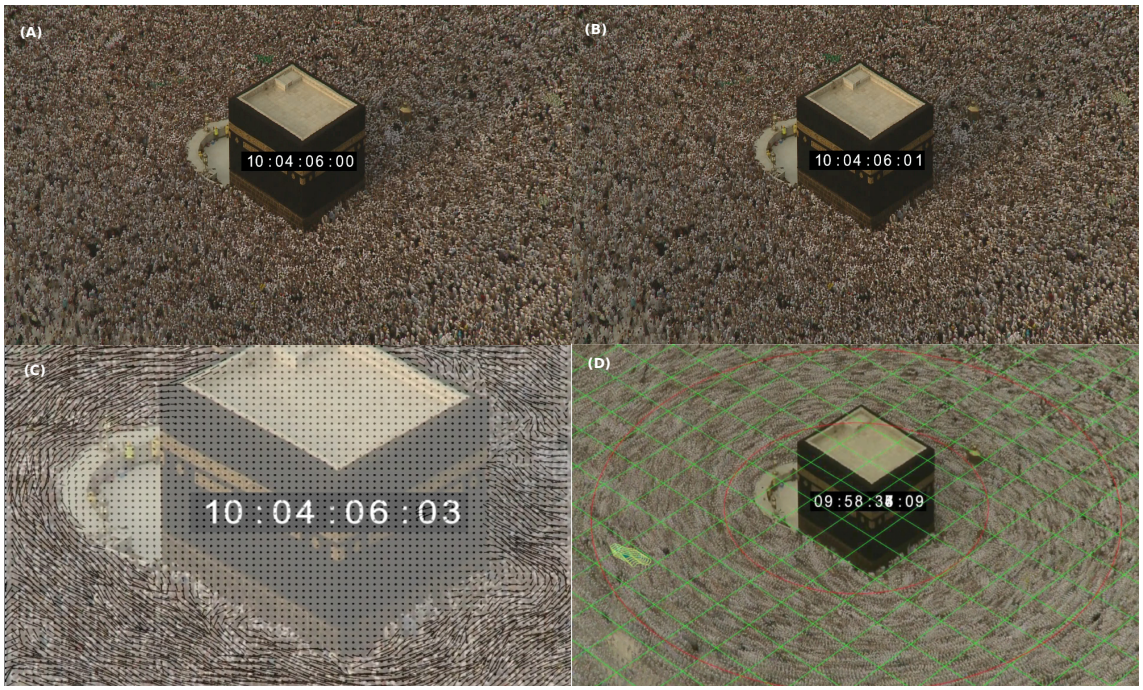

Figure 6.11: Picture Analysis through Optical Flow Tools. Pedestrian flow walking around the Kaaba in the Haram in Mecca: (A) and (B) illustrate two consecutive images in the sequence; each one of them consists of 1920×1080 images pixels, (C) shows a set of velocity vectors obtained by the Lucas and Kanade technique computing at each point of a 64×64 grid centred on the 1920×1080 pixels, (D) shows the echo effect.

The flow fields in figure 6.11 (C) show examples of the rotational movement of pilgrims around the Kaaba. We can clearly observe a kind of oscillation in the pilgrim paths around the Kaaba, this oscillation is caused by the shock-wave effect as a result of the repulsive forces between pedestrians in high density crowd dynamics. This was generated by applying the algorithm to every eighth pixel position on a pair of 1920×1080 pixel images of a surface similar to figure 6.11

(A, B). The rotation field in 6.11(C) was obtained by rotating pedestrian displacement in the Mataf area near the Kaaba wall. Through OpenCV tracking tools, it is possible to see that the movement around the Kaaba is not a perfect circular movement. The tracking of a simple individual in the pilgrim stream indicates some oscillation movement around the main path of the individual. These phenomena are due to the huge physical repulsive and attractive forces influencing the pedestrians movement. The pedestrian motion disturbance caused by high density crowd movement was also clearly visible in our pedestrian tracking on the Mataf area, (see fig.4.19). This finding agrees with the video observation on the piazza of the Haram. For verification of the PedFlow approach we compare our simulation results with those of the optical flow. With help of this approach a lot of phenomena (like the lane formation, oscillation effect and edge effect) can be seen, showing that our simulation reproduces a part of the reality. Therefore we stress that optical flow methods are very efficient for image analysis, structural analysis, image recognition, motion analysis and object tracking.

The above mentioned techniques can be helpful for the validation and verification of simulation tools but is not sufficient, since there are many effects affecting the credibility of this method, for example: ambiguity, aliasing, and the aperture effect. One of these effects the 'aperture problem', has been extensively detailed in optical flow literature [154]. However, the other two short-comings (ambiguity, aliasing) are discussed to a lesser extend. Computer scientists and algorithms developer are working to resolve this problem so that the programs can take into account the three points.

6.4.2 Discussion

We have used a multi-stage validation method. One of the most important parameters was verified, the pedestrian density distribution on the Mataf area as a function of the position $\vec{r}$ and velocity $\vec{v}$. It served in a first step of a comparison of the simulation density results with the observed density behaviour on the Mataf area at different times during the day, before and after the prayer. The maximum registered density obtained by the statistical method was 7 to 8 persons/m^2. One can clearly recognise the similarity between the statistical data and the results given by the simulation, which can reach 7 persons/m^2, especially in the congested area, (see fig. 6.12 (A) and (B)).

From observation of the Mataf it is well-known that the area indicating the beginning and the end of the Tawaf is the area most congested and accumulated by pilgrims, (see fig.6.12) (D). This phenomenon is obviously reproduced by the simulation, (see fig. 6.12 (A)). This area appears in the picture on the right lower

corner of the Kaaaba, known as black stone corner where the observed pilgrim density reached over 9 persons/m^2. All statistical results illustrating the density distribution at the Mataf area at different time intervals are demonstrated in the chapter 4.

The second step of the multi-stage verification was to compare the velocity-density diagram made by the simulation with all well-known fundamental diagrams. According to Predtetschenski and Milinski the average walking speed depends on the the walking facility and the local density which can reach 9 persons/m^2 [1]. In figure 6.12 one clearly recognizes density waves with maximum density near the Kaaba wall. There the average local density can reach a critical value of 7 to 8 persons/m^2. In the congested area the local density increases with significant dropping in the pedestrian velocity. The average local speed $\vec{v}(\vec{r},t)$ as a function of the local density $\rho(\vec{r},t)$ made by the simulation is compared with the Predtetschenski and Milinski densities in figure 6.12 (C). Our own data is shown as red crosses in figure 6.12 (B). Moreover the analysis of the data of the Mataf area showed that a reduction of the available navigation space is responsible for the speed reduction and the density increase. The small deviation in pedestrian walking speeds at lower density can be explained by the fitness level of the pedestrian. Through this comparison two phenomena are clearly demonstrated, the density effect in the Mataf area and the edge effects: the edges of a crowd move faster than the center of the crowd. This phenomenon was clearly demonstrated in the statistical results shown in figure 6.12 (D).

Comparing the results of PedFlow with results of other models in the simulation of a special cases like the Jamarat bridge, (see fig. 6.6), showed that the critical points in the Jamarat facility made by microscopic simulations with Myriad [146] are the same critical points exhibited by the PedFlow microscopic simulations of the Jamarat bridge.

6.4.3 Conclusions

For people working in software development and simulation program evolution the verification and validation of the model is a vital procedure to make sure that the tools apply to reality. The validation of the simulation program ensures the users and decision makers that the simulation results are credible and applicable in the development of the project. Moreover Turing and face validity tests contribute to progressive optimization of the program. The Turing test is a successful method comparing the real world with the simulation output. The output data obtained by the simulation can be presented to people attending the same project and working with the same tools knowledgeable about the system in the same

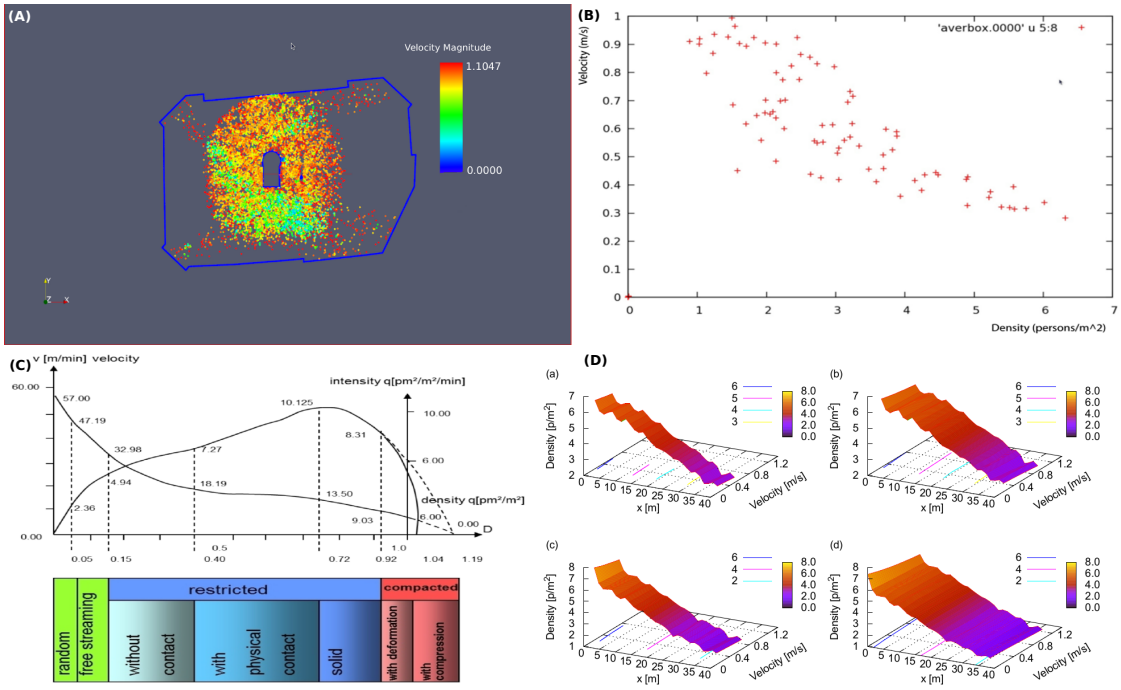

Figure 6.12: (A) A snapshot of tawaf simulation results made by PedFlow with velocity index, the blue color indicates the pedestrian stand still while the red color indicates their maximal walking speed (cf. fig. 6.7); (B) velocity-density diagram: PedFlow simulation results; (C) Predtetschenski and Milinski fundamental diagram (cf. fig. 5.6); (D) velocity-density distribution as a function of the distance from the Kabaa wall, the curves (b, d) illustrate the simulation results while the curves (a, c) show the statistical results and indicate the density behaviour on the Mataf area at different times during the day, obtained by a calculation according to the Predtetschenski and Milinski fundamental diagram see chapter 4 (cf. fig. 6.5).

exact format as the system data. The discussion between the experts about the deviation of the simulation and the system outputs can be helpful to validate the program, their explanation of how they did that should improve the model.

The opinion of the project member and model user for development, progress and verification of the simulation tools is very important. This method will be referred to as face validation. Face validation is necessary to identify the behaviour of the simulation system under the same simulation condition. A preliminary examination of the model one can deduce that this method is useful, necessary, but not sufficient.

In this chapter we have discussed verification and validation of microscopic simulation models. Different approaches and methods for deciding verification and validation of the model development process have been presented, as have been various validation techniques. Optical flow methods are very efficient for image analysis, structural analysis, image recognition, motion analysis and object tracking. This technique can be helpful for the validation and verification of

simulation tools. For the first step we try to compare our video takes with the simulation results. In the second part of this work we compare our simulation results with the optical flow results. With help of this approach a lot of phenomena (like the lane formation, oscillation effect and edge effect) can be seen, showing that our simulation reproduces a part of the reality.

As a practical example, the Haram Mosque in Mecca and the Jamarat Bridge in Saudi Arabia were used for high density crowd simulation: the huge number of pilgrims cramming the bridge during the pilgrimage to Mecca gave rise to serious pedestrian disasters in the nineties. Moreover, the analytical and numerical study of the qualitative behaviour of human individuals in a crowd with high densities can improve traditional socio-biological investigation methods.

CHAPTER 7

THE NEW DESIGN OF MATAF AND FURTHER INVESTIGATIONS

7.1 RECOMMENDATIONS FOR THE FUTURE HAJJ PLANNING AND DEVELOPMENT

With the increasing number of pilgrims every year and with the dramatic evolution of the transportation system in the world, the design and architecture of the Haram mosque in Mecca must be changed to increase the capacity, throughput and performance. The proposed and evaluated design has a specific aim, the safety of pilgrims. In order to ensure that the proposed design satisfies the required criteria of pilgrims safety, especially during overcrowding, many simulations and tests were realized to access the critical points in the Mataf area. The new Mataf area was designed to satisfy the international standard criterion of pedestrians safety, especially during overcrowding. The flow of pilgrims is demanding, since any accumulation in this area can be dangerous and has fatal consequences. The new proposed design offers a significant improvement to the safety of pilgrims. The limited spatial possibilities in and around the Haram area for infrastructural development requires an in-depth analysis and search for solutions to solve the problem of pedestrian flow. From this the concept arises to build a temporary Mataf to take a small capacity from the ground Mataf as best arrangements during the massive extension project in Masjid Al-Haram.

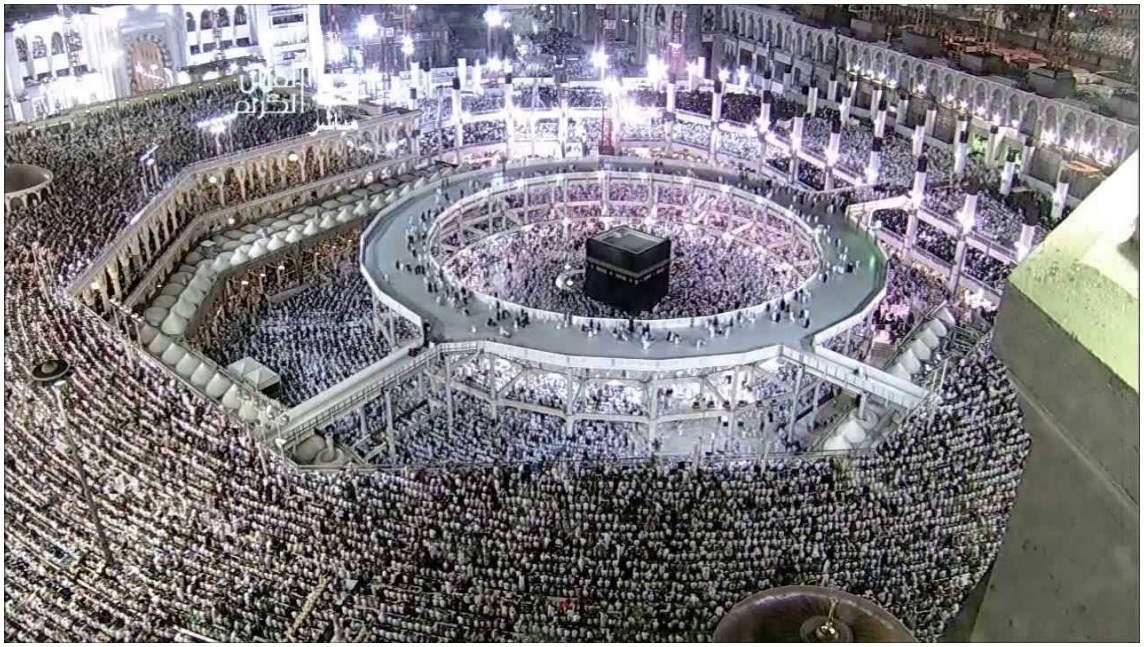

Figure 7.1: The new walk way around the Kaaba is definitely taking shape in this picture (26.07.2013).

The Mataf area is a very restrained plain. The construction of the temporary Mataf within Masjid Al Haram should attempt to resolve many problems to avoid a potential disaster in the future, such as the overcrowding disaster at the Jamarat bridge in 2005. The conceptual design as we can see in figure 7.1 has two problems; the first problem concerns the fluidity of the movement on the platform especially at the exits, the second problem concerns the ground Mataf in that the fluidity of pedestrian flow will be disturbed through the pillars carrying the platform. The Haram building must ensure the international norm of safety to allow the increased number of pilgrims.

To prevent stampede and congestion within the Mataf area during the rush hour of the Hajj events a sufficient study and analysis of the expected inflows and outflows (and, hence, number of pilgrims) must be ascertained and documented, considering the alternation possibility of large pedestrian flows. A narrow passage and bottleneck analysis within the Haram mosque area is crucial for any decision making. Through exact simulation and analysis of pedestrian fluidity on the Haram area the congestion points as the intersection or crossing points must be established and should be removed. Either the passages with counter flow must be detected as early as possible and carefully treated (examined). This analysis can be used to assess the potential safety hazards and can be helpful for the organizers. As critical points the exits of the Haram must be checked. The passage between the Mataf area and the Massaa area and between the pillars of

the temporary Mataf can cause problems for the fluidity of the pilgrim streams.

For the safety of all pilgrims on the Haram area and to ensure a quick and effective response to any occurring problems a sophisticated and continuously monitoring system (e.g. video surveillance) must be established.

An engineering system must be developed within the Haram to allow the security and emergency forces to move as quickly as possible and unobstructed to any place if something happens, to remove or at least mitigate problems.

The main problem in Mecca itself are the traffic jams. The high density of cars and buses combined with walking or road crossing pedestrians make the situation more complex for rescue or evacuation plans. The possibility to be stampeded at Hajj pilgrimage is very high at all places and especially inside the Haram in Mecca, in Muzdalifa, at the Jamarat and on the streets between the so called points of interest.

The changes necessary for a successful Hajj and its activities are all contained in the wider long-term plan for Mecca. The next expansion for Haram and Massaa requires a new infrastructure and regeneration of the east end - which will reclaim old neighbourhoods to Haram for housing and parking area - which is a huge project.

CHAPTER 8

CONCLUSIONS AND RECOMMENDATIONS

8.1 CONCLUSIONS

This work is an attempt to model high density crowd dynamic flows in autonomous and controlled scenarios. A microscopic approach was used to model this problem based on observed collective behaviour in emergency conditions, where the detailed design of interactions is overlapped by group behaviour. We presented a simple means of achieving more complex behaviour in both indoor and outdoor environments. The simulation tools produce results that compare favourably with the real data.

As a practical example, the Haram Mosque in Mecca and the Jamarat Bridge in Saudi Arabia were used for high density crowd simulation: the huge number of pilgrims cramming the bridge during the pilgrimage to Mecca caused serious pedestrian disasters in the 90's. Moreover, the analytical and numerical study of the qualitative behaviour of human individuals in a crowd with high densities can also improve traditional socio-biological investigation methods.

For obtaining empirical data different methods were used, automatic and manual methods. We analysed video recordings of the crowd movement in the Tawaf within the mosque in Mecca during the Hajj of the 27th of November, 2009. We evaluated unique video recordings of a 105$\times$ 154 m large Mataf area taken from the roof of the Mosque, (see chap. 4).

For the validation and calibration of the simulation tools, different methods were used, (see chap. 6).

At medium to high pedestrian densities, the techniques used in PedFlow can produce realistic crowd motion, with pedestrians moving at different speeds and under different circumstances, following believable trails and taking sensible avoidance action.

8.2 Further research recommendations

As possible future work, we would like to have a better understanding of the parameters influencing the crowd behaviour such as the ethnic and psychological parameters. These parameters have a significant impact on the movement of crowds especially in panic situations. The psychological-physiological parameters in the case of riots or emergencies must be investigated further and documented so that they can be implemented into other models. Our proposed approach to simulate crowd behaviours in the future is based on this dichotomy, and we propose separate models for an agent's personality and another one to account for situational factors. This question arises and opens the door to many topics that must be further investigated. There are certain things we can do to help a high density crowd participant like pilgrims, sport or music event spectators to survive a stressful situation, by planning, preparation, training and better management. But this is not sufficient to make sure that hundred percent of the crowd are safe, if we consider the number of accidents happened in the last decade.

Finally, this research is a beginning for new understanding in microscopic pedestrian studies. Limitations of resources and time have been the major constraints. The recommendations below may further improve this study.

- Improvement of the automatic video data collection to prevent the occlusion problem is highly recommended to enhance the performance of the system for higher pedestrian traffic densities.
- Additional models for obstructions and wall avoidance of microscopic pedestrian simulation models are suggested to perform better capacity analysis.
- Further research of microscopic pedestrian characteristics may reveal better understandings of the microscopic behaviour of pedestrian interaction. Comparison of the microscopic pedestrian characteristics with highway capacity manuals may suggest a better design standard than the existing level of service standard.
- Further exploration of many applications of the microscopic pedestrian simulation model is recommended.

The effects of such extreme conditions on the human body and how the people's bodies respond are very interesting to be considered in the simulation model to prevent potential hazard and to answer many questions occupying the scientists for decades. For example:

- What can we humans do to better equip a huge number of people attending an audience safely. And in case of emergency how people cope with and survive extreme environments or conditions?
- Are there decisions or things we can do, to better increase crowd participant chances to survive a crowd disaster or crush?
- Considering the psychological factor, are there some decisions that are simply out of our (conscious) control in case of panic?
- What emergency rescue services are available in the gathering places? What personnel, equipment, and procedures are in place to assist humans in emergencies such as those mentioned in case of crowd disasters? Are there individuals in the emergency staff who have specialized training that can deal with extreme conditions such as crowd panic and crowd injuries?
- Are there experienced people who are able to calm down the people if the crowd breaks out of control in such extreme conditions (like the ones described in crowd forces paragraphs)?

This question arises and opens the door to many topics that must be further investigated. There are certain things we can do to help a high density crowd participant like pilgrims, sport or music event spectator to survive a stressful situation, like planning, preparation, training and better management. But this is not sufficient to make sure that hundred percent of the crowd are safe, if we consider the number of accidents happened in the last decade.

APPENDIX A

PUBLICATIONS RELATED TO THIS THESIS

- Mohamed H. Dridi, Tracking Individual Targets in High Density Crowd Scenes Analysis of a Video Recording in Hajj 2009. Current Urban Studies 3, 35-53 (2015).
- Mohamed H. Dridi, Simulation of high density pedestrian flow: a microscopic model. Open Journal of Modelling and Simulation 3 (2015), 81-95 (2015).
- Mohamed H. Dridi, Pedestrian flow simulation validation and verification techniques. Current Urban Studies 3, 119-134 (2015).
- Mohamed H. Dridi, List of Parameters Influencing the Pedestrian Movement and Pedestrian Database. International Journal of Social Science Studies 3, No. 4, 94-106 (2015).

ACKNOWLEDGMENTS

I would like to express my sincerest thanks and gratitude to my advisor, Prof. Dr. rer. nat. Günter Wunner, who has enlightened me to pursue knowledge and learning. Through his constructive discussions and superb analytical skills, he has helped me greatly in this research. I am also grateful to the committee members, Prof. Dr. Günter Haag and Prof. Dr. Bechinger. I am grateful to Dr. Mahmoud Bodo Rasch for his encouragement and practical advice. I am also thankful to him for supporting this work. I would like to express my sincerest thanks and gratitude to Prof. Dr. G. Wunner for a critical reading of the manuscript, for his important comments and suggestions to improve the manuscript. Many thanks to Dr. H. Cartarius for his support during writing this work. I would like to acknowledge Prof. Dr. R. Löhner, Dr. E. Haug, Dipl.-Ing. B. Gawenat for numerous discussions and lectures on related topics. Many thanks to my friend Dipl.-Ing. Sead Becirovic. Special acknowledgement is also given to Thomas Richter Alender, Dr. Michael Curcic and Carla Sundermann for their support during this research. Finally, I am greatly indebted to Yassine Maaradji, my family for their understanding, patience and support during the entire period of my study.

BIBLIOGRAPHY

[1] W. M. Predtechenski and A. I. Milinski. *Personenströme in Gebäuden*. Verlagsgesellschaft Rudolf Müller, Köln (1971).

[2] V. J. Blue. Cellular automata microsimulation for modeling bi-directional pedestrian walkways. *Transportation Research, Part B: Methodological* 35(3), 293–312 (2001).

[3] C. W. Reynolds. Flocks, herds, and schools: A distributed behavioral model. *Computer Graphics* 21, 25–34 (1987).

[4] D. Helbing, I. Farkas, and T. Vicsek. Simulating dynamical features of escape panic. *Nature* 407, 487–490 (2000).

[5] D. Helbing, A. Johansson, and H. Zein Al-Abideen. The Dynamics of Crowd Disasters: An Empirical Study. *Phys. Rev. E* 75, 046109 (2007).

[6] D. Helbing and P. Molnár. Self-organization phenomena in pedestrian crowds. In *Self-organization of Complex Structures: From Individual to Collective Dynamics*, pp. 569–577. Gordon and Breach (1997).

[7] V. Blue and J. Adler. Emergent fundamental pedestrian flows from cellular automata microsimulation. *Transportation Research Board* 1644, 29–36 (1998).

[8] J.J. Fruin. *Designing for Pedestrians: A Level of Service Concept*. Polytechnic University of Brooklyn; http://books.google.de/ books?id=LM_Etg AACAAJ (1970).

[9] J. J. Fruin. *Pedestrian planning and design*. Metropolitan Association of Urban Designers and Environmental Planners; http://books.google.de/books?id =AydSAAAAMAAJ (1971).

[10] United States Federal Highway Administration. Office of Traffic Operations. *The 1985 Highway Capacity Manual: A Summary*. U. S. Department of Transportation, Federal Highway Administration (1986). http:// books.google.de/books?id=VkpPAAAAMAAJ.

[11] D. Helbing. A mathmatical model for the behavior of pedestrians. *Behavioral Science* 36, 298–310 (1991).

[12] D. Helbing and T. Vicsek. Optimal self-organization. *New Journal of Physics* 1(13), 1–17 (1999).

[13] P. G. Gips and B. Marksjo. A micro-simulation model for pedestrian flows. *Mathmatics and Computer in Simulation* 27, 95–105 (1985).

[14] G. G. Lovas. Modeling and simulation of pedestrian traffic flow. *Tranportation Research* 28B, 429–443 (1994).

[15] S. Okazaki. A study of pedestrian movement in architectural space, part 1: Pedestrian movement by the application on magnetic models. *Trans. of A. I. J.* 283, 111–119 (1979).

[16] S. Okazaki and S. Matsushita. A study of simulation model for pedestrian movement with evacuation and queuing. *In Proceeding of the International Conference on Engineering for Crowd Safety* 12, 271–280 (1993).

[17] P. Thompson and E. Marchant. A computer model the evacuation of large building populations. *Fire and Safety Journal* 24, 131–148 (1995a).

[18] J. Watts. Computer models for evacuation analysis. *Fire and Safety Journal* 12(1237), 245 (1987).

[19] D. Helbing and P. Molnar. Social force model for pedestrian dynamics. *Physical review E* 51(4282), 4282–4286 (1995).

[20] D. Helbing. A fluid-dynamic model for the movement of pedestrians. *Complex Systems* 6, 391–415 (1992).

[21] R. Löhner. On the modeling of pedestrian motion. *Applied Mathematical Modelling* 34(2), 366–382 (2010).

[22] D. Helbing, I. J. Farkas, P. Molnar, and T. Vicsek. Simulation of Pedestrian Crowds in Normal and Evacuation Situations. In *Pedestrian and evacuation dynamics*, edited by Michael Schreckenberg and Som Deo (Eds.) Sharma, pp. 21–58. Springer, Berlin (2002).

[23] M. Fukui and Y. Ishibashi. Self-organized phase transitions in CA-models for pedestrians. *J. Phys. Soc. Japan* 8, 2861–2863 (1999).

[24] M. Muramatsu and T. Nagatani. Jamming transition in two-dimensional pedestrian traffic. *Physica A: Statistical Mechanics and its Applications* 275 (1-2), 281–291 (2000).

[25] S. J. Yuhaski and J. M. Smith. Modeling Circulation Systems in Buildings Using State Dependent Queueing Models. *Queueing Syst.* 4(4), 319–338 (1989).

[26] A. Treuille, S. Cooper, and Z. Popovic. Continuum Crowds. *ACM Trans. Graph* 25, 1160–1168 (2006).

[27] D. Helbing. Traffic and related self-driven manyparticle systems. *Reviews of Modern Physics* 73(4), 1067–1141 (2001).

[28] Craig Reynolds. Steering Behaviors for Autonomous Characters. In *Game Developers Conference 1999*, pp. 763–782. Miller Freeman Game Group, San Francisco, California (1999).

[29] S. R. Musse and D. Thalmann. A Model of Human Crowd Behavior: Group Inter-Relationship and Collision Detection Analysis. In *Proc. Workshop of Computer Animation and Simulation of Eurographics'97*, pp. 39–51 (1997).

[30] N. Pelechano, K. O'Brien, B. Silverman, and N. Badler. Crowd Simulation Incorporating Agent Psychological Models, Roles and Communication. In *First International Workshop on Crowd Simulation, Lausanne, Switzerland, 24-25 November 2005*, pp. 21–30 (2005).

[31] O. C. Cordeiro, A. Braun, C. B. Silveria, S. R. Musse, and G. G. Cavalheiro. Concurrency on social forces simulation model. In *First International Workshop on Crowd Simulation, Lausanne, Switzerland, 24-25 November 2005* (2005).

[32] R. Gayle, W. Moss, M. C. Lin, and D. Manocha. Multi-robot coordination using generalized social potential fields. In *IEEE International Conference on Robotics and Automation, 2009. ICRA '09.*, pp. 106–113 (2009).

[33] A. Sud, R. Gayle, E. Andersen, S. Guy, M. Lin, and D. Manocha. Real-time Navigation of Independent Agents Using Adaptive Roadmaps. In *Proceedings of the 2007 ACM Symposium on Virtual Reality Software and Technology*, VRST '07, pp. 99–106. ACM, New York, NY, USA (2007).

[34] W. Shao and D. Terzopoulos. Autonomous Pedestrians. *Graph. Models* 69(5-6), 246–274 (2007).

[35] S. Paris, J. Pettre, and S. Donikian. Pedestrian reactive navigation for crowd simulation: a predictive approach. *Computer Graphics Forum* 26, 665–674 (2007).

[36] H. Yeh, S. Curtis, S. Patil, J. van den Berg, D. Manocha, and M. Lin. Composite Agents. In *Proceedings of the 2008 ACM SIGGRAPH/Eurographics Symposium on Computer Animation*, SCA '08, pp. 39–47. Eurographics Association, Aire-la-Ville, Switzerland, Switzerland (2008).

[37] P. Fiorini and Z. Shiller. Motion planning in dynamic environments using velocity obstacles. *The International Journal of Robotics Research* 17, 760–772 (1998).

[38] F. Feurtey. *Simulating the Collision Avoidance Behavior of Pedestrians.* Master's thesis, University of Tokyo, School of Engineering, Department of Electronic Engineering. (2000).

[39] S. Guy, J. Chhugani, C. Kim, N. Satish, M. C. Lin, D. Manocha, and P. Dubey. ClearPath: Highly Parallel Collision Avoidance for Multi-Agent Simulation. In *ACM Siggraph/Eurographics Symposium on Computer Animation*, pp. 177–187. ACM (2009).

[40] A. Sud, E. Andersen, S. Curtis, M. Lin, and D. Manocha. Real-time Path Planning for Virtual Agents in Dynamic Environments. In *ACM SIGGRAPH 2008 Classes*, SIGGRAPH '08, pp. 55:1–55:9. ACM, New York, NY, USA (2008).

[41] J. Van den Berg, M. C. Lin, and D. Manocha. Reciprocal velocity obstacles for realtime multi-agent navigation. In *IEEE Conf. Robotics and Automation*, pp. 5917–5922. IEEE (2008).

[42] J. Van den Berg, S. J. Guy, M. C. Lin, and D. Manocha. Reciprocal *n*-Body Collision Avoidance. In *Robotics Research - The 14th International Symposium, ISRR 2009, August 31 - September 3, 2009, Lucerne, Switzerland*, pp. 3–19 (2009).

[43] A. Schadschneider, D. Chowdhury, and K. Nishinari. *Stochastic Transport in Complex Systems: From Molecules to Vehicles*. Elsevier Science; http://books.google.de/books?id=dRcxsa4sobQC (2010).

[44] C. Loscos, D. Marchal, and A. Meyer. Intuitive Crowd Behaviour in Dense Urban Environments using Local Laws. In *Theory and Practice of Computer Graphics (TPCG 03)*, pp. 122–129. IEEE Computer Society Press (2003).

[45] M. C. Lin, S. Guy, R. Narain, J. Sewall, S. Patil, J. Chhugani, A. Golas, J. Van den Berg, S. Curtis, D. Wilkie, P. Merrell, C. Kim, N. Satish, P. Dubey, and D. Manocha. Interactive Modeling, Simulation and Control of Large-Scale Crowds and Traffic. In *Motion in Games, Second International Workshop, MIG 2009, Zeist, The Netherlands, November 21-24, 2009. Proceedings*, pp. 94–103 (2009).

[46] L. Heigeas, A. Luciani, J. Thollot, and N. Castagné. A Physically-Based Particle Model of Emergent Crowd Behaviors. In *Graphicon* (2003).

[47] T. I. Lakoba, D. J. Kaup, and N. M. Finkelstein. Modifications of the Helbing-Molnar-Farkas-Vicsek social force model for pedestrian evolution. *Simulation* 81(339) (2005).

[48] Y. Sugiyama, A. Nakayama, and K. Hasebe. 2-Dimensional optimal velocity models for granular flows. *Pedestrian and Evacuation Dynamics* pp. 155–160 (2002).

[49] L. F. Henderson. The statistics of crowd fluids. *Nature* 229, 381–383 (1971).

[50] B. Maury, A. Roudneff-Chupin, and F. Santambrogio. A Macroscopic Crowd Motion Model of the Gradient-flow Type, Mathematical Models and Methods. *Applied Sciences* 20, 1787–1821 (2010).

[51] J. M. Lasry and P. L. Lions. Mean field games. *Japanese Journal of Mathematics* 2, 229–260 (2007).

[52] R. M. Colombo and M. D. Rosini. Pedestrian flows and non-classical shocks. *Math. Methods Appl. Sci.* 28, 1553–1567 (2005(13)).

[53] V. J. Blue and J. L. Adler. Cellular automata microsimulation of bidirectional pedestrian flows. *Transportation Research Record* 1678, 135–141 (1999).

[54] V. J. Blue and J. L. Adler. Modeling four-directional pedestrian flows. *Transportation Research Record* 1710, 20–27 (2000).

[55] C. Burstedde, K. Klauck, A. Schadschneider, and J. Zittartz. Simulation of-pedestrian dynamics using a two-dimensional cellular automaton. *Physica A* 295, 507–525 (2001).

[56] C. Burstedde, K. Klauck, A. Schadschneider, and J. Zittartz. Cellular Automaton Approach to Pedestrian Dynamics – Applications. In *Proceedings from the first Pedestrian and Evacuation Dynamics Conference, PED01*, pp. 87–98 (2001).

[57] H. L. Klupfel. *A Cellular Automaton Model for Crowd Movement and Egress Simulation.* Ph.D. thesis, Dissertation for the University Duisburg-Essen, Germany. (2003).

[58] D. Helbing, I. Farkas, and T. Vicsek. Simulating dynamical features of escape panic. *Nature* 407, 487–490 (2000).

[59] D. Helbing. *Verkehrsdynamik. Neue physikalische Modellierungskonzepte*. Springer, Berlin (1997).

[60] D. Helbing, I. J. Farkas, and T. Vicsek. Freezing by heating in a driven mesoscopic system. *Phys. Rev. Lett* 84, 1240–1243 (2000).

[61] K. Teknomo. Application of microscopic pedestrian simulation model. *Transportation Research Part F: Traffic Psychology and Behaviour* 9(1), 15–27 (2006).

[62] C. W. Reynolds. Interaction with Groups of Autonomous Characters. In *Proceedings of Game Developers Conference 2000*, pp. 449–460. CMP Game Media Group, San Francisco, California (2000).

[63] G. K. Still. New Computer system can predict human behaviour response to building fires. *Fire 84* pp. 40–41 (1993).

[64] R. Narain, A. Golas, S. Curtis, and M. C. Lin. Aggregate dynamics for dense crowd simulation. In *ACM Transactions on Graphics (TOG)*, volume 28(5), p. 122. ACM (2009).

[65] R. L. Hughes. The flow of human crowds. *Annu. Rev. Fluid Mech.* 35, 169–182 (2003).

[66] D. Helbing, L. Buzna, A. Johansson, and T. Werner. Self-organized pedestrian crowd dynamics: Experiments, simulations, and design solutions. *Transportation Sci.* 39, 1–24 (2005).

[67] P. Dallard, T. Fitzpatrick, A. Flint, S. Le Bourva, A. Low, R. M. Ridsdill, and M. Willford. The London Millennium Footbridge. *The Structural Engineer* 79(22), 17–33 (2001).

[68] K. Rahman, N. Abdul Ghani, A. Abdulbasah Kamil, and M. Mustafa. Analysis of Pedestrian Free Flow Walking Speed in a Least Developing Country: A Factorial Design Study. *Research Journal of Applied Sciences, Engineering and Technology* 4(21), 4299–4304 (2012).

[69] R. L. Knoblauch, M. T. Pietrucha, and M. Nitzburg. Field studies of pedestrian walking speed and start-up time. *Transportation Research Record 1538. Washington (DC): National Research Council, Transportation Research Board* Dec, 27–38 (1996).

[70] H. J. P. Timmermans and Ebooks Corporation. *Pedestrian Behavior: Models, Data Collection and Applications: Models, Data Collection and Applications*. Emerald (2009). http:// books.google.de/books?id=LQVE-pbhMQ0C.

[71] Wikipedia. Usain Bolt. *http://de.wikipedia.org/wiki/Usain_Bolt* (abgerufen am 19. März 2013).

[72] M. Xiong, W. Cai, S. Zhou, M.Y.H. Low, F. Tian, D. Chen, Daren Wee Sze Ong, and B. D. Hamilton. A case study of multi-resolution modeling for crowd simulation. In *SpringSim '09: Proceedings of the 2009 Spring Simulation Multiconference*, pp. 1–8. Society for Computer Simulation International (2009).

[73] J. J. Fruin. Crowd dynamics and auditorium management. *Auditorium News, International Association of Auditorium Managers. Available online at www.iaam.org/CVMS/IAAMCrowdDyn.doc.* (abgerufen am 13. June 2011).

[74] U. Weidmann. Transporttechnik der Fußgänger. Schriftenreihe des IVT 90, ETH Zürich (1992). (in German).

[75] J. Zhang, W. Klingsch, A. Schadschneider, and A. Seyfried. Ordering in bidirectional pedestrian flows and its influence on the fundamental diagram. *Journal of Statistical Mechanics: Theory and Experiment* 2012, P02002 (2012).

[76] J. J. Fruin. The causes and prevention of crowd disasters. In *Smith, R. A., Dickie, J. F. (eds.): Engineering for Crowd Safety*. Elsevier: New York (1993).

[77] P. Pecol, P. Argoul, S. Dal Pont, and S. Erlicher. The non-smooth view for contact dynamics by Michel Frémond extended to the modeling of crowd movements. *Discrete and Continuous Dynamical Systems - Series S (DCDS-S), AIMS* 6, 547–565 (2013).

[78] Campus Police. General Evacuation Procedures. Technical report, Oxford College of Emory University; http://oxford.emory.edu/life-at-oxford/campus-police/fire-safety/general-evacuation-procedures/ (2013).

[79] R. Loehner. Applied CFD Techniques, An introduction Based on Finite Element Methods. *John, Wiley and Sons Ltd, The Atrium, Southern Gate, Chichester, West Sussex PO19 8SQ. England* p. 58 (2008).

[80] B. Delaunay. Sur la sphère vide, Izvestia Akademii Nauk SSSR. *Otdelenie Matematicheskikh i Estestvennykh Nauk* 7, 793–800 (1934).

[81] R. Loehner, K. Morgan, J. Peraire, and M. Vahdati. Finite Element Flux-Corrected Transport (FEM-FCT) for the Euler and Navier-Stokes Equations. *ICASE Rep. 87-4, Int. J. Num. Meth. Fluids 7* pp. 1093–1109 (1987).

[82] R. Loehner and J. Ambrosiano. A Vectorized Particle Tracer for Unstructured Grids. *Journal of Computational Physics* 91(1), 22–31 (1990).

[83] D. Oberhagemann. Static and Dynamic Crowd Densities at Major Public Events. Technical report, vfdb TB 13-01 Ed: Vereinigung zur Förderung des Deutschen Brandschutzes e. V. (vfdb), German Fire Protection Association; http://www.vfdb.de/download/TB_13_01_Crowd_densities.pdf (2012).

[84] R. S. C. Lee and R. L. Hughes. Prediction of human crowd pressures. *Accident Analysis and Prevention* 38, 712–722 (2006).

[85] C. E. Nicholson and B. Roebuck. The investigation of the Hillsborough disaster by the health and safety Executive. *Safety Science* 18(4), 249–259 (1995).

[86] W. Zhen, L. Mao, and Z. Yuan. Analysis of trample disaster and a case study – Mihong bridge fatality in China in 2004. *Safety Science* 46, 1244–1270 (2008).

[87] R. A. Smith and L. B. Lim. Experiments to investigate the level of 'comfortable' loads for people against crush barriers. *Safety Sci.* 18, 329–335 (1995).

[88] E. J. Evans and F. Hayden. Tests on Live Subjects to Determine the Tolerable Forces that may be exerted by Crowd Control Crush Barriers. Technical report, Report on Research in Biomechanics at the University of Surrey, University of Surrey, Guildford, UK. (1971).

[89] A. Collins. Crush Barrier Strengths and Spacings. Technical report, Liverpool Football Club, London (1973). http://hillsborough.independent.gov.uk/repository/TSO000000870001.html.

[90] G. K. Still. *Crowd Dynamics.* Ph.D. thesis, The University of Warwick (2000).

[91] Professor Hyung-Yun Choi. Biomechanical discomfort factors in egress of older drivers. *Hongik University, Korea* (2010).

[92] J. J. Fruin. Crowd Disasters - A Systems Evaluation of Causes and Countermeasures. *Inc. in U.S. National Bureau of Standards, pub. NBSIR 81–3261* p. 146 (July 1981).

[93] S. G. Fattal and L. E. Cattaneo. Investigation of Guardrails for the Protection of Employees From Occupational Hazards. *Nat. Bur. Stds. NBSIR 76–1139* p. 114 (July 1976).

[94] J. J. Fruin. Pedestrian Planning and Design. *Elevator World* (1987).

[95] A. Seyfried. Comparison of Pedestrian Fundamental Diagram Across Cultures. *Advances in Complex Systems.* 12 (3), 393–405 (2009).

[96] B. D. Jacobs and P. Hart. Disaster at Hillsborough Stadium: A comparative analysis. *In: Parker, D. J. & Handmer, J. W. (eds.) Hazard management and emergency planning, Chapt 10. James and James Science, London* (1992).

[97] J. S. Coleman. *Foundations of Social Theory*. Belknap Series. Belknap Press of Harvard University Press; http://books.google.de/books?id=a4Dl8tiX4b8C (1994).

[98] E. L. Quarantelli. *The Behavior of Panic Participants*. National Emergency Training Center; http://books.google.de/books?id=tSAJSQAACAAJ (1957).

[99] R. H. Turner and L. M. Killian. *Collective behavior.* Prentice Hall College Div, third edition (1987).

[100] A. Mintz. Non-adaptive group behavior. *Journal of Abnormal Psychology* 46, 150–159 (1951).

[101] R. A. Smith and J. F. Dickie. *Engineering for crowd safety: proceedings of the International Conference on Engineering for Crowd Safety, London, UK, 17-18 March, 1993*. Elsevier; http://books.google.de/books?id=Rs VRAAAAMAAJ (1993).

[102] D. Elliott and D. Smith. Football stadia disasters in the United Kingdom: Learning from tragedy? *Industrial and Environmental Crisis Quarterly* 7(3), 205–229 (1993).

[103] J. P. Keating. The myth of panic. *Fire Journal* 147, 57–61 (1982).

[104] H. Kessler. Crowd Panic: Proactive versus Reactive Responses. Technical report (1996-2013). http://www.ifpo.org/resources/articles-and-reports/protection-of-specific-environments/ crowd-panic-proactive-versus-reactive-responses/.

[105] F.J. Rutherford and A. Ahlgren. *Science for All Americans*. Oxford University Press, USA; http://books.google.de/books?id=LKadiKAUljEC (1991).

[106] U. Chattaraj, A. Seyfried, and P. Chakroborty. Comparison of pedestrian fundamental diagram across cultures. *Advances in complex systems* 12, 393–405 (2009).

[107] M. Mänty, C. F. de Leon, T. Rantanen, P. Era, A. N. Pedersen, A. Ekmann, M. Schroll, and K. Avlund. Mobility-related fatigue, walking speed, and muscle strength in older people. *Oxford Journals: Medicine & Health & Science & Mathematics: The Journals of Gerontology: Series A* 67A, Issue 5, 523–529 (2011).

[108] T. Cox. Stress. *London: Macmillan Press.* (1978).

[109] L. Berkowitz. On the formation and regulation of anger and aggression: A cognitive-neoassociationistic analysis. *American Psychologist* 45(4), 494–503 (1990).

[110] R. M. Yerkes and J. D. Dodson. The relation of strength of stimulus to rapidity of habit-formation. *Journal of Comparative Neurology and Psychology* 18(5), 459–482 (1990).

[111] C. A. Anderson. Heat and violence. *Current Directions in Psychological Science* 10(1), 33–38 (2001).

[112] G. W. Evans. *Environmental stress*. CUP Archive (1984).

[113] N. Pelechano, K. O'brien, B. Silverman, and N. Badler. Crowd Simulation Incorporating Agent Psychological Models, Roles and Communication. In *1st Int'l Workshop on Crowd Simulation*, pp. 21–30 (2005).

[114] M. Eysenck. Simply psychology. *Psychology Press.* (2002).

[115] S. P. Hoogendoorn and W. Daamen. Pedestrian Behavior at Bottlenecks. *Transportation Science* 39 (2), 147–159 (2005).

[116] A. Johansson and D. Helbing. From crowd dynamics to crowd safety: A video-based analysis. *Advances in Complex Systems* 4 (4), 497–527 (2008).

[117] M. Boltes, A. Seyfried, B. Steffen, and A. Schadschneider. Automatic extraction of pedestrian trajectories from video recordings. In *Pedestrian and Evacuation Dynamics.*, edited by A. Schadschneider In: W. W. F. Klingsch, C. Rogsch and M. Schreckenberg (Eds.), pp. 43–54. Springer-Verlag Berlin Heidelberg (2010).

[118] C. Papageorgiou and T. Poggio. Trainable pedestrian detection. In *Image Processing, 1999. ICIP 99. Proceedings. 1999 International Conference on*, volume 4, pp. 35–39 vol.4 (1999).

[119] A. N. Marana, L. F. Costa, R. A. Lotufo, and S. A. Velastin. On the efficacy of texture analysis for crowd monitoring. In *Computer Graphics, Image Processing, and Vision, 1998. Proceedings. SIBGRAPI '98. International Symposium on*, pp. 354–361 (1998).

[120] Z. Zhang and M. Li. Crowd density estimation based on statistical analysis of local intra-crowd motions for public area surveillance. *Optical Engineering* 51(4), 047204 (2012).

[121] V. Verona and A. Marana. Wavelet packet analysis for crowd density estimation. In *Prnc. the listed International Symposia on Applied Information*, pp. 535–540. Aeta Press, Innsbmck, Austria (2001).

[122] X. Li, L. Shen, and H. Li. Estimation of crowd density based on wavelet and support vector machine. *Trans. Inst. Meas. Control (London)* 28(3), 299–308 (2006).

[123] Xinyu Wu, Guoyuan Liang, Ka Keung Lee, and Yangsheng Xu. Crowd Density Estimation Using Texture Analysis and Learning. In *IEEE International Conference on Robotics and Biomimetics, ROBIO 2006, Kunming, China, 17-20 December 2006*, pp. 214–219 (2006).

[124] G. Sen, L. Wei, and Y. H. Ping. Counting people in crowd open scene based on grey level dependence matrix. In *IEEE International Conference on Information and Automation, 2009, ICIA '09, Zhuhai/Macau, China, 22-25 June 2009*, pp. 228–231 (2009).

[125] B. Heisele and C. Woehler. Motion-based recognition of pedestrians. In *Pattern Recognition. Proceedings. Fourteenth International Conference on*, pp. 1325–1330. IEEE, Brisbane, Australia (1998).

[126] A. Seyfried, B. Steffen, W. Klingsch, and M. Boltes. The Fundamental Diagram of Pedestrian Movement Revisited. *Journal of Statistical Mechanics* p. 10002 (2005).

[127] W. H. K. Lam and C. Y. Cheung. Pedestrian Speed-Flow Relationships for walking facilities in Hong-Kong. *Journal of Transportation Engineering, ASCE* 126(4), 343–349 (2000).

[128] Y. Ricquebourg and P. Bouthemy. Real-time tracking of moving persons by exploiting spatio-temporal image slices. *IEEE Trans. on Pattern Analysis and Machine Intelligence* 22(8), 797–808 (2000).

[129] O. Masoud and N.P. Papanikolopoulos. A novel method for tracking and counting pedestrians in real-time using a single camera. *IEEE Transactions on Vehicular Technology* 50(5), 1267–78 (2001).

[130] S. Murakami and A. Wada. An automatic extraction and display method of walking persons' trajectories. In *15th International Conference on Pattern Recognition, ICPR'00, Barcelona, Spain, September 3–8, 2000*, volume 4, pp. 611–614. IEEE Computer Society (2000).

[131] D. D. Hoffman and Flinchbaugh B. E. The interpretation of biological motion. *Biological Cybernetics* 42, Issue 3, 195–204 (1982).

[132] Saudi Arabia government. Makkah City Profile; http://www.the-saudi.net/saudi-arabia/makkah/makkah_city_ profile.htm (2013).

[133] Ministry of Hajj. Saudi Arabia. Supreme Hajj Committee; http:// haj.gov.sa/en-us/Pages/default.aspx (2013).

[134] Etzel van Kuijk Cor van Dijkum, Dorien DeTombe. *Validation of simulation Models*. Netherlands Universities Institute for Coördination of Research in Social Sciences (1998 / 1999).

[135] P. L. Knepell and D. C. Arangno. *Simulation Validation: A Confidence Assessment Methodology*. Wiley-IEEE Computer Society Press, Los Alamitos (1993).

[136] M. B. Beck, J. R. Ravetz, L. A. Mulkey, and T. O. Barnwell. On the problem of model validation for predictive exposure assessments. *Stochastic Hydrology and Hydraulics* 11, 229–254 (1997).

[137] J. P. C. Kleijnen. Verification and validation of simulation models. *European Journal of Operational Research* 82(1), 145–160 (1995).

[138] R.G. Sargent. Verifying and validating simulation models. In *Proceedings of the 1996 Winter Simulation Conference, eds. J.M. Charnes, D.M. Morrice, D.T. Brunner, and J.J. Swain*, pp. 55–64 (1996).

[139] Jack P. C. Kleijnen. Validation of Models: Statistical Techniques and Data Availability. In *Proceedings of the 31st Conference on Winter Simulation: Simulation—a Bridge to the Future - Volume 1*, WSC '99, pp. 647–654. ACM, New York, NY, USA (1999).

[140] Robert G. Sargent. Verification and Validation of Simulation Models. In *Proceedings of the 37th Conference on Winter Simulation*, WSC '05, pp. 130–143. Winter Simulation Conference (2005).

[141] O. Balci and R. G. Sargent. Validation of multivariate response simulation models by using Hotelling's two-sample T^2 test. *Simulation* 39(6), 185–192 (1982).

[142] O. Balci and R. G. Sargent. Some examples of simulation model validation using hypothesis testing. In *Proceedings of the 1982 winter simulation conference, ed. H. J. Highland, Y. W. Chao, and O. S. Madrigal*, pp. 620–629 (1982).

[143] O. Balci and R. G. Sargent. Validation of simulation models via simultaneous confidence intervals. *American Journal of Mathematical and Management Sciences* 4(3), 375–406 (1984).

[144] Thomas H. Naylor and J. M. Finger. Verification of Computer Simulation Models. *Management Science* 14(2), B–92–B–101 (1967).

[145] S. A. AlGadhi and G. K. Still. Jamarat Bridge; Mathematical models, Computer Simulation and Hajjis Safety analysis. Technical report, Crowd Dynamics Limited; http://www.crowddynamics.com/ (2003).

[146] G. K. Still. Simulex/Myriad. *Copyright © Crowd Dynamics Limited* (2003). http://www. crowddynamics.com/.

[147] L. Kovar, M. Gleicher, and F. H. Pighin. Motion Graphs. In *Proceedings of the 29th Annual Conference on Computer Graphics and Interactive Techniques*, SIGGRAPH '02, pp. 473–482. ACM, New York, NY, USA (2002).

[148] D. P. Noonan, P. Mountney, D. S. Elson, A. Darzi, and G. Yang. A stereoscopic fibroscope for camera motion and 3D depth recovery during Minimally Invasive Surgery. In *2009 IEEE International Conference on Robotics and Automation, ICRA 2009, Kobe, Japan, May 12-17, 2009*, pp. 4463–4468 (2009).

[149] J. L. Barron, D. J. Fleet, and S. S. Beauchemin. Performance of optical flow techniques. *International Journal of Computer Vision* 12(1), 43–77 (1994).

[150] S. S. Beauchemin and J. L. Barron. The Computation of Optical Flow. *ACM Comput. Surv.* 27(3), 433–466 (1995).

[151] C. M. Fan, N. M. Namazi, and P. B. Penafiel. A New Image Motion Estimation Algorithm Based on the EM Technique. *IEEE Trans. Pattern Anal. Mach. Intell.* 18, 348–352 (1996).

[152] D. J. Fleet and A. D. Jepson. Computation of component image velocity from local phase information. *International Journal of Computer Vision* 5(1), 77–104 (1990).

[153] P. M. Hayton, M. Brady, S. M. Smith, and N. Moore. A non-rigid registration algorithm for dynamic breast MR images. *Artificial Intelligence* 114, 125–156 (1999).

[154] B. K. P. Horn and B. G. Schunk. Determining Optical Flow. *Artificial Intelligence* 17, 185–203 (1981).

[155] Q. X. Wu. A correlation-relaxation-labeling framework for computing optical flow -template matching from a new perspective. *IEEE Transactions on Pattern Analysis and Machine Intelligence* 17(8), 843–853 (1995).

[156] J. H. Sun, D. A. Yates, and D. E. Winterbone. Measurement of the flow field in a diesel engine combustion chamber after combustion by cross-correlation of high-speed photographs. *Experiments in Fluids* 20, 335–345 (1996).

[157] W. F. Clocksin. A New Method for Computing Optical Flow. In *Proceedings of the British Machine Vision Conference 2000, BMVC 2000, Bristol, UK, 11-14 September 2000*, pp. 1–10 (2000).

[158] S. A. Velastin, J. H. Yin, A. C. Davies, M. A. Vicencio-Silva, R. E. Allsop, and A. Penn. Automated measurement of crowd density and motion using image processing. In *Seventh International Conference on Road Traffic Monitoring and Control, 26-28 APRIL 1994. Procedings.(IEE Conference Publication 391)*, pp. 127–132 (1994).

[159] S. Velastin, J. Yin, A. Davies, M. A. Vicencio-Silva, R. E. Allsop, and A. Penn. Analysis of Crowd Movements and Densities in Built-up Environments using Image Processing. In *Proceedings IEE Colloquium on Image Processing for Transport Applications*, pp. 8/1–8/6 (1993).

[160] D. Johnston. *Pedestrian Surveillance through Image Processing*. Master's thesis, University of Southampton; http://johnsto.co.uk/ uni/crowd/ Report.pdf (2004).

[161] M. Seki, H. Fujiwara, and K. Sumi. A robust background subtraction method for changing background. In *Proceedings Fifth IEEE Workshop on Applications of Computer Vision, WACV 2000, December 4-6, Palm Springs, California, USA*, pp. 207–213 (2000).

[162] P. Vannoorenberghe, C. Motamed, J. M. Blosseville, and Jack-Gerard Postaire. Monitoring pedestrians in a uncontrolled urban environment by matching low-level features. In *Systems, Man, and Cybernetics, 1996., IEEE International Conference on*, volume 3, pp. 2259–2264 vol.3 (1996).

[163] S. Yonemoto, H. Nakano, and R. Taniguchi. Real-time human figure control using tracked blobs. In *Proc. of 12th International Conference on Image Analysis and Processing*, pp. 127–132 (2003).

[164] B. Lucas and T. Kanade. An iterative image registration technique with an application to stereo vision. In *Proceedings of the 7th international joint conference on Artificial intelligence - Volume 2*, IJCAI'81, pp. 674–679. Morgan Kaufmann Publishers Inc., San Francisco, CA, USA (1981).

[165] G. Bradski. OpenCV. *Dr. Dobb's Journal of Software Tools, Copyright © 1999-2001 Intel Corporation* (2000).

Ehrenwörtliche Erklärung

Ich erkläre, dass ich diese Dissertation, abgesehen von den ausdrücklich bezeichneten Hilfsmitteln, selbständig verfasst habe.

Stuttgart, den 17. April 2015 *Mohamed Hedi Dridi*